

Syracuse University

SURFACE

Theses - ALL

May 2020

Understanding Double Network Theory and Applying it to Synthesis and Biological Applications

Alexander Vincent Struck Jannini
Syracuse University

Follow this and additional works at: <https://surface.syr.edu/thesis>



Part of the [Engineering Commons](#)

Recommended Citation

Struck Jannini, Alexander Vincent, "Understanding Double Network Theory and Applying it to Synthesis and Biological Applications" (2020). *Theses - ALL*. 407.
<https://surface.syr.edu/thesis/407>

This Thesis is brought to you for free and open access by SURFACE. It has been accepted for inclusion in Theses - ALL by an authorized administrator of SURFACE. For more information, please contact surface@syr.edu.

Abstract

The double network synthesis technique has gained popularity in the past few years as a method to create hydrogels with high strength and toughness, making them ideal for a plethora of applications, such as tissue engineering, drug delivery, and biosensors. The technique revolves around creating a ductile, weak network in the same space as a brittle, strong network. With the development of the synthesis technique, researchers have investigated both why these materials have the reported properties and finding new ways to synthesize them or use them in different applications. In this work, I aim to add on both aspects of this research. First, I investigated how brittle network variables affect the mechanical properties of the double network to expand our knowledge of double network behavior. Next, as part of a collaborative project with the Soman Lab, I helped develop a double network hydrogel that could be synthesized using a novel photolithography setup for making complex 3D microstructures. Lastly, a slug glue protein laden hydrogel was developed in the hopes of making a novel double network for the purposes of investigating the effects of glue protein and metal ion interactions.

Understanding Double Network Theory and Applying it to Synthesis and Biological
Applications

Alexander Struck Jannini

M.S., Rowan University, 2014

B.S., Rowan University, 2013

Thesis

Submitted in partial fulfillment of the requirements for the degree of
Master of Science in Bioengineering

Syracuse University

May 2020

Copyright © Alex Jannini 2020

All Rights Reserved

Acknowledgments

I would like to thank my advisors, Dr.'s Julie M. Hasenwinkel and James H. Henderson, for their guidance and support during my time here at Syracuse University. I would also like to thank Dr. Andy Smith for his guidance with the slug glue protein portion of my work. His insight helped me find the perfect place to go hunting for slugs on warm summer mornings.

I would like to express my gratitude towards my committee members, who have taken the time out of their busy schedules to review and critique my work. It is only through their observations and comments that I can grow to become a stronger researcher and scientist, and for that I am grateful.

A special thanks to members of the Biomaterials Institute, especially members of the Henderson group, who have listened to my long spiels about issues with my projects, and have been ever helpful in finding ways to resolve them. I would also like to thank Dr. Puskal Kunwar of the Soman Lab, who came up to me during a Stevenson Poster Session to talk about my work on double networks. It was through this conversation that a chapter of my thesis was developed.

Lastly, I would like to thank my friends and family, for being the source of support and encouragement I needed when experiments just wouldn't work. A special thanks to my partner, who has had to deal with my hectic schedule and sometimes sour moods after particularly rough days in the lab. I couldn't have done it without you.

Table of Contents

Acknowledgments	iv
Table of Contents	v
List of Schemes	viii
List of Figures	viii
List of Tables	x
Chapter 1 Introduction	1
1.1 Double Network Hydrogels	1
1.2 Understanding Double Network Mechanics	2
1.3 Creating Double Networks via Novel Synthesis Methods	3
1.4 Double Networks in Nature – The <i>Arion subfuscus</i> Defensive Glue	5
1.5 Scope of Thesis	7
1.6 References	7
Chapter 2 Using a Central Composite Experimental Design to Investigate the Effects of Brittle Network Variable Interactions on Double Network Mechanics	10
2.1 Synopsis	10
2.2 Introduction	11
2.3 Experimental	14
2.3.1 Materials	14
2.3.2 Methacrylation of Hyaluronic Acid.....	14
2.3.3 Single Network and Double Network Synthesis	15
2.3.4 Mechanical Testing.....	15
2.3.5 Central Composite Design.....	17
2.3.6 Statistical Analysis	17
2.4 Results and Discussion	17
2.4.1 Synthesizing the Double Network	17
2.4.2 Brittle Network Concentration and Crosslinking Affecting Mechanical Properties	20
2.4.3 Model Equations.....	25
2.5 Conclusions	26
2.6 Schemes, Figures, and Tables	28
2.7 References	34
Chapter 3 Developing a Double Network for High-Resolution 3D Printing Using Optical Projection Lithography	37

3.1 Synopsis	37
3.2 Introduction	37
3.3 Experimental	40
3.3.1 Materials	40
3.3.2 LAP Synthesis	40
3.3.3 Fabrication of the DN Structure	41
3.3.4 Mechanical Testing.....	41
3.3.5 Microscopic Imaging.....	42
3.3.6 Statistical Analysis	42
3.4 Results and Discussion	42
3.4.1 Fabrication and Characterization of the DN Structures.....	42
3.4.2 Effect of Light Dose on the Tensile Properties of DN Gel Structures	44
3.4.3 Effect of Composition of Alginate/acrylamide on the Tensile Properties of DN Gel Structures	45
3.4.4 Effect of Cross-linker Amount on the Tensile Properties of DN Gel Structures	45
3.4.5 Effect of Composition of Photoinitiator on the Tensile Properties of DN Gel Structures	46
3.4.6 Printing and Characterization of 3D DN Gel	47
3.4.7 Fabrication of User-Defined 2D/3D Structure of DN Hydrogel	48
3.5 Conclusions	49
3.6 Schemes, Figures, and Tables	50
3.7 References	58
Chapter 4 Determining the Effect of Polymer and Protein Concentration on Adhesive and Mechanical Properties of Protein-Polymer Gels	62
4.1 Synopsis	62
4.2 Introduction	62
4.3 Experimental	67
4.3.1 Materials	67
4.3.2 Extracting the Slug Glue Proteins	67
4.3.3 Gel Synthesis	67
4.3.4 Rheometry	68
4.3.5 Hysteresis.....	68
4.3.6 Lap Shear Test	68

4.3.7 Pull-Off Test	69
4.3.8 Statistical Tests	69
4.4 Results and Discussion	70
4.4.1 Gel Synthesis	70
4.4.2 Stiffness and Hysteresis Energy	71
4.4.3 Cohesive and Adhesive Strength	73
4.5 Conclusions	75
4.6 Schemes, Figures, and Tables	77
4.7 References	83
Chapter 5 Summary	87
5.1 Conclusions	87
5.2 Future Work	88
Appendices	90
Appendix A.1. All tensile, tearing, and swelling data collected for the CCD. Each value is the average \pm standard deviation	90
Appendix A.2. ANOVA Results. Tabular ANOVA data for each of the mechanical responses. Obtained from MINITAB software	91
Appendix A.3. Explanation of the Tearing Energy Results	93
Appendix B.1. Quantification of volume increase during the immersion of DN gel structures in calcium solution.	94
Appendix B.2. Study of the mechanical properties of fabricated DN gel structures with different fabrication speed and fixed laser power.	95
Appendix B.3. Schemes, Tables, and Figures for Appendix B	96
Appendix C. The Strain and Frequency Sweeps of PDMAAm-SGP gels	98
Vita	100

List of Schemes

Scheme 3.1 a) Schematic showing the 3D fabrication of DN hydrogel structure using digital mask-based optical lithography setup. b) Schematic of the alginate/DMAAm DN hydrogel formed by covalent cross-linking of DMAAm and ionic cross-linking of alginate.

Scheme 3.2 Schematic cartoon showing a simplification of the lithography setup. A laser is shined to a digital micromirror device (DMD), which allows for precise polymerization and crosslinking of the photoinitiated gel. Ionic crosslinking is conducted after the lithography by submerging the gel in a calcium bath.

List of Figures

Figure 2.1 The CCD data points used during experiments. The 2^2 factorial design compositions are denoted by the orange points and the blue denotes the CCD compositions, while the red is the centerpoint.

Figure 2.2 Swelling study of individual polymer networks and the double network. Here, “Q” stands for the swelling ratio. Error bars are standard deviation. It is interesting to note that the DN has a slow swelling rate comparable to that of a PDMAAm gel for the first few time points but reaches a maximum comparable to that of the MHA gel.

Figure 2.3 Surface plots that show the a) modulus, b) elongation at break, c) max stress, d) tearing energy, and e) Q_{\max} response to changes in brittle network composition of an MHA-PDMAAm DN gel. Of the five properties, modulus and tearing energy were dependent on the interactions between the weight percent and crosslinking ratio of the brittle MHA network.

Figure 2.4 Comparison of the response predicted from the model equations (“Theoretical”) versus those obtained by direct testing (“Experimental”) for modulus (a), elongation at break (b), max stress (c), tearing energy (d), and Q_{\max} (e). Error bars are 95% confidence intervals. * - significant difference between the theoretical and experimental values.

Figure 3.1. Initial tests to show double network formation. a) Plot showing the tensile stress–strain curve obtained from DN gel structure and its individual parent gel structures. The inset shows a dogbone-shaped structure being stretched more than 4 times its original length. The structure was printed with the laser intensity of 5 mW/cm^2 and exposure time of 5 s. Bar diagrams showing elastic modulus (b), ultimate strain (c), and ultimate stress (d) for the DN gel structures, alginate gel structures, and DMAAM gel structures with LAP as an photoinitiator and MBAAM as a cross-linker. ANOVA test showed significant difference among the groups (p value < 0.001). ANOVA with Bonferroni correction showed significant differences between two groups at $*p < 0.016$, $**p < 0.001$. [Error bars: mean \pm standard deviation (SD)]. e) Plot showing the tearing test for the DN gel representative structures and the individual parent gel structure. f)

Plots showing the stress–strain curve obtained from the DN gel structures exposed to different exposure times.

Figure 3.2 Results of the alginate composition experiments. a) Sample tensile tests results from each of the DN compositions. The elastic moduli (b), ultimate strain (c), and the ultimate stress (d) was collected and compared. * $p < 0.016$, ** $p < 0.001$. (Error bars: mean \pm SD).

Figure 3.3 Results of the crosslinker concentration experiments. a) Sample stress–strain results of the DN gels with the varying amounts of crosslinkers (0.035, 0.07, and 0.14 wt %). The elastic moduli (b), ultimate strain (c), and the ultimate stress (d) was collected and compared. * $p < 0.016$, ** $p < 0.001$. (Error bars: mean \pm SD)

Figure 3.4 The results of the photoinitiator composition experiment. a) Sample stress–strain results of the DN gels with the varying amounts LAP photoinitiator (0.165, 0.33 and 0.66 wt %). The elastic moduli (b), ultimate strain (c), and the ultimate stress (d) was collected and compared. * $p < 0.016$. (Error bars: mean \pm SD)

Figure 3.5 Results of experiments in which the laser power and the fabrication speed were varied. a) Sample stress–strain curves for DN gel structure printed at fixed fabrication speed and varying laser power. b) Scatter plot showing modulus of elasticity, ultimate stress, and ultimate strain of the DN gel structure fabricated with different laser intensity and constant fabrication speed. c) Stress–strain curve for DN gel structure printed at varying fabrication speed and fixed laser power. * p value < 0.05 , ** p value < 0.001 . (Error bars: mean \pm SD)

Figure 3.6 Illustration cartoon of 2D structure (auxetic shaped). (A2) Fabricated DN gel structure before stretching and (A3) after stretching. Structure was printed using optical projection lithography and dipped into calcium solution for 72 h. (B) 2D printed “Syracuse University” before dipping into calcium solution. (C) Log-pile structure demonstrating the smallest feature size/resolution of 120 μm . (D,E) 3D printing of tough and stretchable hydrogel. (D1,D2) Empire State Building structure before and after dipping into the calcium solution. (E) Mayan pyramid structure printed using DN gel structure and image was recorded after the structures are dipped into calcium solution for 72 h. The fabricated images shown in A,D,E were acquired using a digital SLR camera and B,C are recorded using a HIROX microscope.

Figure 4.1 The design space used to investigate the effects of polymer and protein concentration on the adhesive and mechanical properties of the gels.

Figure 4.2 A slug glue protein, poly(dimethylacrylamide) gel that has been exposed to UV light from the OmniCure[®] S2000 Spot UV Cure System. For this particular light source, it was found that the beam was too focused, and would cause denaturing or damaging of the proteins in the area where the light directly shone unto the sample (red dashed circle). These samples were considered unusable.

Figure 4.3 The results of the rheometry experiments with the SGP-DMAAm gels. The order of magnitude increase in storage modulus in the 60 mg DMAAm/mL, 0.8 mg SGP/mL sample was

seen as a potential indication of a SGP network being formed. Error bars are standard deviation. ** - p-value < 0.01. *** - p-value < 0.001.

Figure 4.4 The hysteresis energy of the SGP-DMAAm gels. One point to note is that all error bars cross the 0-point. This indicates that there is little to no energy dissipation that occurs within the gels. If an SGP network was forming, it would be expected that the energy dissipation would increase with incorporation of SGP's into the gel.

Figure 4.5 The cohesive strength of the SGP-DMAAm gels as observed from a lap shear test. No statistical difference could be inferred when comparing the compositions. This could be due to the high variations seen in the SGP-loaded 40 mg DMAAm/mL samples. It should be noted that outlier testing was conducted on all samples, and no outliers could be determined. This data also conforms with the results of the hysteresis testing, which indicated a lack of SGP network formation. An SGP network being formed within the gels would be seen as an increase in the cohesive strength.

Figure 4.6 The adhesive strength of the SGP-DMAAm gels based on the results of a pull-off test. Interestingly, the 40 mg DMAAm/mL, 0.0 mg SGP/mL and 40 mg DMAAm/mL, 0.5 mg SGP/mL compositions had the highest adhesive energy. This is believed to be due to the high water content of these gels, and an increase in the surface tension that would result when a force is applied to the gel and then released. * - p-value < 0.05. ** - p-value < 0.01.

List of Tables

Table 2.1 A comparison of the mechanical properties between the single networks (SN's) and the DN (\pm standard deviation). MHA networks were too fragile to test using either the tensile or tearing procedure. * - Statistically different using Student's t-test with $p < 0.01$. ** - Statistically different from the other two points using Tukey post-hoc with $p < 0.01$.

Table 2.2 The general CCD equation used to model response behavior and the specific coefficient values for each response. These equations are based off the surface response plots as shown in Figure 2.3.

Chapter 1 Introduction

1.1 Double Network Hydrogels

Double networking is a synthesis technique that can be used to develop tough and elastic materials. These networks have these tough and elastic behavior due to a brittle, rigid polymer network that serves to disperse the stress once a crack or deformation forms in the material [1]. The second, more ductile polymer allows the network to extend far beyond the yielding strain of the brittle polymer. The combination of stress dispersion and ductility allows for double network gels with greater mechanical strength and toughness than the individual networks. The technique is not the only way to synthesize strong polymers; other techniques include tetrahedron-like macromonomers [2] or slide-ring crosslinkers [3]. These two techniques provide enough strength to impart elastic deformation in hydrogels, but the toughness was found to be lower than that of double network gels [1]. Another technique, in which the gel is combined with clay nanoparticles [4], does provide higher strength and toughness than using the macromonomer or crosslinker procedures, but not to the same degree as the double network structure [5].

For a classical double network hydrogel, such as those developed by Gong and colleagues, the following criterion must be met: the first network is a brittle polyelectrolyte, which is synthesized as a single network. The polyelectrolyte is usually tightly crosslinked and in some cases heterogeneous in nature [5]. Once the first network has been synthesized, it is placed in a solution containing the monomer of the second network. This second network is comprised of a neutral polymer that, as a single network, would be considered soft and ductile. The first network swells in the second network solution, which can also contain crosslinker and initiator, and then the second network is formed via a second polymerization step. The swelling of the first network allows the second network precursors to diffuse into the bulk, and upon excitation, the second

network forms independently of the first. The second network should be in 20 to 30 molar excess of the first network in order to ensure that there is enough of the ductile polymer present in the material to provide support when strains are applied [1]. The synthesis technique is similar to that of making interpenetrating polymer networks (IPN's); the main difference being that IPN's are made of polymers with similar mechanical properties, while double networks (as stated previously) are made of polymers with differing mechanical properties. This difference causes a synergistic effect, which makes double networks stronger than the IPN's [5].

1.2 Understanding Double Network Mechanics

Ever since the technique was first reported in 2003 [6], there has been considerable interest in understanding how these materials behave, and the underlying mechanisms responsible for this phenomena. Gong provided an extensive discussion on her original material [1]. The theory proposed that the high toughness and strength is due to the synergistic effect between the brittle and ductile network. Specifically, the strong brittle network accepts a majority of the force applied to the gels. When the force applied is enough to break the network, it fractures and creates large damage zones. These large damage zones dissipate energy and allow for more force to be applied before a macroscopic crack forms [1].

To continue to explore these double networks, experiments and modeling were conducted to better understand what causes these large damage zones [7], [8]. From this, it was hypothesized that heterogeneity within the brittle network was responsible for the remarkable mechanical properties. Nakajima et al. continued with this theory by investigating the effects of homogeneity in the first network on the mechanical properties of the double network [9]. To test this, Nakajima et al. developed a method of creating a pure homogeneous first network using a tetra-PEG gel. They found that these homogeneous gels had the same mechanical behavior as the

inhomogeneous gels, and concluded that this aspect of the gel is not necessary for high toughness and tensile strength [9]. This independence on heterogeneity does not occur for all combinations of brittle and ductile networks [10].

This homogeneity of double networks was further investigated by Cui et al. By controlling the osmotic pressure of their polyampholyte double network precursor solution, the researchers were able to scale the homogeneity of the system [11]. High osmotic pressures tended to increase the homogeneity of the system. Using this method, they found that the gels had the highest strength and stiffness as well as highest strains to fracture when a middling osmotic pressure was applied. This is hypothesized to be due to the balance between the benefits of homogeneity and high ionic bond strength. As the osmotic pressure increases, condensation occurs, which leads to more ionic interactions between the polymer networks. However, when the homogeneity increases, the soft network cannot properly transfer stress, resulting in lower fracture strains [11].

While there have been some investigations into the first network, there have also been some investigations into how the second network affects the mechanical properties. For example, Tsukeshiba et al. found that high crosslinking concentration in the second network does not allow for good entanglement between the two, and can lower the toughness of the double network [12]. Another important study looked at how the ability of the gels to neck was dependent on the molecular weight of the polymer chains of the second network. Long chains of the ductile network allow for disentanglement at high elongations, which allows for greater energy dissipation [13].

1.3 Creating Double Networks via Novel Synthesis Methods

While these double network gels do have highly desired mechanical properties, one of their main drawbacks is the long synthesis times. In order to make a double network using the classical

method, the method requires synthesizing one gel, then allowing it to swell in a monomer solution of the second network. As one can imagine, this can make the synthesis time take up to several days. In addition, using the classical method can limit the complexity of the shape that the gels can be formed into. To this end, researchers have explored ways to improve the synthesis methods used to make double networks so that either the time to synthesize can be reduced or more complex shapes can be obtained.

To improve on the timing of double network synthesis, researchers began looking into using one-pot synthesis methods. As it sounds, the one-pot synthesis method is when the components of both the first and second network are combined into one solution, and then the networks are formed individually. This type of synthesis method usually uses a mix of polymerization/crosslinking chemistries in order to ensure that the networks are formed independently from one another. One of the first examples of this synthesis method was published in 2013, in which Chen et al. used an agar-polyacrylamide system to develop a double network [14]. Agar was polymerized to form a gel through heating-and-cooling cycles, while polyacrylamide was polymerized under UV-excitation.

Another popular combination of polymerization/crosslinking chemistries used in one-pot synthesis is covalent and ionic gelation. This method usually uses a strong but brittle polymer that can be crosslinked via metallic ions, and a neutral ductile network that is polymerized and crosslinked via UV excitation. A combination used particularly often is alginate and polyacrylamide, in which the alginate is crosslinked via calcium ions and the polyacrylamide network is synthesized in the presence of photoinitiator and UV light [15]–[19]. An important note about these gels is that they tend to have self-healing behavior due to the presence of ionic

bonds. As such, they have become of interest for applications such as wound healing [20], [21], drug delivery [22], [23], and tissue engineering [22], [24], [25].

While some researchers have focused on synthesis techniques for lowering the timescale, others have focused on methods for creating double networks into complex structures. The most prominent of these methods is 3D printing. In 2013, Muroi and colleagues reported on their fabrication of a 3D printer that could print double networks [26]. The printer works by printing the material while a UV laser was shined underneath the stage. The UV light was focused via an objective lens which allowed for the light to travel through an optical fiber, allowing for controlled UV polymerization. Since then, other groups have developed their own methods to print double networks for biomedical applications. Yang, Tadepalli, and Wiley were able to 3D print a double network hydrogel with a greater compression strength and elastic modulus greater than that of cartilage [27]. The Burdick Lab out of the University of Pennsylvania were able to bioprint a double network gel consisting of two separately modified hyaluronic acid networks for tissue engineering [28]. Liu and Li developed a double network of κ -carrageenan and polyacrylamide that could be 3D printed into complex shapes for biosensor applications [29].

1.4 Double Networks in Nature – The *Arion subfuscus* Defensive Glue

An interesting subsection of double network research is in the characterization of a slug glue. The *Arion subfuscus* slug, a terrestrial slug found in the Eastern United States, secretes an adhesive gel as a defense mechanism [30]. Compositional analysis of the glue found that the glue is comprised of two networks; a flexible carbohydrate network and a rigid protein network that is crosslinked via metal ions [31]. This compositional analysis also found that the protein/metal and carbohydrate networks are in a 1:1 weight ratio with one another. This is a particularly interesting find, as classic double network theory would predict that the ductile network being in

excess of the brittle network. In addition, the two networks were found to have a synergistic effect. When one of the networks was disrupted using enzymes, the gel deteriorates, lacking any substantial strength [32].

Material testing on the *A. subfuscus* glue found that it has similar toughness to synthetic double networks [32]. Slug glue that was subjected to tensile testing had an average strain at failure of around 9.5, and an average peak stress of 101 kPa. This is in accordance with typical double networks [5]. Hysteresis experiments also showed that the glue can partially recover damage received during testing [33]. This would indicate the presence of physical crosslinks, similar to those seen in the covalent-ionic crosslinked double networks discussed in the previous section.

Based off the mechanical properties of the slug glue, there is a heightened interest in understanding the underlying mechanics of this material. To that end, thorough investigations into the proteins have been conducted. RNA sequencing was used to determine if the proteins had a similar sequence to any other groups of proteins [34]. Four groups of proteins were found to be a considerable interest; a set of proteins with a sequence similar to C-lectins, another set with H-lectin similarities, another with C1-q similarities, and one set with a sequence similar to matrilins. Based off of the known information about these families of proteins, it is hypothesized that the lectin-like proteins are responsible for the adhesive properties [35], [36], while the C1-q proteins and the matrilins were responsible for crosslinking and stiffening the gel [37], [38].

With a majority of the biochemical analysis completed, it may be of interest to investigate the proteins through a materials and engineering perspective, seeing how the proteins behave in synthetic gels and determine more about the underlying mechanics.

1.5 Scope of Thesis

This thesis is an overview of how double network theory was researched and applied to synthetic and biological problems. In Chapter 2 (adapted from Struck Jannini et al. manuscript [in peer review]), the focus is on investigating how double network mechanical properties are affected by brittle network composition. The concentration and crosslinking ratio of the brittle network was systematically altered in order to quantify the effects of both variables and their interaction on the tensile, swelling, and tearing properties of the gels. In Chapter 3 (adapted from Kunwar et al. [39]), the focus is on developing a double network system that could be used in a novel optical lithography setup. The material itself is the object of focus, as opposed to the laser setup, and the mechanical tests that were conducted to show successful double network synthesis as well as how material and lithographic variables affect the mechanical properties of the gel. In Chapter 4, the focus is on developing a material to investigate slug glue proteins. The purpose of this material is to determine if a double network could be formed using a synthetic polymer base that is then incorporated with proteins and metal ions to create the tough protein network. This would allow for future studies in which the protein network and metal ions could be methodically altered to determine how certain proteins behave in the presence of specific metal ions.

1.6 References

- [1] J. P. Gong, “Why are double network hydrogels so tough?,” *Soft Matter*, vol. 6, no. 12, pp. 2583–2590, 2010.
- [2] T. Sakai *et al.*, “Design and fabrication of a high-strength hydrogel with ideally homogeneous network structure from tetrahedron-like macromonomers,” *Macromolecules*, vol. 41, no. 14, pp. 5379–5384, 2008.
- [3] Y. Okumura and K. Ito, “The polyrotaxane gels: a topological gel by figure-of eight cross-links,” *Adv. Mater.*, vol. 13, no. 7, pp. 485–487, 2001.
- [4] K. Haraguchi and T. Takehisa, “Nanocomposite hydrogels: A unique organic-inorganic network structure with extraordinary mechanical, optical, and swelling/De-swelling properties,” *Adv. Mater.*, vol. 14, no. 16, pp. 1120–1124, 2002.

- [5] M. A. Haque, T. Kurokawa, and J. P. Gong, “Super tough double network hydrogels and their application as biomaterials,” *Polymer (Guildf.)*, vol. 53, no. 9, pp. 1805–1822, 2012.
- [6] J. P. Gong, Y. Katsuyama, T. Kurokawa, and Y. Osada, “Double-Network Hydrogels with Extremely High Mechanical Strength,” *Adv. Mater.*, vol. 15, no. 14, pp. 1155–1158, 2003.
- [7] R. E. Webber, C. Creton, H. R. Brown, and J. P. Gong, “Large strain hysteresis and Mullins effect of tough double network hydrogels,” *Macromolecules*, vol. 40, pp. 2919–2927, 2007.
- [8] T. Nakajima, T. Kurokawa, S. Ahmed, W. Wu, and J. P. Gong, “Characterization of internal fracture process of double network hydrogels under uniaxial elongation,” *Soft Matter*, vol. 9, no. 6, pp. 1955–1966, 2013.
- [9] T. Nakajima, Y. Fukuda, T. Kurokawa, T. Sakai, U. Il Chung, and J. P. Gong, “Synthesis and fracture process analysis of double network hydrogels with a well-defined first network,” *ACS Macro Lett.*, vol. 2, no. 6, pp. 518–521, 2013.
- [10] Q. Chen, H. Chen, L. Zhu, and J. Zheng, “Fundamentals of double network hydrogels,” *J. Mater. Chem. B*, vol. 3, pp. 3654–3676, 2015.
- [11] K. Cui *et al.*, “Effect of Structure Heterogeneity on Mechanical Performance of Physical Polyampholytes Hydrogels,” *Macromolecules*, vol. 52, no. 19, pp. 7369–7378, 2019.
- [12] H. Tsukeshiba *et al.*, “Effect of polymer entanglement on the toughening of double network hydrogels,” *J. Phys. Chem. B*, vol. 109, no. 34, pp. 16304–16309, 2005.
- [13] S. S. Es-Haghi, A. I. Leonov, and R. A. Weiss, “Deconstructing the double-network hydrogels: The importance of grafted chains for achieving toughness,” *Macromolecules*, vol. 47, no. 14, pp. 4769–4777, 2014.
- [14] Q. Chen, L. Zhu, C. Zhao, Q. Wang, and J. Zheng, “A robust, one-pot synthesis of highly mechanical and recoverable double network hydrogels using thermoreversible sol-gel polysaccharide,” *Adv. Mater.*, vol. 25, no. 30, pp. 4171–4176, 2013.
- [15] J.-Y. Sun *et al.*, “Highly stretchable and tough hydrogels,” *Nature*, vol. 489, no. 7414, pp. 133–136, 2012.
- [16] X. F. Li, C. Wu, C. Jiang, Q. W. Chen, and D. Zou, “Fracture Behavior of Two Highly Stretchable Double Network Hydrogels,” *Int. J. Polym. Anal. Charact.*, vol. 18, no. 7, pp. 504–509, 2013.
- [17] M. C. Darnell *et al.*, “Performance and biocompatibility of extremely tough alginate/polyacrylamide hydrogels,” *Biomaterials*, vol. 34, no. 33, pp. 8042–8048, 2013.
- [18] C. H. Yang *et al.*, “Strengthening alginate/polyacrylamide hydrogels using various multivalent cations,” *ACS Appl. Mater. Interfaces*, vol. 5, no. 21, pp. 10418–10422, 2013.
- [19] Q. Zheng, L. Zhao, J. Wang, S. Wang, Y. Liu, and X. Liu, “High-strength and high-toughness sodium alginate/polyacrylamide double physically crosslinked network hydrogel with superior self-healing and self-recovery properties prepared by a one-pot method,” *Colloids Surfaces A Physicochem. Eng. Asp.*, 2020.

- [20] Y. Wang *et al.*, “Synthesis of cellulose-based double-network hydrogels demonstrating high strength, self-healing, and antibacterial properties,” *Carbohydr. Polym.*, 2017.
- [21] Q. Wei, Y. Chang, G. Ma, W. Zhang, Q. Wang, and Z. Hu, “One-pot preparation of double network hydrogels: Via enzyme-mediated polymerization and post-self-assembly for wound healing,” *J. Mater. Chem. B*, vol. 7, no. 40, pp. 6195–6201, 2019.
- [22] I. S. Cho and T. Ooya, “Tuned cell attachments by double-network hydrogels consisting of glycol chitosan, carboxymethyl cellulose and agar bearing robust and self-healing properties,” *Int. J. Biol. Macromol.*, 2019.
- [23] Y. Qiao, S. Xu, T. Zhu, N. Tang, X. Bai, and C. Zheng, “Preparation of printable double-network hydrogels with rapid self-healing and high elasticity based on hyaluronic acid for controlled drug release,” *Polymer.*, vol. 186, no. 121994, 2020.
- [24] D. M. Kirchmayer and M. In Het Panhuis, “Robust biopolymer based ionic-covalent entanglement hydrogels with reversible mechanical behaviour,” *J. Mater. Chem. B*, vol. 2, no. 29, pp. 4694–4702, 2014.
- [25] L. Weng, A. Gouldstone, Y. Wu, and W. Chen, “Mechanically strong double network photocrosslinked hydrogels from N,N-dimethylacrylamide and glycidyl methacrylated hyaluronan,” *Biomaterials*, vol. 29, no. 14, pp. 2153–2163, 2008.
- [26] H. Muroi, R. Hidema, J. Gong, and H. Furukawa, “Development of Optical 3D Gel Printer for Fabricating Free-Form Soft & Wet Industrial Materials and Evaluation of Printed Double-Network Gels,” *J. Solid Mech. Mater. Eng.*, vol. 7, no. 2, pp. 163–168, 2013.
- [27] F. Yang, V. Tadepalli, and B. J. Wiley, “3D Printing of a Double Network Hydrogel with a Compression Strength and Elastic Modulus Greater than those of Cartilage,” *ACS Biomater. Sci. Eng.*, vol. 3, no. 5, pp. 863–869, 2017.
- [28] L. L. Wang, C. B. Highley, Y. C. Yeh, J. H. Galarraga, S. Uman, and J. A. Burdick, “3D extrusion bioprinting of single- and double-network hydrogels containing dynamic covalent crosslinks,” *J. Biomed. Mater. Res. - Part A*, vol. 106, no. 4, pp. 865–875, 2018.
- [29] S. Liu and L. Li, “Ultrastretchable and Self-Healing Double-Network Hydrogel for 3D Printing and Strain Sensor,” *ACS Appl. Mater. Interfaces*, vol. 9, no. 31, pp. 26429–26437, 2017.
- [30] A. M. Smith, “Adhesive Gels,” in *Biological Adhesives*, Berlin: Springer-Verlag, 2006, pp. 167–182.
- [31] A. M. Smith, “Multiple Metal-Based Cross-Links: Protein Oxidation and Metal Coordination in a Biological Glue,” in *Biological and Biomimetic Adhesives: Challenges and Opportunities*, Cambridge: Royal Society of Chemistry, 2013, pp. 3–15.
- [32] A. M. Wilks, S. R. Rabice, H. S. Garbacz, C. C. Harro, and A. M. Smith, “Double-network gels and the toughness of terrestrial slug glue,” *J. Exp. Biol.*, vol. 218, no. Pt 19, pp. 3128–37, 2015.
- [33] T. M. Fung, C. Gallego Lazo, and A. M. Smith, “Elasticity and energy dissipation in the double network hydrogel adhesive of the slug *Arion subfuscus*,” *Philos. Trans. R. Soc. B*

- Biol. Sci.*, vol. 374, no. 1784, 2019.
- [34] A. M. Smith, C. Papaleo, C. W. Reid, and J. M. Bliss, “RNA-Seq reveals a central role for lectin, C1q and von Willebrand factor A domains in the defensive glue of a terrestrial slug,” *Biofouling*, vol. 33, no. 9, pp. 741–754, 2017.
- [35] A. N. Zelensky and J. E. Gready, “The C-type lectin-like domain superfamily,” *FEBS J.*, vol. 272, no. 24, pp. 6179–6217, 2005.
- [36] J. F. Sanchez *et al.*, “Biochemical and structural analysis of *Helix pomatia* agglutinin: A hexameric lectin with a novel fold,” *J. Biol. Chem.*, vol. 281, no. 29, pp. 20171–20180, 2006.
- [37] S. Ressler, B. K. Vu, S. Vivona, D. C. Martinelli, T. C. Südhof, and A. T. Brunger, “Structures of C1q-like proteins reveal unique features among the C1q/TNF superfamily,” *Structure*, vol. 23, no. 4, pp. 688–699, 2015.
- [38] M. Paulsson and R. Wagener, “Matrilins,” in *Methods in Cell Biology*, vol. 143, L. Wilson and P. Tran, Eds. Cambridge: Elsevier, 2018, pp. 429–446.
- [39] P. Kunwar *et al.*, “High-Resolution 3D Printing of Stretchable Hydrogel Structures Using Optical Projection Lithography,” *ACS Appl. Mater. Interfaces*, vol. 12, no. 1, pp. 1640–1649, 2020.

Chapter 2 Using a Central Composite Experimental Design to Investigate the Effects of Brittle Network Variable Interactions on Double Network Mechanics

2.1 Synopsis

Double networking is a hydrogel synthesis technique that reinforces gels through a synergistic effect occurring when a ductile, loosely crosslinked gel is synthesized in the same space as a previously polymerized brittle, tightly crosslinked gel. While there have been investigations undertaken to better understand the mechanisms by which these double network gels behave, there have been none that specifically investigate and quantify the effect of the interactions of different variables on the mechanical properties of these systems. To investigate the interactions of brittle network variables, a central composite design was used to systematically alter the concentration and crosslinking ratio of a poly(ethylene glycol) diacrylate (PEGDA) crosslinked, methacrylated hyaluronic acid network (MHA) used in an MHA-poly(dimethyl acrylamide)

double network, and the tensile, tearing, and swelling properties of these networks were studied. Through changing the weight percent of MHA and the ratio of PEGDA:MHA (0.793 to 2.207 wt% and 1.586:1 and 4.414:1, respectively), the modulus and tearing energy were found to change by an order of magnitudes (19.19 kPa to 282.45 kPa and 6.16 to 102.10 J/m², respectively). Using this design, it was found that the interactions of these two variables affect both the modulus and the tearing energy of the DN gels. As these properties of the material are indicative of the strength and toughness, this work shows the importance of these interactions, and that they should be considered when other materials researchers develop their own double networks.

2.2 Introduction

Double networking is a synthesis technique used to reinforce hydrogels. The method was first developed by Gong et al. [1] which made use of a brittle, tightly crosslinked poly(2-acrylamido-2-methylpropane sulfonic acid) network and a ductile, loosely crosslinked poly(acrylamide) network. Since then, double networks (DN's) have been developed using several different combinations of brittle and ductile polymers, including poly(methacrylic acid)-poly[oligo(ethylene glycol) methyl ether methacrylate] [2], alginate-poly(acrylamide) [3], and graphene-poly(dimethylacrylamide) [4]. The advantage of DN gels is the orders of magnitude increases in the strength and toughness as compared to the respective singular networks. This technique has been used to develop materials for a diverse array of applications, such as tissue engineering [5]–[8], drug delivery [4], [9], [10], and biosensors [11], [12].

There has been considerable interest in understanding the mechanics and underlying mechanisms that govern these gels. Gong ran several experiments to investigate what the mechanism was for DN toughness [13]. It was determined that the brittle, strong polymer acts as a “sacrificial

network”, in which the imparted forces are isolated. This causes the brittle network to fracture, but the polymer is held together by the ductile network. This allows the DN to stretch beyond the limits of the brittle network, but still benefit from the strength and toughness of the brittle network [13].

Weng and colleagues developed a DN gel for load-bearing tissue scaffolds and investigated mechanical property changes based on compositional modifications to the ductile network [14]. In this work, the authors attempted to optimize the ductile PDMAAm gel network by changing both the concentration of the monomer and the crosslinker in the DMAAm solution. The second network was optimized for compressive strength, and it was found that a DMAAm concentration of 3 mol/L and a crosslinking concentration of 0.002 moles crosslinker per mole DMAAm led to a maximum compressive fracture stress of 5.2 MPa. This optimization shows how the ductile network should be concentrated enough to provide mechanical integrity when the brittle network breaks, and be loosely crosslinked to ensure high ductility [13].

Tsukeshiba et al. also ran an investigation to elucidate the mechanics of double network behavior, and determined that self-entanglement of the second network is imperative for high toughness [15]. The researchers were able to determine the average molecular weight of synthesized poly(acrylamide) polymers and found that decreasing photoinitiator concentration led to higher average molecular weights. These high molecular weight polymer branches were found to lead to DN's with higher fracture stresses and fracture energies. These high molecular weight polymer strands are believed to be beneficial to DN structures because it allows for more entanglement of the ductile network strands. This provides better dispersion of energy during compressive loading, and allows for resistance to fracture, as the entangled networks fill in void spaces within the DN [15].

While these investigations have furthered our understanding of DN gel mechanics, there are still many aspects that have not been considered. For example, there has been little work in understanding how brittle network variables and their interactions affect the mechanical responses of the DN gels. Tavsanlı, Can, and Okay ran investigations into the degree of methacrylation of an MHA gel and how that affected the modulus of a MHA-PDMAAm DN gel [16]. The degree of methacrylation was varied from 4 to 25%, which had an optimal value of 8%, resulting in a modulus of 549 kPa for a DN with a DMAAm concentration of 0.30 g/mL. However, a majority of this study was focused on the development of a triple network, and the investigative efforts were mainly concentrated on optimizing the second and third DMAAm network [16].

Tavsanlı and Okay also developed MHA-PDMAAm DN gels using a one-pot synthesis method [17]. Again, the degree of methacrylation was investigated as part of the overall study design, with the researchers running tensile and compressive tests on DN gels containing MHA of different degrees of methacrylation. They noted a significant increase in the behavior of the gels as the degree of methacrylation increased, with a maximum Young's modulus of 30 kPa at 25% degree of methacrylation [17]. Recently, Murai et al. investigated water content and crosslinking ratio in a cellulose and poly(ethyl acrylate) DN gel [18]. The investigators briefly looked at the effects of water content and crosslinking ratio of the cellulose network and the effects on the tensile behavior of the DN gel, finding the optimal crosslinking ratio of 0.46 g crosslinker/g cellulose and a water ratio of 10 μ L/g cellulose led to the optimal strength and ductility.

Although these investigations looked into the brittle networks, the interactions of the multiple variables were not explored. These interactions could significantly affect the mechanical properties of a gel and, if overlooked, could lead to less than optimal material compositions for

intended applications. In this work, we investigated the effect of changes in composition of the brittle MHA network on the mechanical properties of a MHA-PDMAAm DN gel. A surface response experimental design was used to quantify the effects of MHA concentration and the ratio of crosslinker (in this experiment poly(ethylene glycol diacrylate) or PEGDA) to MHA as well as their interactions through surface response plots. Quadratic equations were also developed to model the responses, and their accuracy was tested using gel compositions within the design space. It was found that the interactions of weight percent and crosslinking ratio significantly affected the modulus and the tearing energy of these DN gels. These findings show that the brittle network composition is an important aspect of DN design, and should be taken into consideration along with the ductile network.

2.3 Experimental

2.3.1 Materials

Sodium hyaluronate (HA) of average molecular weight 950 kDa was obtained from Bloomage Freda Biopharm Company. Poly(ethylene glycol) diacrylate (PEGDA) of molecular weight 575 Da was purchased from Sigma Aldrich. N,N-Dimethylacrylamide (DMAAm), N,N'-Methylenebis(acrylamide) (MBAAm), glycidyl methacrylate (GMA), and hydrochloric acid (HCl) were obtained from Sigma Aldrich. Irgacure 2959 (Irg 2959) was purchased from BASF. The HCl solution was diluted down to 1.0 M before use.

2.3.2 Methacrylation of Hyaluronic Acid

Methacrylated hyaluronic acid was prepared as described by Varde [19]. Briefly, a 0.33 wt% HA solution was created, and GMA was added at 20 molar excess. The pH of the solution was lowered down to 1.5 using the 1.0 M HCl solution, and then allowed to react for two days at 50 °C. The solution was then placed in Spectra/Por[®] 1 dialysis tubing and allowed to dialyze in a

deionized water bath for two days. Once dialysis was complete, the solution was placed in a -80 °C freezer overnight, and lyophilized for at least 4 days.

2.3.3 Single Network and Double Network Synthesis

Single networks of MHA and DMAAm were prepared. A 2 wt% solution of MHA was created, and PEGDA was added to the solution at a ratio of 4 mol PEGDA to 1 mol MHA (4:1).

DMAAm gels were synthesized by making a 30 wt% DMAAm solution and adding MBAAm so that there were 0.002 moles MBAAm per mol DMAAm [14]. Irg 2959 was added to a concentration of 1.5×10^{-5} mol/mL. All solutions were vortexed until all solids were dissolved. The gels were then subjected to 365 nm UV curing for 2 hours.

For the double network (DN) gels, MHA gels were prepared as described previously. After curing, the gels were placed in excess DMAAm solution of the same composition as described above. After swelling overnight, the gels were removed from the solution and once again cured under UV light for 2 hours.

2.3.4 Mechanical Testing

To determine the swelling characteristics of the different gels, MHA, DMAAm, and DN gels were prepared using cylindrical molds with a diameter of 15.5 mm. Solutions were injected into these molds before curing. Once all samples were made, the gels were lyophilized for 5 days so that all gels had a uniform initial water content. Samples were removed from the lyophilizer, and then placed in excess deionized water ($n=3$ per composition). Mass measurements were taken at regular time intervals, and the swelling ratio (Q) was calculated using Equation 1, where m_0 is the initial mass of the sample and m_i is the mass of the sample at timepoint “ i ”. The average maximum swelling ratio (Q_{\max}) was calculated for comparison.

$$Q = \frac{(m_i - m_0)}{m_0} \quad (1)$$

The rubber elastic properties of the gels were determined using tensile testing. Tensile testing was conducted only on DMAAm and DN gels, as the MHA gel lacked sufficient mechanical integrity. Samples were prepared into sheets using glass slides and a 1.15 mm thick spacer. After curing, the sheets were submerged in deionized water for at least three days. Tensile samples were created by using a dogbone punch with a gauge length and gauge width of 6.25 mm and 1.50 mm, respectively. The samples were clamped into a TestResources 100 Series Universal Test Machine with a 25 N force transducer. The clamps of the machine were modified by adhering sandpaper to reduce the slippage of samples. The samples were pulled at a rate of 150% strain per minute until the material failed. Five samples from five batches were tested for each type of gel. The average Young's modulus, elongation at break, and the max stress were calculated for comparison.

Tearing tests were used to determine the toughness of the gels. Again, only the DMAAm and DN gels were tested, as the MHA gel lacked the necessary mechanical integrity to test. Briefly, samples were cut into rectangles of 25 mm length and 10 mm width. A razor blade was used to make a defect in the middle of the sample, but not all the way through it. The tear path length (TPL) was recorded by measuring the length between the non-defective end of the sample to the defect. A trouser tear test was performed on five batches of each network at a rate of 10 mm/min in the Test Resources tensile tester. The tearing energy was calculated according to Equation 2 [20], where t is the thickness, L_{path} is the TPL, and $\int_{x_1}^{x_n} F dx$ is the area under the force curve versus the position.

$$\text{Tearing Energy} = \frac{1}{(t * L_{\text{path}})} * \int_{x_1}^{x_n} F dx \quad (2)$$

2.3.5 Central Composite Design

To determine the effect of brittle network composition changes on the DN mechanical properties, a surface response experimental design known as a central composite design (CCD) was developed. A CCD design is capable of testing for the effects of multiple variables, their interactions, and also any nonlinear effects on the responses [21]. For this design, the MHA concentration and the crosslinking ratio, or the PEGDA:MHA molar ratio, was altered. The MHA concentration was changed over a range of 0.793 wt% to 2.207 wt%, while the PEGDA:MHA ratio was changed from 1.586:1 to 4.414:1. The experimental design space can be seen in *Figure 2.1*.

2.3.6 Statistical Analysis

A student's t-test was used to compare between the DMAAm and the DN gel for tensile and tearing tests. Analysis of variance (ANOVA) followed by Tukey post-hoc test was used for the swelling study comparison between the PDMAAm, MHA, and DN gels. For the CCD, ANOVA was used to determine significant effects via the Minitab statistical analysis software package. Surface plots and quadratic equations were also collected using the Minitab software.

2.4 Results and Discussion

2.4.1 Synthesizing the Double Network

Running tensile, tearing, and swelling experiments showed that PEGDA-crosslinked MHA-DMAAm gels behaved in a manner indicative of a DN structure. From the tensile testing, the modulus was found to increase by an order of magnitude between the PDMAAm single network (SN) and the DN while there was no significant loss of ductility, as shown in Table 2.1. The max

stress was also found to increase significantly when compared to the PDMAAm SN. When comparing the swelling data, the PDMAAm gel had a significantly higher maximum swelling (Q_{\max}) than the other two gels. No significant difference was found between the MHA network and the DN gel. This would indicate that the swelling of the DN was constrained or limited by the brittle MHA network.

The MHA network was found to be too fragile to test with the tensile or tearing protocols. In both instances, the MHA network samples lacked the structural integrity to be loaded into the testing machine.

The swelling data also provides some evidence of double network formation. As stated above, the maximum swelling ratio of the DN was similar to that of the MHA network, but had an initial rate of swelling similar to the PDMAAm gels. This behavior is better visualized in Figure 2.2. The swelling study shows that the DN has a behavior that is a combination of the two single networks. During the early stages of the swelling study, the absorption rate of the PDMAAm network limits the DN from swelling as fast as the MHA network. However, at longer times, the MHA network in the DN limits it from swelling to the same extent as the PDMAAm single network. It should be noted that Q for the MHA gel did decrease over time due to the gel swelling to rupture at later time points. It should also be noted that while this is the case, no statistical difference was found between the last time point and the timepoint where Q_{\max} occurs for these MHA gels.

This difference in water uptake could be explained by both the differences in crosslinking densities of the two single networks and a difference in the inherent hydrophilicity of the two materials. While the data collected in this study would suggest PDMAAm is the more hydrophilic of the two polymers, some literature would suggest that MHA is more hydrophilic.

Weeks et al. found that adding hyaluronic acid to DMAAm/methacryloxypropyltris (trimethylsiloxy) silane (TRIS) hydrogels ended up reducing the contact angle from around 80° to 60° [22]. Another study by Weeks et al. investigated the degree of methacrylation on the contact angle of MHA networks, and found that contact angle also decreased when the degree of methacrylation increased [23]. In this study, the group also found that adding the methacrylated HA to DMAAm/TRIS hydrogels again decreased the contact angle, but the degree of methacrylation had no additional effect. This suggests that the difference in swelling ability is more likely due to the difference in the crosslinking densities than the inherent hydrophilicity of the two materials.

The main difference between the MHA-PDMAAm gels developed in this work and those developed previously is the use of a separate crosslinker in the brittle MHA network. In the Weng et al. paper, as well as the two Okay papers, a crosslinker was not added to the MHA network [14], [16], [17]. The addition of PEGDA appears to have some effect on the strength of these gels, but not on the ductility. In the Tavsanlı and Okay paper from 2017, a series of 1 wt% MHA, 30 wt% DMAAm gels were subjected to tensile tests. Tavsanlı and Okay showed that with varying degrees of MHA methacrylation, the modulus of these gels stayed roughly a constant 35 kPa [17]. In comparison to the 1 wt% gels synthesized in the present study, it was found that the modulus for the highly crosslinked 1 wt% gel (1 wt% 4:1) had a higher modulus than that reported by Tavsanlı and Okay (92 kPa), and the lower crosslinked gel (1 wt% 2:1) had a smaller modulus (19 kPa). When looking at the elongation at break, the 1 wt% gels developed in this paper are comparable to the gels developed by Tavsanlı and Okay (281 % for 4:1, 270% for 2:1, and between 200 and 400%). The maximum stress increased for the 4:1 gel but decreased for the 2:1 gel (146 kPa for 4:1 and 30 kPa for 2:1, as compared to 60 to 120 kPa).

This implies that the low concentration of PEGDA used in this study provided no structural reinforcement.

2.4.2 Brittle Network Concentration and Crosslinking Affecting Mechanical Properties

The differences seen within this design space are interesting considering the relatively small range of values used for both concentration and crosslinking ratios. The importance of the brittle network composition is clearly evident when designing a DN gel. Other researchers interested in developing a DN for their intended application would do well to investigate the brittle network for an optimal composition.

Using the CCD, the response of several mechanical properties were observed while varying the concentration and the crosslinking ratio of the brittle network. As part of the experimental design, the MHA concentration and crosslinking ratio was systematically changed from 0.793 wt% to 2.207 wt% and 1.586:1 to 4.414:1, respectively. Over this compositional range, the Young's Modulus was found to vary by an order of magnitude (19.92 – 282.4 kPa). There is a similar range seen in the max stress (30.32 – 314.6 kPa) and in the tearing energy (6.164 – 102.1 J/m²). For elongation at break, the range of difference was less extreme (222 – 305 %). The swelling results show almost a quadruple difference over the range of compositions (4.58 – 16.9 g/g). A full table of data is provided in Appendix A.1.

In regards to mechanical properties, decreasing the MHA wt% and [PEGDA]/[MHA] led to a decrease in modulus, max stress, and tearing energy while also an increase in the elongation at break and Q_{\max} . When looking at the surface plots generated from the CCD, there is similarity in the overall shape of response curves between the modulus and the max stress (Figure 2.3.a and Figure 2.3.c, respectively). The main difference is the slight curvature that can be seen in the modulus surface plot. This can be explained from the ANOVA results, which found that

interactions between MHA wt% and [PEGDA]/[MHA] significantly affected the modulus response. ANOVA results can be found in Appendix A.2.

To explain the modulus (E) results, we define the modulus as described from rubber elasticity theory, shown below in Equation 3:

$$E = 3nRT \quad (3)$$

Where R and T are the gas constant and temperature, respectively, and n is the number of active chain units per unit volume. This term is related to the density of the polymer, as well as the molecular weight between crosslinks (M_c) [24]. Based off the definition, M_c is affected by the concentration of the polymer and the crosslinking ratio. A compounding effect occurs with increases in both variables, effectively reducing M_c and causing an increase in n and subsequently E.

From the elongation at break plot (Figure 2.3.b), the parabolic relationship suggests a local maximum at mid-level crosslinking ratios. It is interesting to note this shape, as the ANOVA results showed that the MHA wt% was the only significant variable that affected the response. The parabolic relationship can be explained by the additional crosslinks giving the sample more strength and allows the sample to be stretched farther before stress is imparted to the ductile network. If too many crosslinks are added, then the sample becomes too brittle, and the sample fails at a lower strain as stress is imparted to the ductile network. This indicates that the most ductile DN composition can be achieved without sacrificing strength altogether and highlights the importance of synergistic effects between the brittle and ductile network.

As discussed previously, the max stress has a surface plot with very little curvature (Figure 2.3.c). This lack of curvature is also reflected in the ANOVA data, which shows that the MHA

wt% and [PEGDA]/[MHA] ratio affected the response, but not the interactions or nonlinear factors. The shape of the response curve is similar to that of the modulus. Interactions affecting the modulus but not the max stress can be explained from a thermodynamic perspective. The max stress, from a thermodynamic stance, can be defined as the force necessary to break the bonds present in the system normalized to the area. This force necessary to break the bonds can be related back to the enthalpy needed to break the bonds (ΔH_{bonds}). Specifically, for this example, ΔH_{bonds} would be the summation of the weakest bond energies (i.e. the bonds that break during tensile testing) present in the system. Since this is a summation, both crosslinking and concentration would have an effect on the max stress, but the two would not have a compounding effect.

The tearing energy appears to have minima at high MHA wt%, low crosslinking, and low MHA wt% and high crosslinking (Figure 2.3.d). To explain this behavior, we use the model for fracture energy (G) as shown in Equation 4 [13]:

$$G = G_0 + \sigma_c \varepsilon_c h \quad (4)$$

Here, G_0 is the intrinsic fracture energy, σ_c is the yielding stress, ε_c is the strain where the necking finishes, and h is the length of the softened zone around the crack. Of these variables, the one that is theoretically higher in the low-concentration, low-crosslinking gel is h , since the material has less brittle network to keep the size of the softened zone low. Relating h to the intrinsic fracture energy of the material (G_0) as well as the characteristic elastic energy density (W), as seen in Equation 5 [25], we can further explain this behavior.

$$h \cong \frac{G_0}{W} \quad (5)$$

It is important to note the inverse relation between h and W . For low-concentration, low-crosslinking brittle network gels, the density of the elastic energy must be lower when compared to a more concentrated, crosslinked network, as there is not enough brittle network available to absorb the mechanical energy being applied to the system. At our low-concentration, low-crosslinking gel composition, the W must be small enough that the h value is actually raised past that of either the low-concentration, high-crosslinking gel or the high-concentration, low-crosslinking gel. And because the size of the softened zone is larger, this also means that the critical length that the sample must be pulled is also larger [13]. Due to this critical length increase, the sample must be pulled to a higher length in order to fully propagate the crack, which in turn increases the area under the curve for the force versus position graphs. This type of behavior can be seen in Appendix A.3. This type of relationship is discussed in more detail in the Yu et al. paper which shows a direct correlation between h and G [25].

From the ANOVA results, the MHA wt%, [PEGDA]/[MHA], and the interactions between these two variables significantly affected the tearing energy. These results can be explained by discussing the size of the damage zone (h in Equations 4 and 5). As described in other works, when a double network is stretched or torn, a region around the crack tip becomes soft due to the defect [13], [25], [26]. As discussed, h can be related to G_0 , which can be defined as the energy required to break polymer chains along the crack plane during a tearing test [27]. This energy is in turn related to the energy required to rupture polymer chains in the gel and the number of chains per unit area [28]. Both concentration and crosslinking affect the number of chains per unit area and the energy requirement to rupture, causing a compounding increase on G_0 , and therefore the tearing energy.

As expected, increases in MHA wt% causes a decrease in the Q_{\max} (Figure 2.3.e). An interesting note, however, is the slight convex structure that occurs with increasing $[\text{PEGDA}]/[\text{MHA}]$ at low MHA wt%. A possible explanation for this behavior would be based off of Flory and Rehner theory; specifically the entropy change caused by the reduction in the numbers of possible chain conformation on swelling (entropy change due to elongation) versus the entropy of mixing the polymer and the solvent [24]. PEGDA can be used as a polymer for hydrogels^(25–27), and has been used in the development of double networks^(28–30). Of important note for this discussion, Mazzoccoli used PEGDA blends in order to crosslink and make mechanically robust tissue engineering scaffolds [35]. It is therefore reasonable to suggest that long chains of PEGDA may be produced during the synthesis process, linking MHA chains farther away from one another than the length of a single PEGDA unit of 575 Da molecular weight. This would explain the convex behavior seen in the response plot. Initially, adding more PEGDA to the system causes the entropy change due to elongation to increase, because the crosslinking bonds are reducing the amount of conformational changes overall, inhibiting swelling. However, as even more PEGDA is added, the PEGDA chains become longer. Because the long chains allow for more conformation changes overall, the entropy change due to elongation is reduced, allowing the gel to swell further.

ANOVA results for the Q_{\max} data showed that not only were MHA wt% and $[\text{PEGDA}]/[\text{MHA}]$ significantly affecting the results, but so too was the nonlinear effects of MHA wt% (Appendix A.2). The concentration and crosslinking ratio affecting the response is explained simply using the Flory-Rehner theory, and again thinking about the entropy change due to elongation. This could also explain the compounding concentration factor; as the concentration of the brittle network increases, these long polymer strands (the HA used had an average molecular weight of

950 kDa) take up more space in the fixed volume. Due to this, the polymer strands do not have the same amount of free volume available to make conformation changes, so the entropy change due to elongation increases.

The experiments that were run in this investigation highlight the importance of the first network composition in DN synthesis. For example, while only a relatively small range was used for the compositional space, there was considerable variation in the mechanical responses. Another important finding was the local maxima regarding the elongation at break that was at mid-level crosslinking ratios. From a materials design perspective, this shows that ductility does not have to be sacrificed entirely for strength. Lastly, the interactions of both the crosslinking and weight percent of the brittle network affect the modulus and tearing energy of the DN. Again, this is important from a materials design perspective, because the interplay should be considered in the creation of other DN gels.

2.4.3 Model Equations

Model equations were developed from the CCD to predict the mechanical behavior of the DN gel based on the brittle network composition. The model equations take into account linear and nonlinear effects of the two variables, as well as the interaction effects. The general equation, as well as the value of the coefficients for each response, can be seen in Table 2.2. It should be noted that these model equations are based off the surface response plots that were discussed in the previous section.

Two compositions were synthesized to test for the accuracy of these equations. These compositions (1.75 wt% 2.5:1, and 1.25 wt% 3:1) existed within the design space while also not being used for the development of the CCD. The 2 wt% 4:1 and 1 wt% 2:1 gels used in the CCD were also tested. The same testing was conducted for the new compositions, and these results

were compared to those generated using the model equations. For all tests, there was agreement between the theoretical and experimental results for the 2 wt% 4:1 and 1 wt% 2:1 gels as seen in Figure 2.4. For the two new compositions, there was good fit between the theoretical and experimental values for modulus, tearing energy, and Q_{\max} . For elongation at break, there was a significant difference between the values predicted and collected for the 1.75 wt% 2.5:1 gel. The max stress equation was also found to significantly overestimate the response for the 1.75 wt% 2.5:1 and 1.25 wt% 3:1 compositions.

The overestimation of the max stress equation could be due to the variability of max stresses that were collected. By reviewing the max stress data (Appendix A.1), there are several points within the CCD design that have large variation in max stress. Nonetheless, the modulus, tearing energy, and maximum swelling equations all show strong predictive power of a composition's behavior. This highlights the benefits of using a CCD design, which is that model equations can be used to find optimized compositions over the compositional range used during experimentation.

2.5 Conclusions

A double network composed of PEGDA-crosslinked MHA and PDMAAm was synthesized for the purpose of determining the effects of brittle network composition on the mechanical properties of the DN gel. A central composite experimental design was used to systematically alter weight percent and crosslinking ratio of the brittle network and mechanical tests were conducted to determine the strength, ductility, toughness, and swelling properties of the gels. Using ANOVA, it was found that the modulus and tearing energy were both affected by the interactions of the concentration and crosslinking ratio of the brittle network. An important design aspect to consider is that elongation at break has a local maxima at middling crosslinking

ratios of 3:1, meaning that materials can be designed where ductility does not need to be sacrificed for strength or toughness. Model equations were also developed, and the modulus, tearing energy, and maximum swelling equations were found to accurately predict behavior. Future work would involve running another design of experiments looking at the interplay between brittle network and ductile network composition variables.

2.6 Schemes, Figures, and Tables

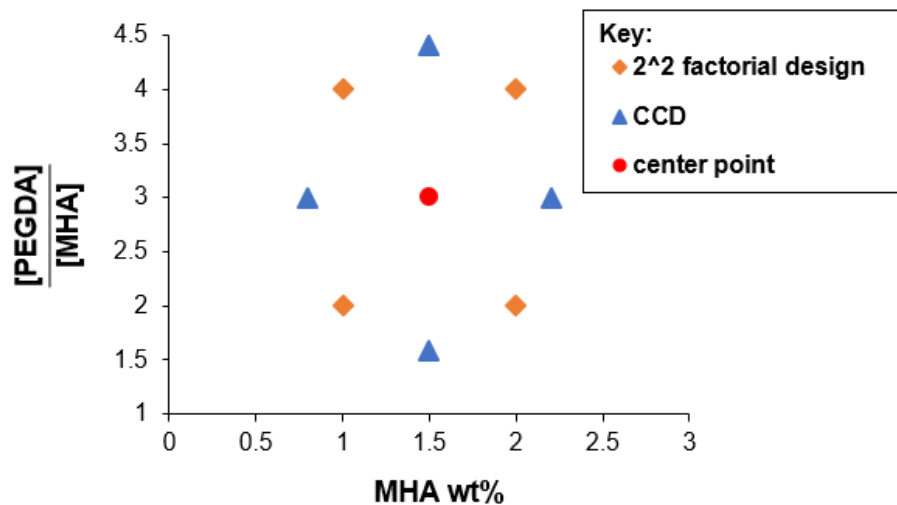


Figure 2.1 The CCD data points used during experiments. The 2^2 factorial design compositions are denoted by the orange points and the blue denotes the CCD compositions, while the red is the centerpoint.

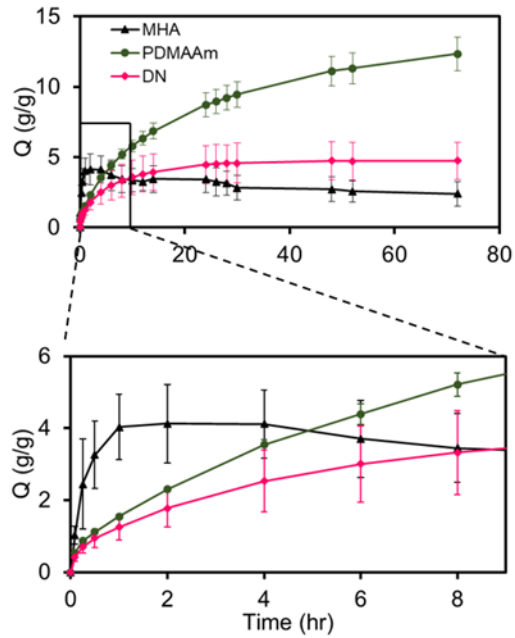


Figure 2.2 Swelling study of individual polymer networks and the double network. Here, “ Q ” stands for the swelling ratio. Error bars are standard deviation. It is interesting to note that the DN has a slow swelling rate comparable to that of a PDMAAm gel for the first few time points but reaches a maximum comparable to that of the MHA gel.

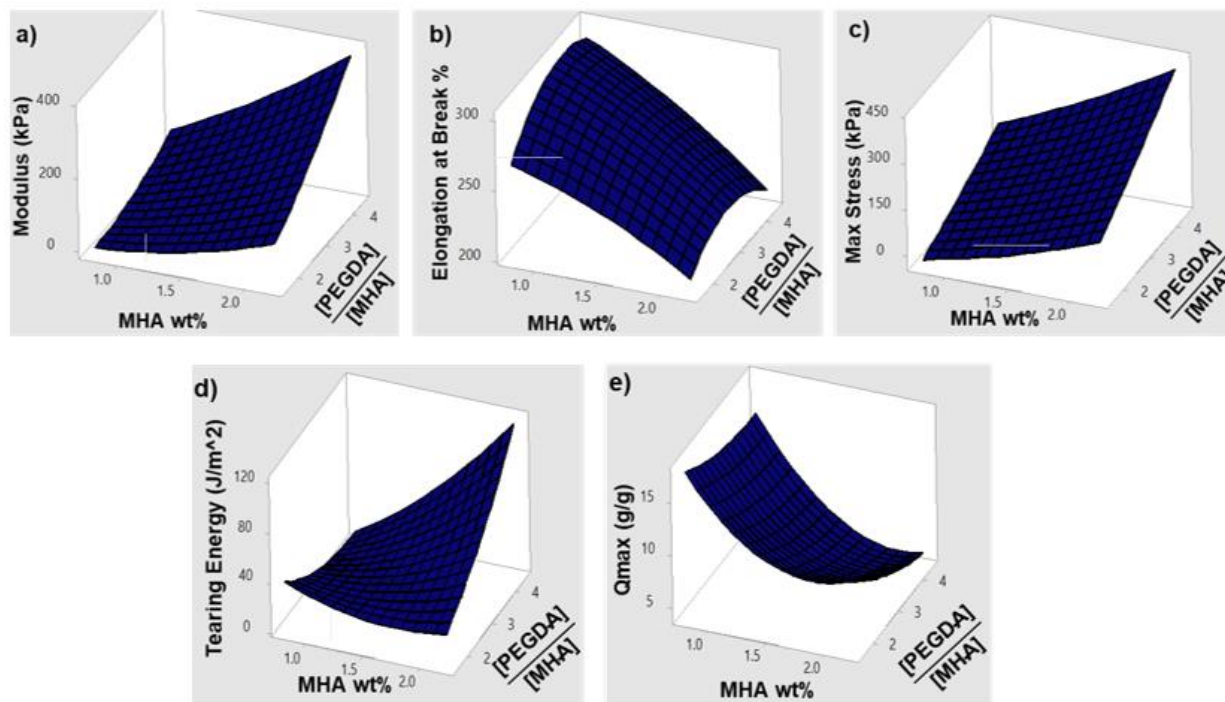


Figure 2.3 Surface plots that show the a) modulus, b) elongation at break, c) max stress, d) tearing energy, and e) Q_{\max} response to changes in brittle network composition of an MHA-PDMAAm DN gel. Of the five properties, modulus and tearing energy were dependent on the interactions between the weight percent and crosslinking ratio of the brittle MHA network.

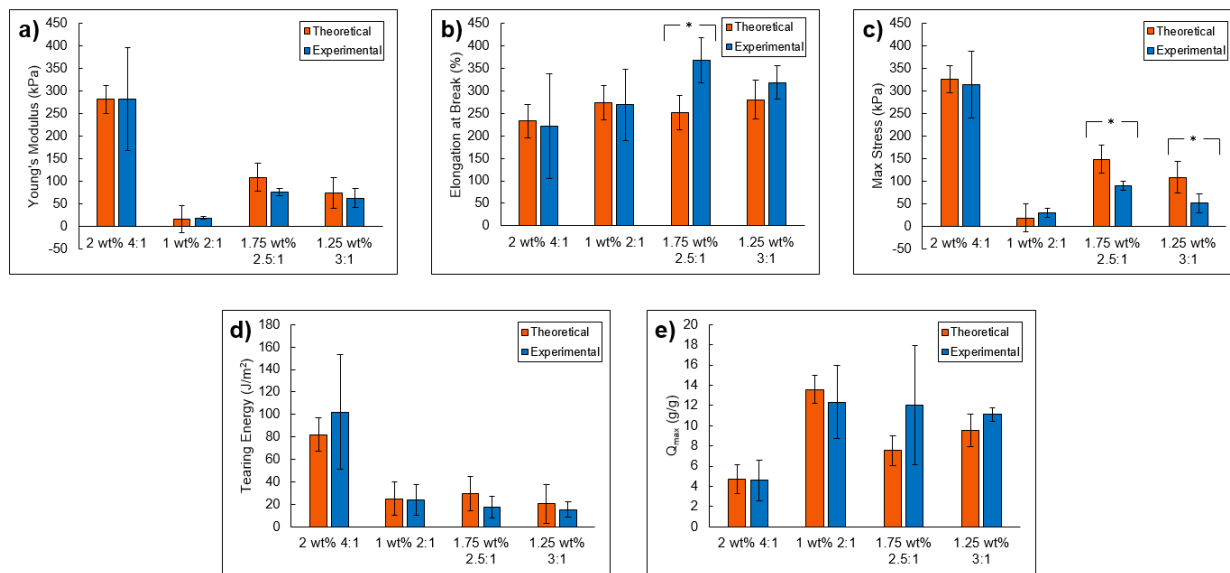


Figure 2.4 Comparison of the response predicted from the model equations (“Theoretical”) versus those obtained by direct testing (“Experimental”) for modulus (a), elongation at break (b), max stress (c), tearing energy (d), and Q_{\max} (e). Error bars are 95% confidence intervals. * - significant difference between the theoretical and experimental values.

Table 2.1 A comparison of the mechanical properties between the single networks (SN's) and the DN (\pm standard deviation). MHA networks were too fragile to test using either the tensile or tearing procedure. * - Statistically different using Student's t-test with $p < 0.01$. ** - Statistically different from the other two points using Tukey post-hoc with $p < 0.01$.

Property	MHA	PDMAAm	DN
Young's Modulus (kPa)	N/A	18.5 (\pm 2.6)	282 (\pm 92)*
Elongation at Break (%)	N/A	281 (\pm 75)	222 (\pm 94)
Max Stress (kPa)	N/A	24.4 (\pm 4.4)	315 (\pm 59)*
Tearing Energy (J/m^2)	N/A	-0.87 (\pm 5.7)	102 (\pm 41)*
Q_{\max}	4.12 (\pm 1.09)	12.34 (\pm 1.19)**	4.74 (\pm 1.34)

Table 2.2 The general CCD equation used to model response behavior and the specific coefficient values for each response. These equations are based off the surface response plots as shown in Figure 2.3.

Response	Coefficients for the Equation: $Response = a + b * MHA \text{ wt}\% + c * \frac{[PEGDA]}{[MHA]} + d * (MHA \text{ wt}\%)^2 + e * \left(\frac{[PEGDA]}{[MHA]}\right)^2 + f * MHA \text{ wt}\% * \frac{[PEGDA]}{[MHA]}$					
	a	b	c	d	e	f
Modulus (kPa)	88	-112	-63.8	35.6	8.9	48.5
Elongation at Break (%)	188	7	70.9	-12.4	-9.3	-6.8
Max Stress (kPa)	-85	-15	8.4	28.4	3.5	29.8
Tearing Energy (J/m ²)	172.5	-119.5	-65.1	19.6	4.65	32.01
Q _{max} (g/g)	34.77	-23.17	-2.08	6.84	0.369	-1.087

2.7 References

- [1] J. P. Gong, Y. Katsuyama, T. Kurokawa, and Y. Osada, “Double-Network Hydrogels with Extremely High Mechanical Strength,” *Adv. Mater.*, vol. 15, no. 14, pp. 1155–1158, 2003.
- [2] L. Alfheid, W. D. Seddon, N. H. Williams, and M. Geoghegan, “Double-network hydrogels improve pH-switchable adhesion,” *Soft Matter*, vol. 12, pp. 5022–5028, 2016.
- [3] C. H. Yang *et al.*, “Strengthening alginate/polyacrylamide hydrogels using various multivalent cations,” *ACS Appl. Mater. Interfaces*, vol. 5, no. 21, pp. 10418–10422, 2013.
- [4] P. Chen *et al.*, “Double network self-healing graphene hydrogel by two step method for anticancer drug delivery,” *Mater. Technol.*, vol. 29, no. 4, pp. 210–213, 2014.
- [5] K. Yasuda *et al.*, “A novel double-network hydrogel induces spontaneous articular cartilage regeneration in vivo in a large osteochondral defect,” *Macromol. Biosci.*, vol. 9, no. 4, pp. 307–316, 2009.
- [6] T. Nonoyama *et al.*, “Double-Network Hydrogels Strongly Bondable to Bones by Spontaneous Osteogenesis Penetration,” *Adv. Mater.*, vol. 28, no. 31, pp. 6740–6745, 2016.
- [7] L. Cai, R. E. Dewi, and S. C. Heilshorn, “Injectable hydrogels with in situ double network formation enhance retention of transplanted stem cells,” *Adv. Funct. Mater.*, vol. 25, no. 9, pp. 1344–1351, 2015.
- [8] A. Pourjavadi, E. Tavakoli, A. Motamedi, and H. Salimi, “Facile synthesis of extremely biocompatible double-network hydrogels based on chitosan and poly(vinyl alcohol) with enhanced mechanical properties,” *J. Appl. Polym. Sci.*, vol. 135, no. 7, pp. 1–8, 2018.
- [9] S. Pacelli *et al.*, “Design of a tunable nanocomposite double network hydrogel based on gellan gum for drug delivery applications,” *Eur. Polym. J.*, vol. 104, no. April, pp. 184–193, 2018.
- [10] Y. Zhang, Q. Chen, J. Ge, and Z. Liu, “Controlled display of enzyme activity with a stretchable hydrogel,” *Chem. Commun.*, vol. 49, no. 84, pp. 9815–9817, 2013.
- [11] S. Liang, Q. M. Yu, H. Yin, Z. L. Wu, T. Kurokawa, and J. P. Gong, “Ultrathin tough double network hydrogels showing adjustable muscle-like isometric force generation triggered by solvent,” *Chem. Commun.*, no. 48, pp. 7518–7520, 2009.
- [12] J. Wang and Y. Han, “Tuning the stop bands of inverse opal hydrogels with double network structure by controlling the solvent and pH,” *J. Colloid Interface Sci.*, vol. 353, no. 2, pp. 498–505, 2011.
- [13] J. P. Gong, “Why are double network hydrogels so tough?,” *Soft Matter*, vol. 6, no. 12, pp. 2583–2590, 2010.
- [14] L. Weng, A. Gouldstone, Y. Wu, and W. Chen, “Mechanically strong double network photocrosslinked hydrogels from N,N-dimethylacrylamide and glycidyl methacrylated hyaluronan,” *Biomaterials*, vol. 29, no. 14, pp. 2153–2163, 2008.

- [15] H. Tsukeshiba *et al.*, “Effect of polymer entanglement on the toughening of double network hydrogels,” *J. Phys. Chem. B*, vol. 109, no. 34, pp. 16304–16309, 2005.
- [16] B. Tavsanlı, V. Can, and O. Okay, “Mechanically strong triple network hydrogels based on hyaluronan and poly(N,N-dimethylacrylamide),” *Soft Matter*, vol. 11, no. 43, pp. 8517–8524, 2015.
- [17] B. Tavsanlı and O. Okay, “Mechanically strong hyaluronic acid hydrogels with an interpenetrating network structure,” *Eur. Polym. J.*, vol. 94, no. May, pp. 185–195, 2017.
- [18] J. Murai *et al.*, “Tough double network elastomers reinforced by the amorphous cellulose network,” *Polymer (Guildf.)*, vol. 178, no. July, p. 121686, 2019.
- [19] P. S. Varde, “Crosslinked Hyaluronic Acid Hydrogel Networks Designed as Mechanical Actuators,” Syracuse University, 2015.
- [20] D. R. King *et al.*, “Extremely tough composites from fabric reinforced polyampholyte hydrogels,” *Mater. Horizons*, vol. 2, no. 6, pp. 584–591, 2015.
- [21] D. C. Montgomery, G. C. Runger, and N. F. Hubele, *Engineering Statistics*, 5th ed. Hoboken: John Wiley & Sons, 2010.
- [22] A. Weeks, D. Luensmann, A. Boone, L. Jones, and H. Sheardown, “Hyaluronic acid as an internal wetting agent in model DMAA/TRIS contact lenses,” *J. Biomater. Appl.*, vol. 27, no. 4, pp. 423–432, 2012.
- [23] A. Weeks, D. Morrison, J. G. Alauzun, M. A. Brook, L. Jones, and H. Sheardown, “Photocrosslinkable hyaluronic acid as an internal wetting agent in model conventional and silicone hydrogel contact lenses,” *J. Biomed. Mater. Res. - Part A*, vol. 100 A, no. 8, pp. 1972–1982, 2012.
- [24] L. H. Sperling, *Introduction to Physical Polymer Science*, 4th ed. Hoboken: John Wiley & Sons, 2006.
- [25] Q. M. Yu, Y. Tanaka, H. Furukawa, T. Kurokawa, and J. P. Gong, “Direct observation of damage zone around crack tips in double-network gels,” *Macromolecules*, vol. 42, no. 12, pp. 3852–3855, 2009.
- [26] Y. Tanaka, “A local damage model for anomalous high toughness of double-network gels,” *EPL*, vol. 78, no. 5, 2007.
- [27] X. Zhao, “Multi-scale multi-mechanism design of tough hydrogels: Building dissipation into stretchy networks,” *Soft Matter*, vol. 10, no. 5, pp. 672–687, 2014.
- [28] G. J. Lake and A. G. Thomas, “The strength of highly elastic materials,” *Proc. R. Soc. London. Ser. A. Math. Phys. Sci.*, vol. 300, no. 1460, pp. 108–119, 1967.
- [29] M. B. Browning, S. N. Cereceres, P. T. Luong, and E. M. Cosgriff-Hernandez, “Determination of the in vivo degradation mechanism of PEGDA hydrogels,” *J. Biomed. Mater. Res. - Part A*, vol. 102, no. 12, pp. 4244–4251, 2014.
- [30] T. Eshel-Green, S. Eliyahu, S. Avidan-Shlomovich, and H. Bianco-Peled, “PEGDA hydrogels as a replacement for animal tissues in mucoadhesion testing,” *Int. J. Pharm.*,

- vol. 506, no. 1–2, pp. 25–34, 2016.
- [31] A. Cavallo, M. Madaghiele, U. Masullo, M. G. Lionetto, and A. Sannino, “Photo-crosslinked poly(ethylene glycol) diacrylate (PEGDA) hydrogels from low molecular weight prepolymer: Swelling and permeation studies,” *J. Appl. Polym. Sci.*, vol. 134, no. 2, pp. 1–9, 2017.
- [32] G. C. Ingavle, A. W. Frei, S. H. Gehrke, and M. S. Detamore, “Incorporation of Aggrecan in Interpenetrating Network Hydrogels to Improve Cellular Performance for Cartilage Tissue Engineering,” *Tissue Eng. Part A*, vol. 19, no. 11–12, pp. 1349–1359, 2013.
- [33] G. C. Ingavle, S. H. Gehrke, and M. S. Detamore, “The bioactivity of agarose-PEGDA interpenetrating network hydrogels with covalently immobilized RGD peptides and physically entrapped aggrecan,” *Biomaterials*, vol. 35, no. 11, pp. 3558–3570, 2014.
- [34] X. Yin *et al.*, “Macroporous Double-Network Hydrogel for High-Efficiency Solar Steam Generation under 1 sun Illumination,” *ACS Appl. Mater. Interfaces*, vol. 10, no. 13, pp. 10998–11007, 2018.
- [35] J. P. Mazzoccoli, D. L. Feke, H. Baskaran, and P. N. Pintauro, “Mechanical and Cell Viability Properties of Crosslinked Low and High MW PEGDA blends,” *J. Biomed. Mater. Res. A*, vol. 93, no. 2, pp. 558–566, 2010.

Chapter 3 Developing a Double Network for High-Resolution 3D Printing Using Optical Projection Lithography¹

3.1 Synopsis

Double-network (DN) hydrogels, with their unique combination of mechanical strength and toughness, have emerged as promising materials for soft robotics and tissue engineering. In the past decade, significant effort has been devoted to synthesizing DN hydrogels with high stretchability and toughness; however, shaping the DN hydrogels into complex and often necessary user-defined two-dimensional (2D) and three-dimensional (3D) geometries remains a fabrication challenge. In this project, a collaboration project was formed between myself and Dr. Puskal Kunwar to create a new fabrication method based on optical projection lithography to print DN hydrogels into customizable 2D and 3D structures within minutes. The focus of my work for this project was on developing a DN synthesis method that would work within this optical projection lithography setup, and then determine the mechanical properties of the printed gels. The DN was synthesized by first photo-crosslinking a single network structure via spatially modulated light patterns followed by immersing the printed structure in a calcium bath to induce ionic cross-linking. It was found that the strain and elastic modulus of printed structures can be tuned based on the hydrogel composition, cross-linker and photoinitiator concentrations, and laser light intensity.

3.2 Introduction

Hydrogel materials, characterized by their high degree of water content, have been extensively used in areas such as drug delivery and pharmaceuticals, diagnostics and biosensors, soft

¹ This chapter is adapted from Kunwar et al.'s publication in *ACS Applied Materials & Interfaces* [47].

robotics, flexible electronics, tissue engineering, and organ-on-a-chip models [1]–[3]. However, most hydrogels are mechanically weak and possess poor toughness and low elastic moduli that have limited their usage in applications that require superior mechanical properties, such as tissue engineering and soft robotics [4]–[6]. To expand the utility of hydrogels for applications that requires a combination of stretchability and toughness, double network (DN) hydrogels, or DN gel, were developed [7]–[10]. DN gel typically consists of two networks: the first network possesses covalently cross-linked polymer chains that allow for the dissipation of large amount of energy during deformation, whereas the second network is soft and often ionically cross-linked, providing superior toughness and stretchability [7], [10]–[13].

Over the years, a variety of DN gel with unique mechanical properties have been synthesized [14]–[20]. For instance, DN gel formed by using ionically cross-linked alginate and covalently cross-linked polyacrylamide (PAAm) have been shown to exhibit remarkable fracture toughness of 9000 J/m^2 [10]. In another study, alginate was replaced by polyvinyl alcohol (PVA) to enable the formation of crystallites upon heating within the intertwined network of PVA/PAAm DN gel [21], [22].

Furthermore, Cai et al. have reported the fabrication of porous DN gel with high toughness and stretchability using the freeze-drying method [23]. Thermoreversible polysaccharide agar/PAAm DN gel with excellent recoverability have also been demonstrated [24]. Chen, et al. have developed biocompatible polyethylene glycol (PEG)/agarose DN gel with excellent mechanical strength [13]. In another study, cell-encapsulated DN network hydrogel fiber that showed tunable mechanical strength, and stretching behavior was synthesized using alginate and poly(N-isopropylacrylamide)/PEG [25]. There are few reports of one-pot synthesis of DN gel such as synthesis of highly mechanical and recoverable agar/PAAm (agar/PAM) DN hydrogels [26]–

[28]. Most current studies choose conventional molding or casting methods to shape DN gel into simple geometries. For instance, clover, snowflakes, and the letters “ICCAA” have been molded using PEG/agarose hydrogel [8]. In another study, DN gel structures in the geometry of a meniscus have been casted using an acrylamide/PAMPS network [29]. Although DN gel with simple geometries such as sheets, slabs, blocks, discs, and dumbbells have been made, DN gel with user-defined and often complex two-dimensional (2D) or three-dimensional (3D) structures will be necessary for a variety of applications in tissue engineering and soft robotics.

To address the need of creating customized 2D and 3D geometries for a range of application of DN gel, 3D printing methods based on extrusion-based fused deposition modeling have been widely used. Complex shapes, such as human ears and noses, have been fabricated using stretchable alginate/PEG DN gel [8], [9], [29]–[33]. 3D printers have also been used to extrude DN gel made from a κ -carrageenan network and PAAm to make structures that can self-heal [31]. Extrusion printing assisted by a heated cartridge was used to print DN structures of PAAm mixed with agar and alginate [34]. However, extrusion-based methods for printing DN gel have low resolution (300–500 μm) and are limited in throughput due to the serial nature of fabrication [8], [9]. To print DN gel at high resolution and at high speeds, light-based 3D printing methods such as stereolithography, digital light processing lithography, and direct laser writing can be transformative as they allow fabrication of structures with high resolution and improved design flexibility, in a highly automated, assembly-free manner [35]–[45]. However, printing DN gel using light-based methods currently, in general, requires an extremely long cross-linking time (several hours), making these methods impractical [10].

In this work, we demonstrate quick and high-resolution printing of user-defined 2D and 3D structures made of DN gel using optical projection lithography. The polymer solution, composed

of sodium alginate, dimethyl acrylamide (DMAAm), methylenebis-acrylamide (MBAAm), and lithium phenyl-2,4,6-trimethylbenzoylphosphinate (LAP), was polymerized by projecting digital patterns of ultraviolet light, followed by immersion of printed structures into calcium chloride solution to undergo ionic polymerization. The quick lithography process (within minutes) and high-resolution printing of DN gel enables customized 3D structures that exhibit high toughness and stretchability. To our knowledge, this is the first report demonstrating fabrication of DN gel into complex 2D and 3D geometries within minutes, and we anticipate that this work will open new avenues in the areas of soft robotics and tissue engineering.

3.3 Experimental

3.3.1 Materials

2,4,6-trimethylbenzoyl chloride was purchased from Fisher Scientific[®]. All other materials were purchased from Sigma-Aldrich[®].

3.3.2 LAP Synthesis

LAP was synthesized using an established method as described below [45]. Briefly, 2,4,6-trimethylbenzoyl chloride (4.5 g, 25 mmol) was added dropwise to continuously stirred dimethyl phenylphosphonite (4.2 g, 25 mmol) at room temperature and under argon gas. This solution was stirred for 24 h before adding an excess of lithium bromide (2.4 g, 28 mmol) in 50 mL of 2-butanone to the reaction mixture at 50 °C, to obtain a solid precipitate after 10 min. The mixture was then cooled to room temperature, allowed to rest overnight and then filtered. The filtrate was washed with 2-butanone (3 × 25 mL) to remove unreacted lithium bromide and dried under vacuum to give LAP (6.2 g, 22 mmol, 88% yield) as a white solid. All chemicals were used as received and were of analytical grade.

3.3.3 Fabrication of the DN Structure

Hydrogel prepolymer solution was synthesized by mixing the DMAAm, alginate, MBAAm, and LAP in aqueous solution (Scheme 3.1). The hydrogel prepolymer solution consisted of DMAAm (22 wt %), alginate (2.4 wt%), MBAAm (0.07 wt % or 0.2 mol MBAAm/mol DMAAm), and LAP (0.33 wt %). To create the gel, the solution was placed in a custom-built, digital mask-based optical lithography setup (Scheme 3.2). Briefly, a 400 nm laser beam modulated by a digital micromirror device (DMD) selectively photocrosslinks the prepolymer solution in a continuous fashion. Postfabrication, the gel structures were dipped into a calcium chloride solution for 72 h to enable the formation of ionic bonds between guluronic acid units in alginate [10]. To make intricate 3D structures, a 3D model of any user-defined structures was drawn using AutoCAD and sliced horizontally to create a stack of binary portable network graphics (png) image files using a custom-written MATLAB code. The png files were uploaded to the DMD, which allowed for the structure to be fabricated via the laser.

3.3.4 Mechanical Testing

All mechanical tests were performed in air at room temperature. After allowing the samples to sit in the ionic bath, rectangular samples were cut into dog bones using a cutter dye with a gauge length of 6.25 mm and gauge width of 1.50 mm. Samples were placed into a tensile tester with a 25 N load cell and stretched at a rate of 9.375 mm/min until failure. For tearing tests, samples were cut into rectangles of 25 mm length and 10 mm width. A razor blade was used to then cut the samples nominally at the center, along the length of the rectangular sample. The tear path length (TPL) was measured as the distance from the end-tear, to the uncut end of the sample. A trouser tear test was performed at a rate of 10 mm/min. The tearing energy was calculated using

Equation 1, where t is the thickness, L_{path} is the TPL, and $\int_{x_1}^{x_n} F dx$ is the area under the force curve versus the position [46].

$$Tearing\ Energy = \frac{1}{(t * L_{path})} * \int_{x_1}^{x_n} F dx \quad (1)$$

3.3.5 Microscopic Imaging

The fabricated structures were imaged and characterized using a digital optical microscope (HIROX, KH-8700). An MX(G)-2016(z) objective lens was used to image the fabricated structures, which provided a resolution of 1.16 μm .

3.3.6 Statistical Analysis

Statistical analysis was performed using analysis of variance (ANOVA) with three independent samples for each test. Post hoc t-tests with Bonferroni correction were also performed between two groups to determine significant differences.

3.4 Results and Discussion

3.4.1 Fabrication and Characterization of the DN Structures

First, we printed a planar slab structure using a single exposure of light pattern and characterized its mechanical properties (Figure 3.1). A rectangular shaped patterned fs laser beam of wavelength 400 nm with a laser intensity of 5 mW/cm² was exposed for 5 s to print planar rectangular shaped structures. During this process of fabrication, the UV exposure induced cross-linking of acrylamide by covalent bonding; at this stage, the alginate within the acrylamide network does not form a network. When UV-crosslinked structures are subsequently immersed into the 100 mM calcium chloride solution, ionic cross-linking of alginate occurs. Alginate

chains consist of mannuronic acid (M unit) and guluronic acid (G unit), and the introduction of the divalent cations results in cross-linking of G units in different alginate chains forming an ionic network [10].

For optimal soak times in the calcium bath, we studied the swelling behavior of the structures after submerging them to the calcium solution (Appendix B.1) These structures swelled to 208% of its original dimension during the first 24 h of immersion and further swelled to 248% at the end of 96 h. As a result, all mechanical property characterizations, such as stress–strain relationships, tearing resistance, and tensile properties such as elastic modulus, strain, and maximum stress, were performed 72 h post-immersion to ensure repeatability and minimal influence of swelling on the tests.

The stress–strain plots for the DN gel structure and structures printed using its individual parent gel (acrylamide-only and alginate-only) show that the DN gel structure stretched more than four times its original length without rupture (Figure 3.1.a and inset). The acrylamide gel structure was softer and more stretchable compared to the DN gel structure; however, the alginate structures were more tough and less stretchable than that of the DN gel structure.

Tensile parameters (elastic modulus, ultimate strain, ultimate stress) of the structures printed using DN gel, alginate-only gel and acrylamide-only gel are plotted (Figure 3.1 parts b through d). The modulus of elasticity was 124 ± 17 kPa for alginate structure, 49 ± 4.3 kPa for the DN gel structure, and 5.3 ± 0.15 kPa for DMAAm structure. It required stress of 65 ± 4 kPa to stretch the DN gel structure by 4.10 ± 0.5 times of its original length. The stress and associated strain for the acrylamide gel structure was 6.6 ± 0.5 kPa and 6.25 ± 0.44 . For the case of the alginate gel, the ultimate strain was 1.54 ± 0.23 , with a corresponding ultimate stress of 118 ± 22 kPa. The elastic modulus of the DN gel structure is close to the average of the elastic moduli of the

DMAAm and alginate gel (Figure 3.1). A similar trend is also observed in the ultimate stress and ultimate strain of the fabricated structures. Essentially, these results show that the DN gel structure acquires its stretching properties from the acrylamide gel and stiffness properties from the alginate gel.

Furthermore, tearing tests were performed to characterize the tear resistance of the printed structure (Figure 3.1.e). In the case of the DN gel structure, the position moved by the upper clamp was 26 mm, whereas for case of the alginate sample the clamp moved 24 mm, and for acrylamide the clamp only moved 5 mm. The tearing energy was 92 J/m² for the DN hydrogel structure, 0.4 J/m² for the acrylamide-only structure, and 98 J/m² for the alginate-only structure. This study suggests that the tearing resistance for the DN gel structure is similar to that of the alginate sample and higher compared to that of the acrylamide structure.

3.4.2 Effect of Light Dose on the Tensile Properties of DN Gel Structures

To investigate the effect of light dose on the tensile properties of DN gel structures, we varied the exposure time from 3 to 10 s while keeping a constant light intensity of 5 mW/cm² (Figure 3.1.f). For the sample exposed less than 3 s, no cross-linking was detected; therefore, we used exposure times of 3, 5, 8, and 10 s. Samples exposed to 3 s were partially cross-linked, and the structures were partially formed. However, 5 s exposure was able to completely cross-link the structure. The strain was highest for the structure which is exposed for 5 s. The structures fabricated with exposure times of 8 and 10 s were considered overexposed, as they exhibit less stretchability and break with lower ultimate stress as compared to the sample exposed to 5 s.

3.4.3 Effect of Composition of Alginate/acrylamide on the Tensile Properties of DN Gel Structures

In this set of experiments, the laser intensity and exposure time were kept constant at 5 mW/cm² and 5 s, respectively. Samples were prepared using a constant amount of DMAAm (22 wt %), and the amount of alginate was varied (1.2, 2.4 and 4.8 wt %) to change the acrylamide/alginate ratio of the printed samples. The amount of the cross-linker and photoinitiator was fixed to 0.07 and 0.33 wt %, respectively. A stress–strain curve with representative samples was plotted as shown in Figure 3.2.a.

An increase in the concentration of the alginate was found to increase the modulus of elasticity and maximum stress, while the stretchability of the structure decreases (Figure 3.3 parts b through d). The elastic modulus of the structure decreases from 148.5 ± 12.5 to 12 ± 1.88 kPa, when the concentration of alginate was decreased from 4.8 to 1.2 wt %. The strain was 3.7 ± 0.38 for the structure with alginate concentration of 4.8 wt %. There was a small increase in ultimate strain when the alginate concentration was lowered to 2.4 wt % and the highest ultimate strain of 4.76 ± 0.30 was obtained with the alginate concentration of 1.2 wt %. Ultimate stress follows the decreasing trend seen with the elastic modulus. The stress decreases from the 159.3 ± 14.5 to 21.33 ± 1.5 kPa when the alginate concentration is decreased from 4.8 to 1.2 wt %.

3.4.4 Effect of Cross-linker Amount on the Tensile Properties of DN Gel Structures

Tensile properties of the DN gel structures were studied by varying the MBAAm cross-linker concentration (0.035, 0.07, and 0.14 wt %) while keeping the amounts of the acrylamide, alginate, and photoinitiator constant at 22, 2.4, and 0.33 wt % respectively. Structures were printed using a laser power of 5 mW/cm² and an exposure time of 5 s. The fabricated structures were loaded into the tensile tester, and the stress strain curve was recorded as shown in Figure

3.3.a. Results show that the elastic modulus of the structure is highest (51.31 ± 1.75 kPa) for the structure printed with MBAAm concentration of 0.07 wt %, and the modulus decreases when the concentration of MBAAm increases to 0.14 or decreases to 0.035 wt % (Figure 3.3.b). Similarly, the ultimate strain is also highest (3.85 ± 0.55) for the structure printed with the MBAAm concentration of 0.07 wt % (Figure 3.3.c). The strain is decreased to 1.9 ± 0.06 and 2.65 ± 0.26 , when the MBAAm concentration is 0.14 and 0.035 wt %, respectively. A similar trend is also shown in the ultimate stress as seen in Figure 3.3.d). The stress is highest (65 ± 4 kPa) for the DN gel structures fabricated with MBAAm concentration 0.07 wt % compared to that of the structures printed with the MBAAm concentration of 0.14 and 0.035 wt %.

3.4.5 Effect of Composition of Photoinitiator on the Tensile Properties of DN Gel Structures

DN gel slab samples were prepared with three concentrations of LAP photoinitiator (0.165, 0.33, and 0.66 wt %). The amount of the acrylamide, alginate and cross-linker was fixed to 22, 2.4, and 0.07 wt %, respectively. Structures were printed using a DMD based fabrication with the laser power of 200 mW (laser intensity of 5 mW/cm²) and exposure time of 5 s. The concentration of the LAP also strongly affects the stretchability and stiffness of the DN gel structures Figure 3.4. The highest elastic modulus of 60.91 ± 2.91 kPa is obtained for the structure fabricated with the LAP concentration of 0.66 wt %. This figure also shows that the modulus remains at the similar level for the LAP concentrations of 0.33 and 0.16 wt %.

However, the ultimate strain of 3.89 ± 0.51 is obtained for the structure printed with the LAP concentration of 0.33 wt % and is highest among the structures printed with the three different concentrations of the LAP photoinitiator as shown in Figure 3.4.c. Similarly, the ultimate stress is 65 ± 4 kPa, which is obtained for the structures fabricated using a DN gel with a LAP of 0.33 wt % (Figure 3.4.d).

Results showed that the optimized prepolymer composition of DMAAm (22 wt %), alginate (2.4 wt %), MBAAm (0.07 wt %), LAP (0.33 wt %), and laser parameters (laser intensity of 5 mW/cm², exposure time of 5 s) can result in mechanically robust yet stretchable structures.

3.4.6 Printing and Characterization of 3D DN Gel

Optimized prepolymer composition and printing conditions were used to demonstrate the ability to print complex 3D structures using DN gel. In the case of the 3D fabrication, an UV absorber quinoline yellow (QY) dye was used to limit the light scattering and penetration of depth of the light. We observed that the QY dye washed away when the sample was dipped into the calcium solution. First, the stress–strain curve was obtained by fabricating the DN gel rectangular slab structures with varying the laser intensity of 0.65 mW/cm² (laser power of 40 mW), 1 mW/cm² (laser power of 60 mW), 1.35 mW/cm² (laser power of 80 mW), and 1.65 mW/cm² (laser power of 100 mW) at a constant fabricating speed of 0.02 mm/s. Sample tensile test results are shown in Figure 3.5.a. The elastic modulus does not vary significantly for the fabricated structures with different laser intensities (Figure 3.5.b). It is also evident from the figure that the ultimate stress is 35 kPa for the structure fabricated with a laser intensity of 0.6 mW/cm² and the stress increases to highest (66 kPa) for the laser intensity 1 mW/cm²; however, further increase in laser intensity leads to decrease in the stress. The structure printed with a laser intensity of 1 mW/cm² stretches almost 480% of its original length, and the ultimate strain is decreased for the structure printed with laser intensity lower and higher than 1 mW/cm².

Further, the effect of the fabrication (scanning) speed on the tensile properties of the DN gel structure was also studied. To perform a test, DN gel structures were printed by a constant laser intensity of 1.65 mW/cm² and varying scanning speed of 0.045–0.09 mm/s. The exposure laser dose for fabrication speed of more than 0.075 mm/s was not able to fully cross-link the DMAAm

hydrogel. These printed structures were stretched to obtain a stress–strain curve as shown in Figure 3.5.c. Increasing the fabrication speed from 0.045 to 0.06 mm/s, the ultimate strain increases from 150 to 290% and decreases when the printing speed is increased to 0.075 mm/s and above (Appendix B.2). The trend is also consistent with the result obtained in stress–strain curve obtained from structure with different laser powers and stress–strain curves obtained from the 2D structure printed with different exposure time.

3.4.7 Fabrication of User-Defined 2D/3D Structure of DN Hydrogel

Next, we demonstrate the printing of user-defined 2D DN gel structures using an “auxetic” shape design. A cartoon of auxetic shape with re-entrant cell structure before and after stretching is shown in Figure 3.6.a1. The auxetic structure was printed as shown in Figure 3.6.a2 using the DN gel with the laser intensity of 5 mW/cm² and exposure time of 5 s. This structure did not lose its breadth when stretched to 200% of its original length (Figure 3.6.a3). Next, we also fabricated the 2D structure of DN hydrogel by writing “Syracuse University” using a laser intensity of 5 mW/cm² and exposure time of 5 s. The results of which are shown in Figure 3.6.b.

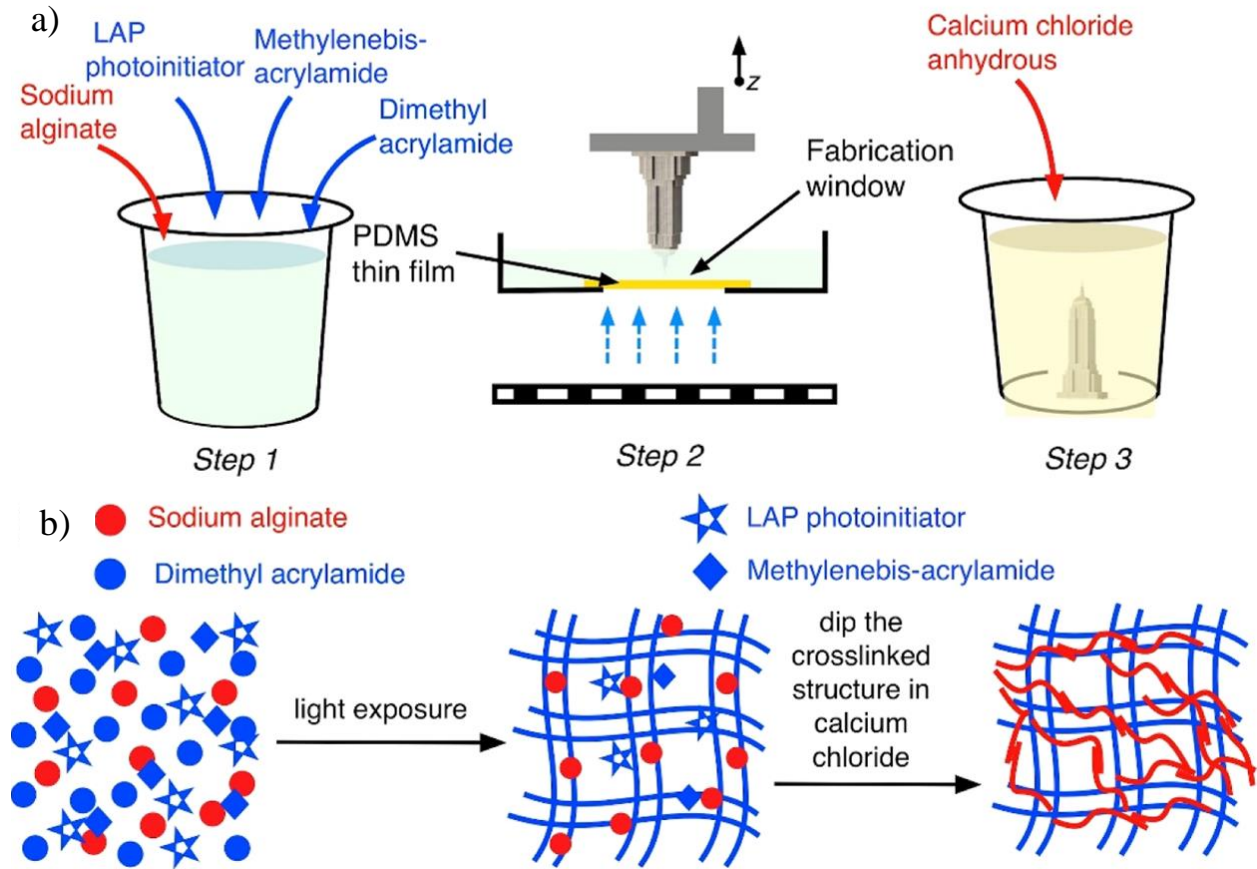
We further tested the smallest feature size of DN gel structures fabricated using our optical lithography system as shown in Figure 3.6.c. The smallest feature size of the printed structure is mostly influenced by the size of a mirror in DMD (~12 μm) and the material properties of DN gel. In this experiment, we designed masks of intersecting lines and the linewidth of the lines were varied to 3, 5, and 10 pixels, with a laser intensity of 5 mW/cm² and exposure time of 5 s. No observable crosslinking was observed in the case of 3 pixels’ line. Only partial cross-linking was observed for 5 pixels’ line, and the partially cross-linked structures were easily destroyed during the subsequent washing steps. The smallest linewidth of printed stable line of the DN gel was 120 μm using a mask of 10 pixels lines.

Further, 3D printing of the DN hydrogel structures is demonstrated (Figure 3.6 parts d and e). This is done by printing the Empire State Building printed using digital mask-based optical lithography. Post-printing, the structure is dipped into the calcium chloride solution for 72 h as shown in Figure 3.6.d. In order to fabricate the structure, a laser power of 60 mW (=laser intensity of 1 mW/cm²) and stage speed of 0.02 mm/s was used. Mayan pyramid printing is also demonstrated using DN gel hydrogel, and the structure was printed using the laser power of 1 mW/cm² and scanning speed of 0.02 mm/s (Figure 3.6.e).

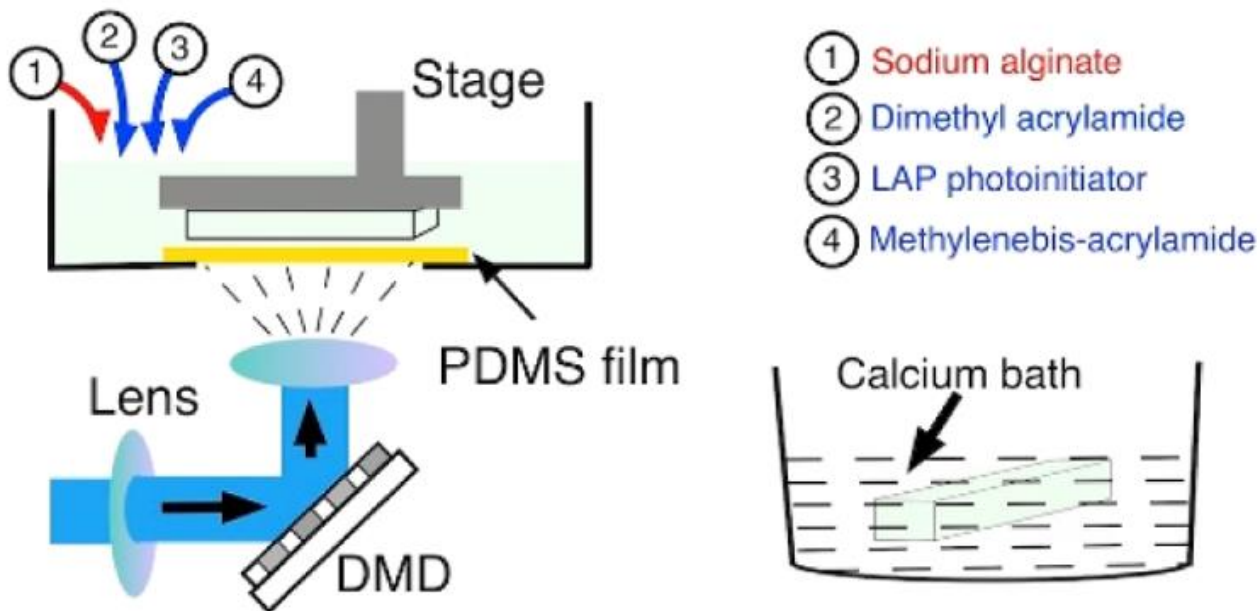
3.5 Conclusions

In summary, we have demonstrated that an alginate, poly(dimethylacrylamide) gel can be used in a 3D additive printing method of synthesis using optical projection lithography. Material testing found that increasing the crosslinker concentration from 0.07 to 0.14 wt% results in weaker gels overall. When the photoinitiator concentration was increased from 0.16 to 0.33 wt%, a similar trend occurred for the ultimate stress and strain. At a laser power of 60 mW, materials had the highest ultimate stress and strains, but the lowest moduli. The power level with the highest moduli was either 40 or 100 mW. This new method can be extended to other material compositions with broad implications in the areas of soft robotics and tissue engineering.

3.6 Schemes, Figures, and Tables



Scheme 3.1 a) Schematic showing the 3D fabrication of DN hydrogel structure using digital mask-based optical lithography setup. b) Schematic of the alginate/DMAAm DN hydrogel formed by covalent cross-linking of DMAAm and ionic cross-linking of alginate.



Scheme 3.2 Schematic cartoon showing a simplification of the lithography setup. A laser is shined to a digital micromirror device (DMD), which allows for precise polymerization and crosslinking of the photoinitiated gel. Ionic crosslinking is conducted after the lithography by submerging the gel in a calcium bath.

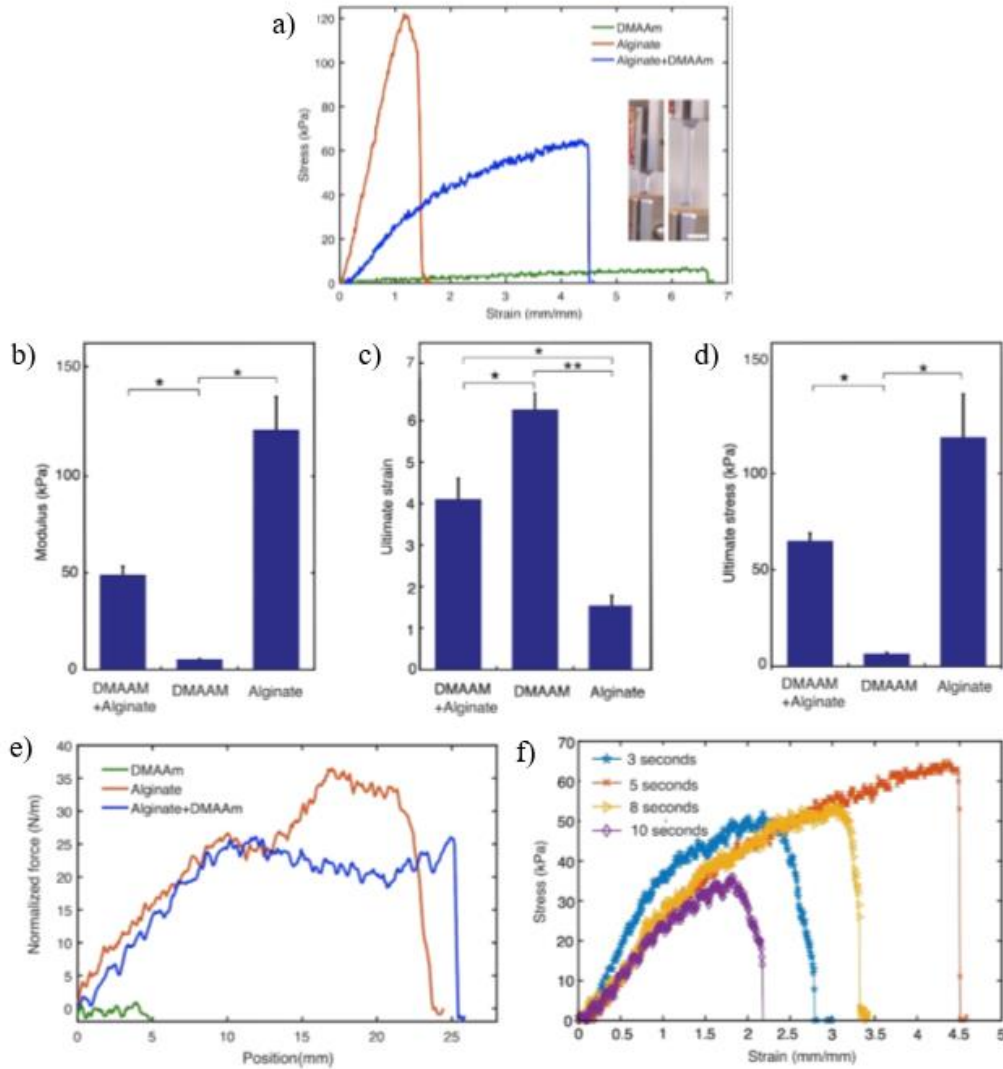


Figure 3.1. Initial tests to show double network formation. a) Plot showing the tensile stress–strain curve obtained from DN gel structure and its individual parent gel structures. The inset shows a dogbone-shaped structure being stretched more than 4 times its original length. The structure was printed with the laser intensity of 5 mW/cm^2 and exposure time of 5 s. Bar diagrams showing elastic modulus (b), ultimate strain (c), and ultimate stress (d) for the DN gel structures, alginate gel structures, and DMAAM gel structures with LAP as an photoinitiator and MBAAM as a cross-linker. ANOVA test showed significant difference among the groups (p value < 0.001). ANOVA with Bonferroni correction showed significant differences between two groups at $*p < 0.016$, $**p < 0.001$. [Error bars: mean \pm standard deviation (SD)]. e) Plot showing the tearing test for the DN gel representative structures and the individual parent gel structure. f) Plots showing the stress–strain curve obtained from the DN gel structures exposed to different exposure times.

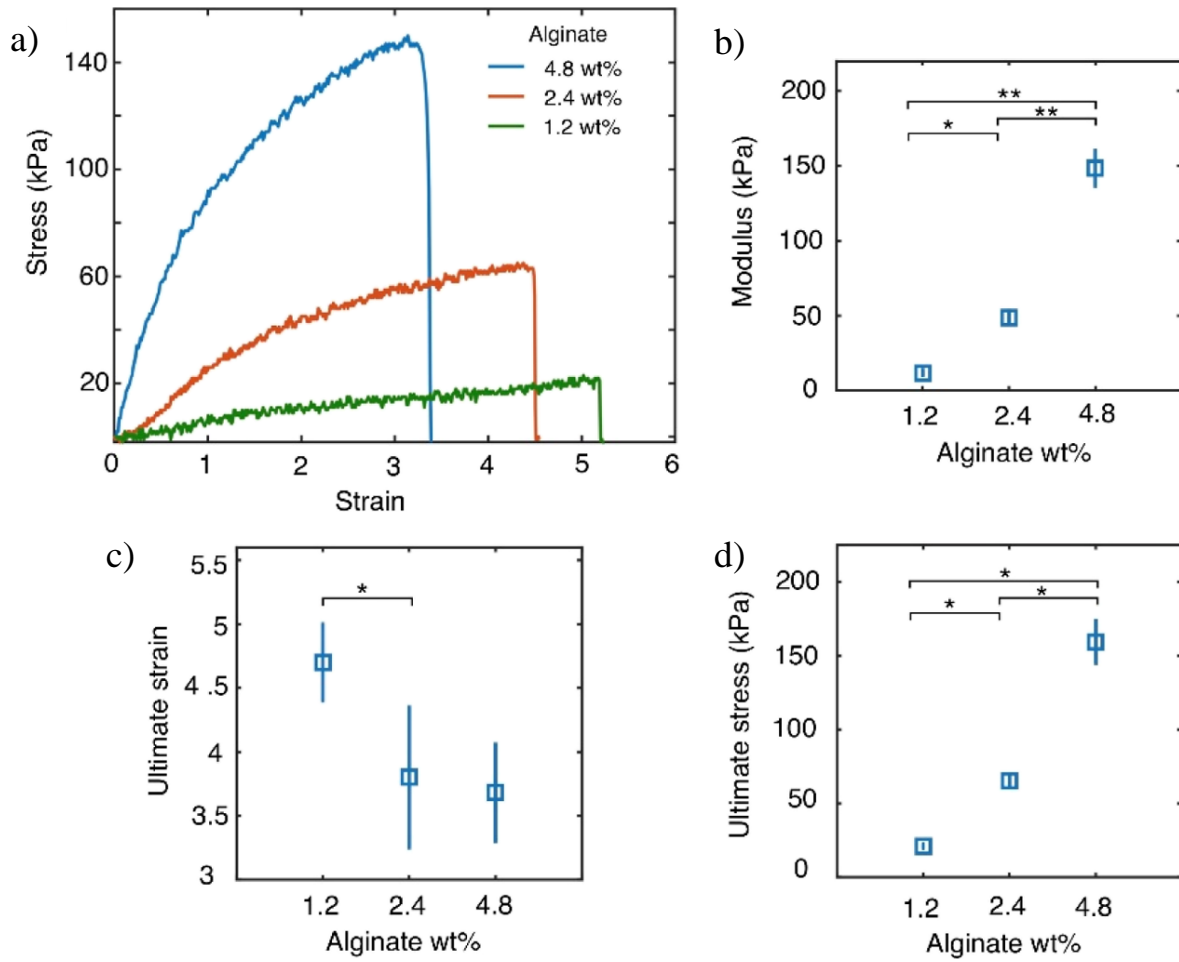


Figure 3.2 Results of the alginate composition experiments. a) Sample tensile tests results from each of the DN compositions. The elastic moduli (b), ultimate strain (c), and the ultimate stress (d) was collected and compared. * $p < 0.016$, ** $p < 0.001$. (Error bars: mean \pm SD).

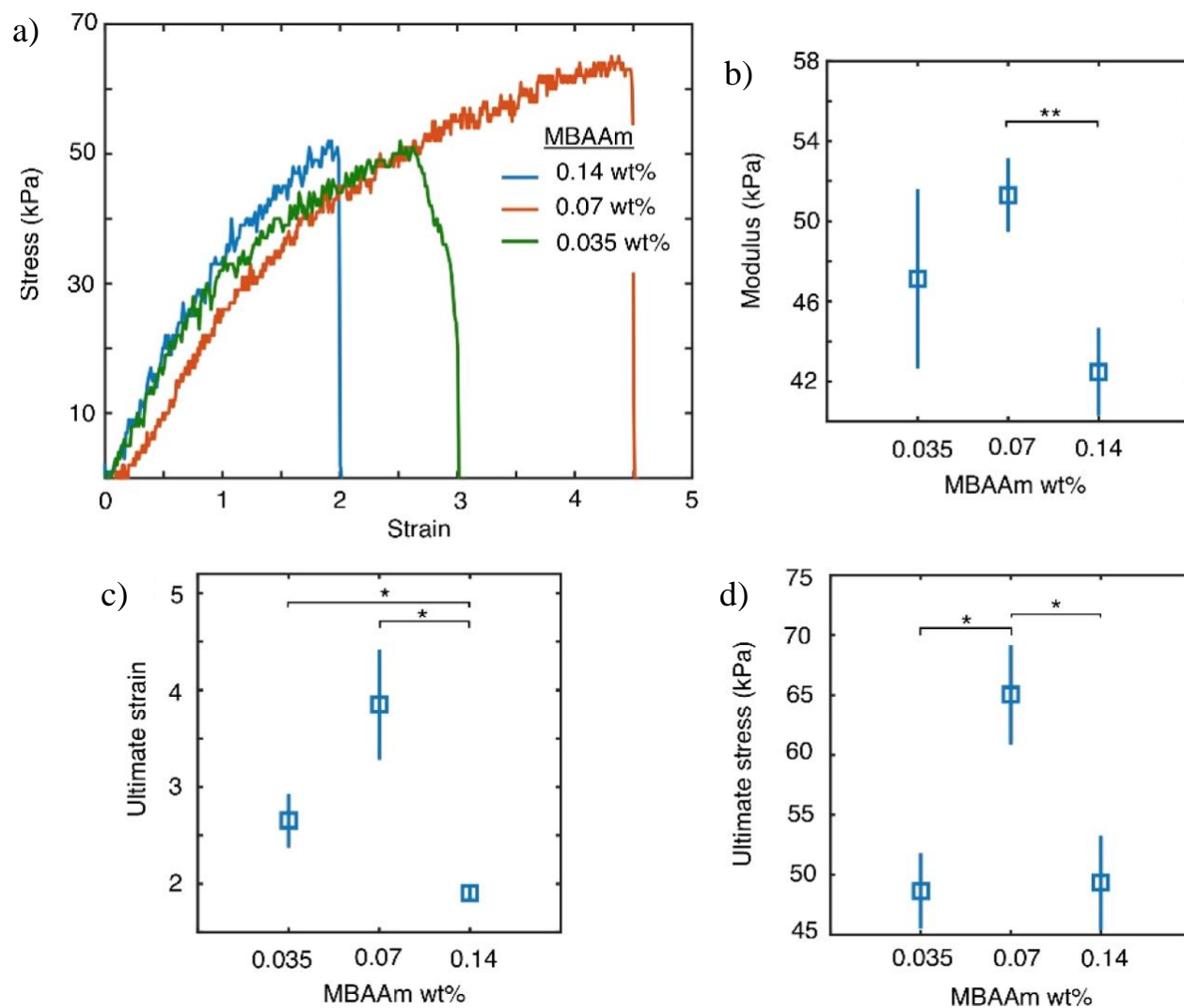


Figure 3.3 Results of the crosslinker concentration experiments. a) Sample stress–strain results of the DN gels with the varying amounts of crosslinkers (0.035, 0.07, and 0.14 wt %). The elastic moduli (b), ultimate strain (c), and the ultimate stress (d) was collected and compared. * $p < 0.016$, ** $p < 0.001$. (Error bars: mean \pm SD)

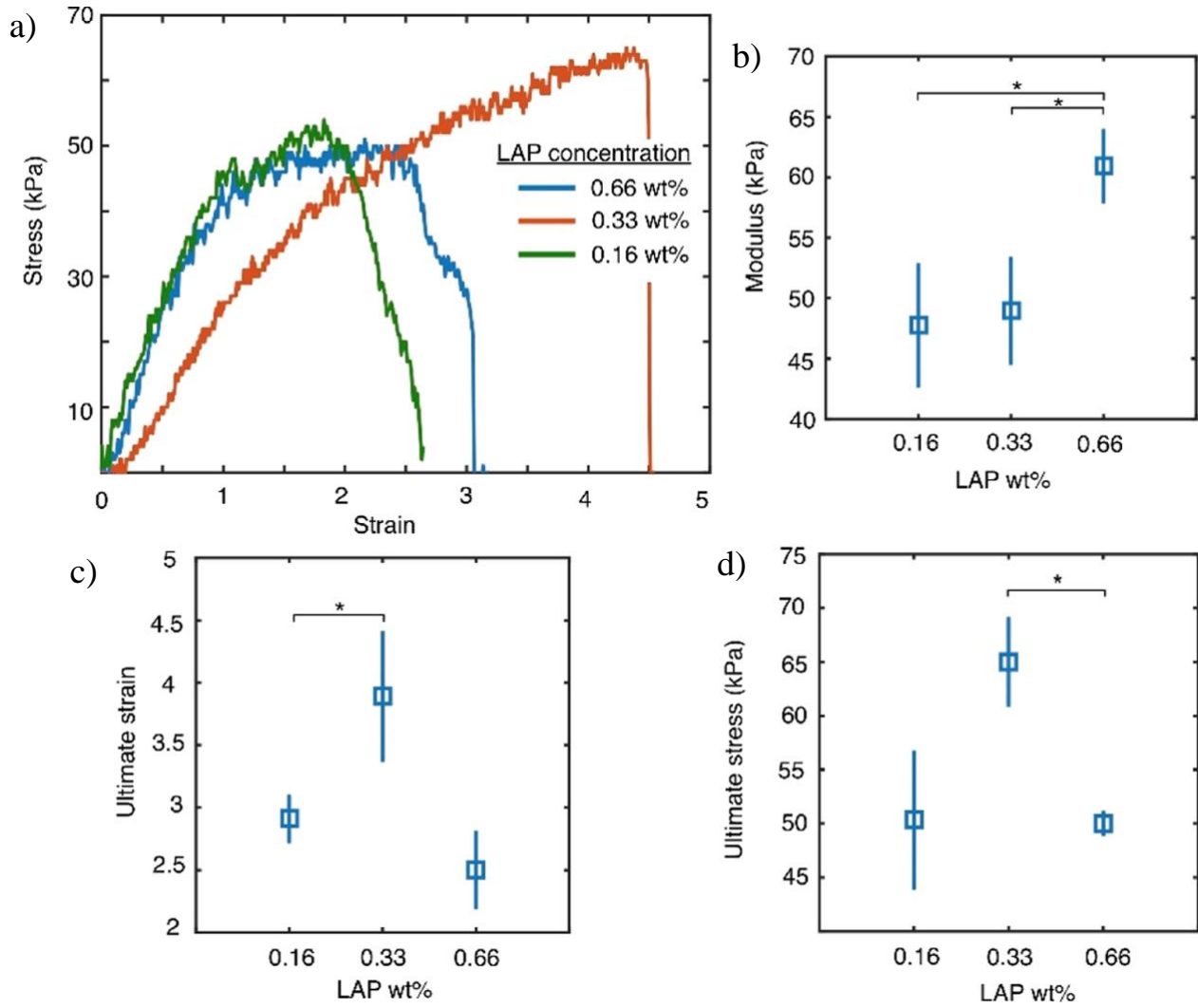


Figure 3.4 The results of the photoinitiator composition experiment. a) Sample stress–strain results of the DN gels with the varying amounts LAP photoinitiator (0.165, 0.33 and 0.66 wt %). The elastic moduli (b), ultimate strain (c), and the ultimate stress (d) was collected and compared. * $p < 0.016$. (Error bars: mean \pm SD)

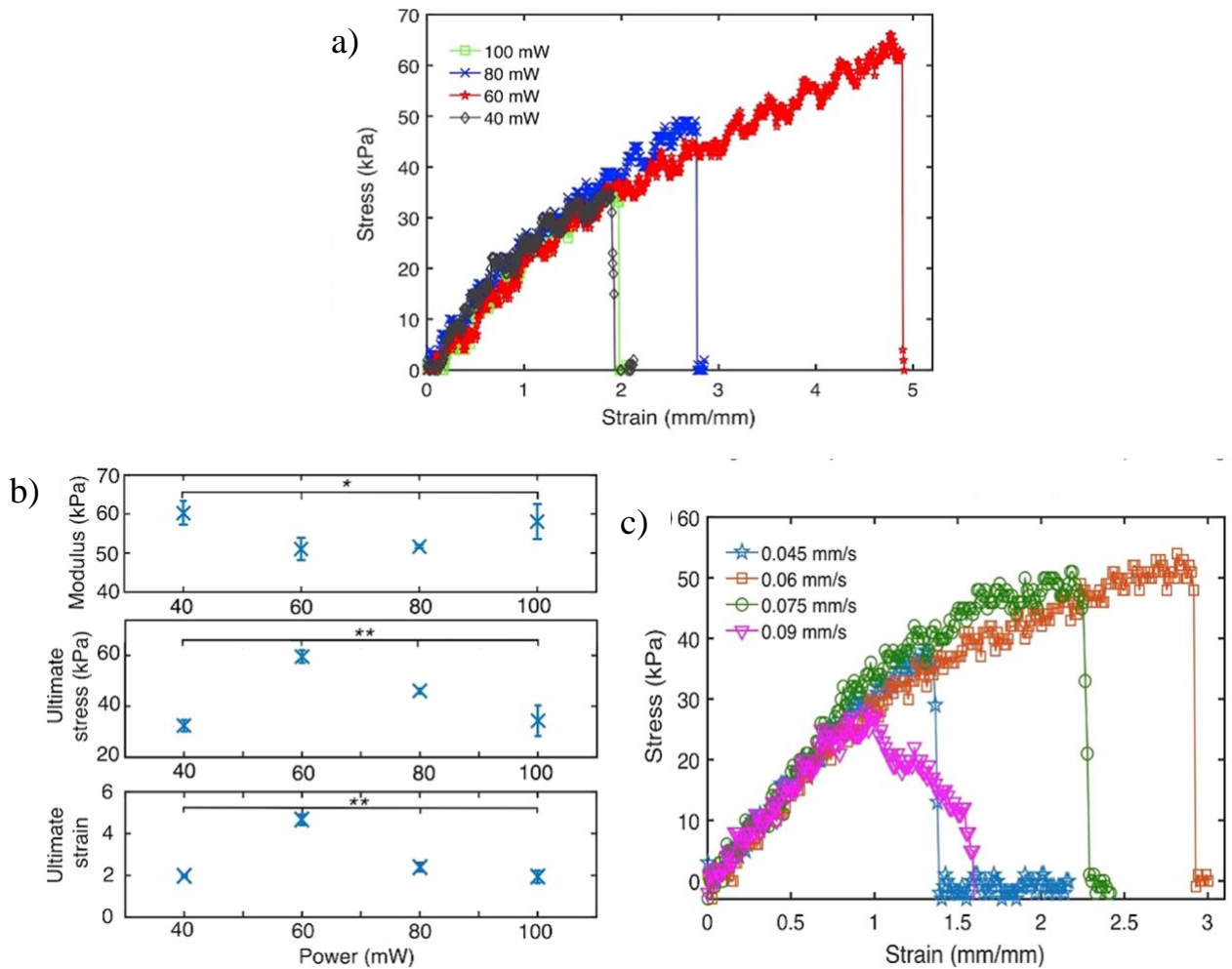


Figure 3.5 Results of experiments in which the laser power and the fabrication speed were varied. a) Sample stress-strain curves for DN gel structure printed at fixed fabrication speed and varying laser power. b) Scatter plot showing modulus of elasticity, ultimate stress, and ultimate strain of the DN gel structure fabricated with different laser intensity and constant fabrication speed. c) Stress-strain curve for DN gel structure printed at varying fabrication speed and fixed laser power. *p value < 0.05, **p value < 0.001. (Error bars: mean \pm SD)

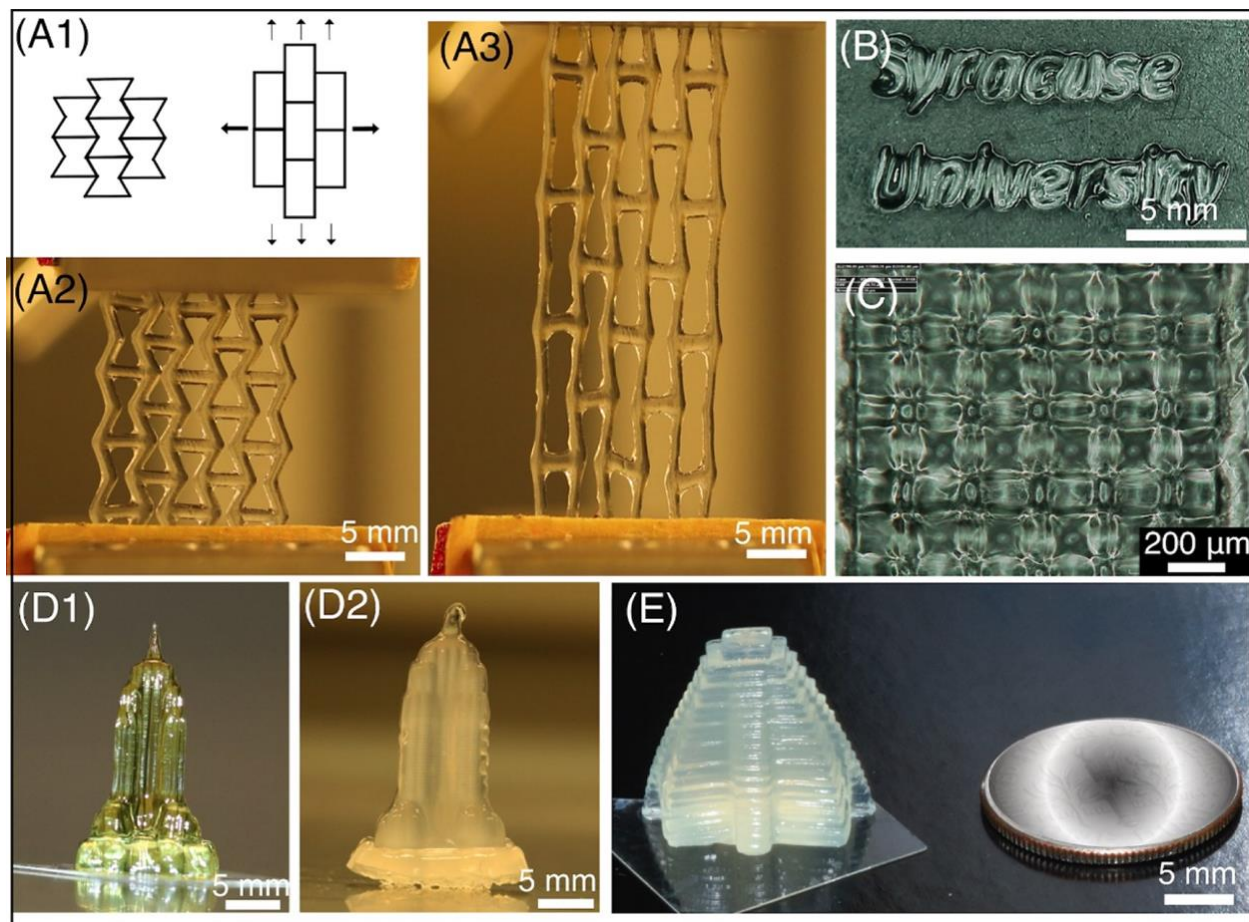


Figure 3.6 Illustration cartoon of 2D structure (auxetic shaped). (A2) Fabricated DN gel structure before stretching and (A3) after stretching. Structure was printed using optical projection lithography and dipped into calcium solution for 72 h. (B) 2D printed “Syracuse University” before dipping into calcium solution. (C) Log-pile structure demonstrating the smallest feature size/resolution of 120 μm . (D,E) 3D printing of tough and stretchable hydrogel. (D1,D2) Empire State Building structure before and after dipping into the calcium solution. (E) Mayan pyramid structure printed using DN gel structure and image was recorded after the structures are dipped into calcium solution for 72 h. The fabricated images shown in A,D,E were acquired using a digital SLR camera and B,C are recorded using a HIROX microscope.

3.7 References

- [1] Y. S. Zhang and A. Khademhosseini, “Advances in Engineering Hydrogels,” *Science*, vol. 356, no. 6337, pp. 1–27, 2017.
- [2] J. Kopeček, “Hydrogel biomaterials: A smart future?,” *Biomaterials*, vol. 28, no. 34, pp. 5185–5192, 2007.
- [3] J. Elisseeff, “Structure Starts to Gel,” *Nat. Mater.*, vol. 7, pp. 271–274, 2008.
- [4] I. M. El-Sherbiny and M. H. Yacoub, “Hydrogel scaffolds for tissue engineering: Progress and challenges,” *Glob. Cardiol. Sci. Pract.*, vol. 2013, no. 3, p. 38, 2013.
- [5] Y. He, F. Yang, H. Zhao, Q. Gao, B. Xia, and J. Fu, “Research on the printability of hydrogels in 3D bioprinting,” *Sci. Rep.*, vol. 6, pp. 1–13, 2016.
- [6] T. S. Jang, H. Do Jung, H. M. Pan, W. T. Han, S. Chen, and J. Song, “3D printing of hydrogel composite systems: Recent advances in technology for tissue engineering,” *Int. J. Bioprinting*, vol. 4, no. 1, pp. 1–28, 2018.
- [7] Q. Chen, H. Chen, L. Zhu, and J. Zheng, “Fundamentals of double network hydrogels,” *J. Mater. Chem. B*, vol. 3, no. 18, pp. 3654–3676, 2015.
- [8] Y. Bu, H. Shen, F. Yang, Y. Yang, X. Wang, and D. Wu, “Construction of tough, in situ forming double-network hydrogels with good biocompatibility,” *ACS Appl. Mater. Interfaces*, vol. 9, no. 3, pp. 2205–2212, 2017.
- [9] J. E. Samorezov, C. M. Morlock, and E. Alsberg, “Dual Ionic and Photo-Crosslinked Alginate Hydrogels for Micropatterned Spatial Control of Material Properties and Cell Behavior,” *Bioconjug. Chem.*, vol. 26, no. 7, pp. 1339–1347, 2015.
- [10] J.-Y. Sun *et al.*, “Highly stretchable and tough hydrogels,” *Nature*, vol. 489, no. 7414, pp. 133–136, 2012.
- [11] Y. Liu, W. He, Z. Zhang, and B. Lee, “Recent Developments in Tough Hydrogels for Biomedical Applications,” *Gels*, vol. 4, no. 2, p. 46, 2018.
- [12] M. C. Darnell *et al.*, “Performance and biocompatibility of extremely tough alginate/polyacrylamide hydrogels,” *Biomaterials*, vol. 34, no. 33, pp. 8042–8048, 2013.
- [13] Y. M. Chen, K. Dong, Z. Q. Liu, and F. Xu, “Double network hydrogel with high mechanical strength: Performance, progress and future perspective,” *Sci. China Technol. Sci.*, vol. 55, no. 8, pp. 2241–2254, 2012.
- [14] D. A. Rennerfeldt, A. N. Renth, Z. Talata, S. H. Gehrke, and M. S. Detamore, “Tuning mechanical performance of poly(ethylene glycol) and agarose interpenetrating network hydrogels for cartilage tissue engineering,” *Biomaterials*, vol. 34, no. 33, pp. 8241–8257, 2013.
- [15] L. Weng, A. Gouldstone, Y. Wu, and W. Chen, “Mechanically strong double network photocrosslinked hydrogels from N,N-dimethylacrylamide and glycidyl methacrylated hyaluronan,” *Biomaterials*, vol. 29, no. 14, pp. 2153–2163, 2008.

- [16] G. C. Ingavle, N. H. Dormer, S. H. Gehrke, and M. S. Detamore, "Using chondroitin sulfate to improve the viability and biosynthesis of chondrocytes encapsulated in interpenetrating network (IPN) hydrogels of agarose and poly(ethylene glycol) diacrylate," *J. Mater. Sci. Mater. Med.*, vol. 23, no. 1, pp. 157–170, 2012.
- [17] K. Yasuda *et al.*, "A novel double-network hydrogel induces spontaneous articular cartilage regeneration in vivo in a large osteochondral defect," *Macromol. Biosci.*, vol. 9, no. 4, pp. 307–316, 2009.
- [18] Y. Tanabe *et al.*, "Biological responses of novel high-toughness double network hydrogels in muscle and the subcutaneous tissues," *J. Mater. Sci. Mater. Med.*, vol. 19, no. 3, pp. 1379–1387, 2008.
- [19] D. Myung *et al.*, "Glucose-Permeable Interpenetrating Polymer Network Hydrogels for Corneal Implant Applications: A Pilot Study," *Curr. Eye Res.*, vol. 33, no. 1, pp. 29–43, 2009.
- [20] R. Kishi, K. Kubota, T. Miura, T. Yamaguchi, H. Okuzaki, and Y. Osada, "Mechanically tough double-network hydrogels with high electronic conductivity," *J. Mater. Chem. C*, vol. 2, no. 4, pp. 736–743, 2014.
- [21] J. Li, Z. Suo, and J. J. Vlassak, "Stiff, strong, and tough hydrogels with good chemical stability," *J. Mater. Chem. B*, vol. 2, no. 39, pp. 6708–6713, 2014.
- [22] H. Bodugoz-Senturk, C. E. Macias, J. H. Kung, and O. K. Muratoglu, "Poly(vinyl alcohol)-acrylamide hydrogels as load-bearing cartilage substitute," *Biomaterials*, vol. 30, no. 4, pp. 589–596, 2009.
- [23] B. Sun, Z. Wang, Q. He, W. Fan, and S. Cai, "Porous double network gels with high toughness, high stretchability and fast solvent-absorption," *Soft Matter*, vol. 13, no. 38, pp. 6852–6857, 2017.
- [24] Q. Chen *et al.*, "Simultaneous enhancement of stiffness and toughness in hybrid double-network hydrogels via the first, physically linked network," *Macromolecules*, vol. 48, no. 21, pp. 8003–8010, 2015.
- [25] Z. Liang *et al.*, "Double-Network Hydrogel with Tunable Mechanical Performance and Biocompatibility for the Fabrication of Stem Cells-Encapsulated Fibers and 3D Assemble," *Sci. Rep.*, vol. 6, no. August, pp. 1–11, 2016.
- [26] Q. Chen, L. Zhu, C. Zhao, Q. Wang, and J. Zheng, "A robust, one-pot synthesis of highly mechanical and recoverable double network hydrogels using thermoreversible sol-gel polysaccharide," *Adv. Mater.*, vol. 25, no. 30, pp. 4171–4176, 2013.
- [27] P. Chen, R. Wu, J. Wang, Y. Liu, C. Ding, and S. Xu, "One-pot preparation of ultrastrong double network hydrogels," *J. Polym. Res.*, vol. 19, no. 3, 2012.
- [28] T. Lin *et al.*, "One-Pot Synthesis of a Double-Network Hydrogel Electrolyte with Extraordinarily Excellent Mechanical Properties for a Highly Compressible and Bendable Flexible Supercapacitor," *ACS Appl. Mater. Interfaces*, vol. 10, no. 35, pp. 29684–29693, 2018.

- [29] J. Saito *et al.*, “Robust bonding and one-step facile synthesis of tough hydrogels with desirable shape by virtue of the double network structure,” *Polym. Chem.*, vol. 2, no. 3, pp. 575–580, 2011.
- [30] L. L. Wang, C. B. Highley, Y. C. Yeh, J. H. Galarraga, S. Uman, and J. A. Burdick, “Three-dimensional extrusion bioprinting of single- and double-network hydrogels containing dynamic covalent crosslinks,” *J. Biomed. Mater. Res. - Part A*, vol. 106, no. 4, pp. 865–875, 2018.
- [31] S. Hong *et al.*, “3D Printing of Highly Stretchable and Tough Hydrogels into Complex, Cellularized Structures,” *Adv. Mater.*, vol. 27, no. 27, pp. 4035–4040, 2015.
- [32] S. Liu and L. Li, “Ultrastretchable and Self-Healing Double-Network Hydrogel for 3D Printing and Strain Sensor,” *ACS Appl. Mater. Interfaces*, vol. 9, no. 31, pp. 26429–26437, 2017.
- [33] F. Yang, V. Tadepalli, and B. J. Wiley, “3D Printing of a Double Network Hydrogel with a Compression Strength and Elastic Modulus Greater than those of Cartilage,” *ACS Biomater. Sci. Eng.*, vol. 3, no. 5, pp. 863–869, 2017.
- [34] S. E. Bakarich, M. In Het Panhuis, S. Beirne, G. G. Wallace, and G. M. Spinks, “Extrusion printing of ionic-covalent entanglement hydrogels with high toughness,” *J. Mater. Chem. B*, vol. 1, no. 38, pp. 4939–4946, 2013.
- [35] J. Wei *et al.*, “3D printing of an extremely tough hydrogel,” *RSC Adv.*, vol. 5, no. 99, pp. 81324–81329, 2015.
- [36] V. Chan, P. Zorlutuna, J. H. Jeong, H. Kong, and R. Bashir, “Three-dimensional photopatterning of hydrogels using stereolithography for long-term cell encapsulation,” *Lab Chip*, vol. 10, no. 16, pp. 2062–2070, 2010.
- [37] P. Kunwar, Z. Xiong, Y. Zhu, H. Li, A. Filip, and P. Soman, “Hybrid Laser Printing of 3D, Multiscale, Multimaterial Hydrogel Structures,” *Adv. Opt. Mater.*, vol. 7, no. 21, pp. 1–13, 2019.
- [38] K. Arcaute, B. K. Mann, and R. B. Wicker, “Stereolithography of three-dimensional bioactive poly(ethylene glycol) constructs with encapsulated cells,” *Ann. Biomed. Eng.*, vol. 34, no. 9, pp. 1429–1441, 2006.
- [39] P. Kunwar, L. Turquet, J. Hassinen, R. H. A. Ras, J. Toivonen, and G. Bautista, “Holographic patterning of fluorescent microstructures comprising silver nanoclusters,” *Opt. Mater. Express*, vol. 6, no. 3, p. 946, 2016.
- [40] J.-W. Choi, M. D. Irwin, and R. B. Wicker, “DMD-based 3D micro-manufacturing,” in *Proceedings of SPIE*, 2010, vol. 7596, no. February 2010, p. 75960H.
- [41] Z. Xiong *et al.*, “Diffraction analysis of digital micromirror device in maskless photolithography system,” *J. Micro/Nanolithography, MEMS, MOEMS*, vol. 13, no. 4, p. 043016, 2014.
- [42] J. R. Tumbleston *et al.*, “Continuous liquid interface production of 3D objects,” *Science (80-.)*, vol. 347, no. 6228, pp. 1349–1352, 2015.

- [43] P. Kunwar, J. Hassinen, G. Bautista, R. H. A. Ras, and J. Toivonen, “Direct laser writing of photostable fluorescent silver nanoclusters in polymer films,” *ACS Nano*, vol. 8, no. 11, pp. 11165–11171, 2014.
- [44] Z. Xiong *et al.*, “Femtosecond laser induced densification within cell-laden hydrogels results in cellular alignment,” *Biofabrication*, vol. 11, no. 3, 2019.
- [45] B. D. Fairbanks, M. P. Schwartz, C. N. Bowman, and K. S. Anseth, “Photoinitiated polymerization of PEG-diacrylate with lithium phenyl-2,4,6-trimethylbenzoylphosphinate: polymerization rate and cytocompatibility,” *Biomaterials*, vol. 30, no. 35, pp. 6702–6707, 2009.
- [46] D. R. King *et al.*, “Extremely tough composites from fabric reinforced polyampholyte hydrogels,” *Mater. Horiz.*, vol. 2, no. 6, pp. 584–591, 2015.
- [47] P. Kunwar *et al.*, “High-Resolution 3D Printing of Stretchable Hydrogel Structures Using Optical Projection Lithography,” *ACS Appl. Mater. Interfaces*, vol. 12, no. 1, pp. 1640–1649, 2020.

Chapter 4 Determining the Effect of Polymer and Protein Concentration on Adhesive and Mechanical Properties of Protein-Polymer Gels

4.1 Synopsis

The *Arion subfuscus* slug secretes a defensive glue that has unique properties of toughness and adhesion, even though it is 95-97% water by mass. The hypothesized reason as to why these glues have such remarkable mechanical properties is due to a double network structure between a rigid protein network and a ductile carbohydrate network. It is also believed that the proteins are responsible for the adhesive properties observed, and both the rigidity and the adhesiveness is a product of protein and metal-ion interactions. In this work, poly(dimethyl acrylamide) (PDMAAm) gels were synthesized in the presence of extracted slug glue proteins (SGP's) and metal ions. A robust set of mechanical tests were performed to determine the full extent of SGP effects on gel properties and to determine if an ion-crosslinked protein network could be formed. To do this, a design space of nine compositions were tested for stiffness, hysteresis energy, cohesive strength, and adhesive strength.

4.2 Introduction

As the field of hydrogel research continues to expand, investigators are looking at ways of developing adhesive gels for different purposes. Due to the hydrophilic nature of hydrogels, adhesive materials would be advantageous for biomedical applications. A majority of focus for these adhesive gels is based on their use for wound dressings, suture replacements, and drug delivery [1], [2]. One of the issues in the development of these gels is their design. The majority of hydrogels that have been researched do not have inherently adhesive properties, and the adhesive hydrogel literature is scarce [3]. A few examples of adhesive systems discussed early in the literature would be poly(acrylic acid)-based oral drug delivery systems [1] and modified

poly(ethylene glycol) gels, such as FocalSeal® [2]. To develop adhesive gels, many researchers have turned to materials from nature as a source of inspiration.

One of the most famous muses for these bioadhesive materials is the mussel. Mussels secrete a byssus, or bundle of filaments, that allows them to adhere to surfaces [4]. The proteins found in the byssus have been studied thoroughly, and have been used in the design of bioadhesive materials [5], [6]. Messersmith created an adhesive hydrogel based on the covalent adhesion of mussel byssus combined with thermosensitive block copolymer chemistry [7]. This allowed the hydrogel network to shrink under heat, making it useful for wound dressing and sealing. Ren and Lu have also developed materials inspired off of the mussel adhesive mechanism using a polydopamine-polyacrylamide single network gel which had high ductility, toughness, and self-healing abilities [8]. Wang developed a mussel-inspired tissue adhesive by creating dopamine-grafted gelatin crosslinked using both Fe^{3+} ions and genipin [9].

While many other sources of inspiration exist, such as geckos [10] and mushrooms [11], one that is gaining significant attention is slugs. Karp and del Nido developed a blood resistant surgical glue for use in minimally-invasive heart surgeries, inspired by water-immiscible components in slug and sandworm secretions that allow for adhesion even in aqueous environments [12]. For this reason, focus has been applied to the *Arion subfuscus* slug, which secretes a defensive glue with interesting properties, including stiffness and adhesion. The glue consists of 95% water by mass, and contains a mixture of carbohydrates and proteins [13].

While investigating the composition of the gel, Dr. Andy Smith found that it seems to have a structure that is comparable to those of double networks [14]. To briefly review double networks, these materials are developed by incorporating a ductile, loosely crosslinked polymer network into an already existing brittle, highly crosslinked polymer network [15]. The two polymers work

in a synergistic manner, providing strength and ductility that are absent in either of the single networks. The first double network (DN) study was seen in 2003 from Gong and coworkers [16]. While initially developed using covalently crosslinked networks, researchers have also developed DN's that use both covalent and ionic crosslinking methods. Sun et al. developed double networks that used an ionically crosslinked alginate gel as the strong network and a covalently crosslinked polyacrylamide gel as the ductile network, which showed remarkable elasticity and toughness even when a defect is cut into the samples [17]. It is also useful to note that the alginate-polyacrylamide gels were shown to have self-healing properties, on account of the ionic crosslinking of alginate. The slug glue is believed to have a double network structure, as the two major materials that make up the glue (aside from water) were found to be carbohydrates and proteins at roughly similar quantities [14]. The carbohydrates and the proteins may form ionic or coordinate covalent crosslinks, both dependently and independently from one another, using various metal ions.

The defensive slug glue is similar to the structure of its trail glue [18]; however, the glue contains a different set of proteins, and a considerable concentration of metal ions [14]. Metal ions that are known to be in the glue include calcium (Ca^{2+}), magnesium (Mg^{2+}), zinc (Zn^{2+}), and iron (Fe^{3+}). The set of proteins that are native to the defensive glue consist of two groups; a set of proteins that have a molecular weight of approximately 15 kDa (asmp-15) and another with a molecular weight around 61 kDa (asmp-61) [19]. In addition, the metals that exist in the glue are imperative to its stiff and adhesive behavior. For instance, removing calcium from the slug glue causes around a 30% decrease in stiffness [20]. Based on this information, Smith decided to use RNA sequencing to determine the sequence of the proteins so information could be gleaned about how the proteins and the metals interact [21]. It was found that the asmp-15 proteins

consist of three different groups; a set of proteins with a sequence similar to C-lectins, another set with H-lectin similarities, and another with C1-q similarities. The asmp-61 proteins were found to have a sequence similar to matrilins.

It's important to note how the protein structure correlates with the metals that exist in the glue. Lectins in general are known as binding proteins involved in many different biological functions, such as cell binding [22] or immunoresponses [23]. C-lectins are a large group of proteins that are known for having a characteristic double-loop (or a loop within a loop) structure [24]. The C-lectin superfamily is found mainly in the extracellular matrix of many Metazoan animals, including humans. C-lectins are known to bind to other proteins and carbohydrates through coordination with Ca^{2+} ions [24]. While the function varies between the individual proteins, C-lectins have been documented in signaling inflammatory responses [25]. H-lectins are known for similar binding behavior, but use Zn^{2+} ions for intermolecular connections [26]. Unlike C-lectins, H-lectins have not been documented in many different species; they have been documented mainly in snails, but recent work has found a variant that exists in a species of algae [27]. In snails, H-lectins are involved in the protection of fertilized eggs from harmful bacteria [26].

The C1q protein superfamily has been studied by those interested in brain and nervous system physiology, as that is where these proteins are found [28]. While there are many different types of C1q proteins, only a small subset of these proteins interacts with metals, mainly calcium. This subset of proteins is believed to use the metal ions to either stabilize their structure or use the ions as a method to mediate protein-protein interactions [28]. Matrilins have a very specific structure consisting mainly of von Willebrand factor type A and epidermal growth factor domains [29]. The protein ends in a coiled-coil domain. Matrilins also rely on Ca^{2+} ions, and sometimes Mg^{2+} ions, as part of a mechanism for crosslinking [29], [30]. This explains why the

stiffness of the glue drops when calcium is removed from the glue, but no change in the stiffness is seen when zinc is removed [20]. It should be noted, however, that both calcium and magnesium are easily removed from the glue, raising the possibility that these ions are not the sole mechanism by which the protein network is formed [31].

To continue discussing crosslinking mechanics, the current working theory is that there are multiple metal-based crosslinking mechanisms that are occurring within the glue. While calcium is the most abundant of the metal ions that exist within the glue, iron is also present [14]. Iron is difficult to remove from the gel, and even when chelators that selectively target iron are added to the glue, the concentration is only slightly reduced [20]. The theory is that iron is responsible for additional ligand-bonding coordination and the binding affinity for these bonds is high enough to resist chelation [20], [31]. Iron may also be responsible for covalent crosslinks formed via oxidation [14], [20]. Briefly, the oxidation of iron in the glue causes the formation of carbonyl groups, which react with amine groups in lysine sidechains to form imine bonds. Oxidized proteins are known to exist in the glue, and disruption of imine bonds is known to decrease its stiffness [20], [32].

An interesting aspect of these proteins is that adding them to gel networks has been shown to cause an increase in stiffness. Smith found that incorporating these proteins into citrus pectin gels caused significant increases in the storage modulus [13], [19], [33]. While stiffening behavior has been observed, neither adhesive nor self-healing behavior has been documented with the incorporation of proteins into synthetic gels.

While these proteins have been investigated significantly, most of the work so far has been focused on the biochemical and structural aspects of the protein to determine the underlying mechanisms of the glue's behavior. To further understand the importance of the proteins, and

how they directly contribute to the adhesive, stiffening, and possible self-healing abilities, a material science centered investigation would be beneficial. With some materials already developed based on the mechanisms of the glue [34], further characterization and understanding can help researchers to develop novel biomaterials for uses in biomedical applications.

4.3 Experimental

4.3.1 Materials

Raw slug glue was either donated from Dr. Smith of Ithaca College or collected from samples in nature. The collection process is as follows: Slugs were obtained from local wilderness and parks. The backs of these slug were rubbed with a metal spatula to trigger the defensive reaction, causing the slug to secrete the glue. The glue was collected, and slugs returned to the wilderness where they were found. The glue was stored in a -80 °C freezer until protein extraction was necessary.

4.3.2 Extracting the Slug Glue Proteins

Slug glue samples were soaked overnight in a solution of 10 mM tris(hydroxymethyl) aminomethane (Tris) and 20 mM ethylenediaminetetraacetic acid (EDTA) at 4 °C at a concentration of 40 mg slug glue per mL Tris-EDTA solution. The mixtures were homogenized, sonicated, and then centrifuged at 13.0×10^3 g's for 10 minutes. The supernatant was collected and considered SGP solution. The protein concentration of the SGP solution was determined via BCA assay.

4.3.3 Gel Synthesis

Solutions of DMAAm and SGP were mixed to obtain the concentrations as described in Figure 4.1. MBAAm and Irg ratios, used as crosslinker and photoinitiator for the DMAAm network respectively, were held constant throughout the compositions at 0.2 mol% MBAAm to DMAAm

and 25 wt% Irg. A concentrated metal ion solution was created with a ratio of 40 mol Ca^{2+} :15 mol Mg^{2+} : 1 mol Zn^{2+} and a concentration of 48 mg/mL CaCl_2 , 33 mg/mL $\text{MgCl}_2 \cdot 6\text{H}_2\text{O}$, and 1.5 mg/mL ZnCl_2 . The concentrated metal ion solution was added to the DMAAm-SGP mixture so that there is a ratio of 0.8 g metal ion for every gram of SGP. The DMAAm-SGP mixtures were injected into molds made with two microscope slides and a spacer with a thickness of 1.13 mm. Gels were subjected to 365 nm UV light for 2 hours to ensure polymerization of the PDMAAm network.

4.3.4 Rheometry

Rheometry experiments were run on an AR-G2 rheometer with an 8 mm plate-plate geometry setup. The storage modulus was recorded at 0.5 % strain and a frequency of 0.5 Hz. These values were chosen based off of strain and frequency sweeps conducted between 0.1 to 100% and 0.1 to 10 Hz, respectively. The data for these sweeps can be found in Appendix C.

4.3.5 Hysteresis

Hysteresis experiments were based off a procedure used by Fung, Gallego Lazo, and Smith [31]. Briefly, gels were cut into samples of a length and width of 15 mm and 4 mm, respectively. The samples were clamped in an AR-G2 rheometer with a specialized tensile clamp setup. Samples were stretched three times to 10,000 mm, 15,000 mm, and then 20,000 mm. After each stretch, the strain was released and the sample was allowed to sit for 5 minutes before the next strain was applied. The hysteresis energy was calculated for each loop and calculated to determine energy dissipation in the gels.

4.3.6 Lap Shear Test

Lap shear tests were performed to determine the cohesive strength of the gels. The tests were performed based on the standard ASTM F2255 [35]. Briefly, rectangles of fake tattoo skin were

cut to the dimensions of 75 mm by 26 mm to act as the substrate. Samples of the gel were sandwiched between two rectangles so that there was a small portion of overlap (roughly 20-25% of the length of one rectangle), and then a force of 1 N was applied to the bonded area for 1 hour in a humidity-controlled room at $30\% \pm 5\%$ relative humidity. After the force had been applied, samples were loaded into a Test Resources® tensile tester and pulled apart at a rate of 5 mm/min. The cohesive strength of the samples was calculated as the maximum load divided by the area of the bonded site.

4.3.7 Pull-Off Test

To determine the adhesive strength of these gels, a pull-off test was conducted. This test was based off of a similar test used by Robertson [36]. Cylindrical samples of 8 mm diameter were made using a handheld press punch. Samples were loaded in a dynamic mechanical analysis machine (DMA) with a compression clamp attachment. Samples were compressed to a load of 1 N, and the load was held for 1 hour. The load was removed at a constant rate of 0.5 N/min. The test was performed until the top clamp hit its maximum height, which corresponded to an adhesive failure. The adhesive strength was determined by dividing the maximum load before failure by the surface area of the sample.

4.3.8 Statistical Tests

For all mechanical tests, three replicates from two batches were tested for a total of six samples per composition. All results were tested for outliers via GraphPad. To test for differences between the compositions, two-way analysis of variance (ANOVA) followed by Tukey post-hoc tests were conducted using Minitab statistical software.

4.4 Results and Discussion

4.4.1 Gel Synthesis

The gel synthesis process was considered successful due to qualitative observations. It was noted that all compositions behaved as low-viscosity fluids before UV exposure, and changed to either semisolid or solid gels for the 40/50 mg DMAAm/mL samples and the 60 mg DMAAm/mL samples, respectively. Control samples maintained a clear white color, while SGP-loaded samples tended to have a pale-yellow color that increased in intensity with increases in SGP concentration.

The time and intensity of the UV exposure was also found to be of importance via qualitative observations. Samples were exposed to three different UV sources; a low intensity (SBI general purpose UV box), middle intensity (OmniCure[®] S2000 Spot UV Cure System with a 200 Watt UV Lamp), and high intensity source (Dymax[®] 2000-EC Series Lamp with a 400 Watt UV Lamp). The times of exposure were changed based on the time it took a control sample of the same concentration to polymerize; this corresponded to 2 hr exposure to the low intensity source, 10 min exposure to the middle intensity source, and 2 min exposure to the high intensity source. In the cases of both the middle intensity and high intensity sources, samples were found to change color from a pale yellow to a clear white as shown in Figure 4.2.

The color change that was observed after UV irradiation may be an indirect marker of protein damage during the synthesis process.¹ It is theorized by Dr. Smith that the yellow color observed in the SGP solution as well as the gels is due to a pigment molecule that exists within the glue. The theorized purpose of this pigment would be to make the glue a bright color, as a warning to

¹Conversation with Dr. Andy Smith of Ithaca College.

predators. The color change after exposure to UV irradiation may indicate a change in the structure of this hypothesized pigment or other molecules derived from the slug glue, including the target proteins for double network formation.

It should also be noted that rheometry tests on samples that lost this yellow tint were found to have storage moduli comparable to that with controls (data not shown). Based off of these results, if samples loaded with protein became clear after UV exposure, it was considered unusable. Since the low intensity light source was the only instance when exposure did not lead to a color change within the gels, this setup was solely used for sample creation.

4.4.2 Stiffness and Hysteresis Energy

The stiffness and hysteresis energy of the SGP-PDMAAm gels was collected to determine if a protein network was formed. If an SGP network had formed within the sample, these gels were hypothesized to take on a double network structure. This would be seen as sharp increases in both the stiffness and hysteresis energy when the SGP was added.

The stiffness of the samples was measured based off the results of a rheometry experiment, in which the storage modulus (G') was recorded at a strain and frequency of 0.5% and 0.5 Hz, respectively. Based on the results shown in Figure 4.3, the 60 mg DMAAm/mL, 0.8 mg SGP/mL had the highest stiffness of any sample, with a storage modulus of 233 ± 106 Pa. This storage modulus was an order of magnitude higher than each of the 40 mg DMAAm/mL and 50 mg DMAAm/mL compositions. This result was considered promising, as such an increase in a mechanical property can be interpreted as indicative of double network formation.

The 60 mg DMAAm/mL, 0.5 mg SGP/mL was also found to have a significant increase in storage modulus when compared to the 40 mg DMAAm/mL samples. Again, the increase in

storage modulus was found to be an order of magnitude. This composition was also considered as a possible sample where a double network may have been formed.

While the data from the rheometry experiments was promising, the results alone were not enough to confirm SGP network formation. In order to determine if the network was being formed, the hysteresis energy of the samples was determined. If the gels which showed significant increases in their stiffness also showed higher hysteresis energy, this would be indicative of the SGP forming, as double networks have been documented to have significant hysteresis energy [17], [37].

From the results of the hysteresis tests, as shown in Figure 4.4, there was no evidence to suggest an SGP network was being formed. All hysteresis energy measurements were remarkably low, with all values being within a standard deviation of 0 kJ/m³. This implies that the hysteresis energy for all of these gels is at or near zero, which would conform to the understanding of PDMAAm gels as described in Chapter 2.

When comparing the performance of these gels to the raw slug glue, it is evident that the SGP-DMAAm gels have weaker mechanical properties. Specifically when reviewing the hysteresis results, raw slug glue tends to have a hysteresis energy between 20 and 60 kJ/m³ [31]. This indicates a lack of SGP network formation in these materials. If an SGP network were forming within these materials, it would be expected that the hysteresis energy would be significantly higher with statistical analysis.

Previous work conducted by Dr. Andy Smith had shown that gels would stiffen when protein solutions were incorporated into them [13], [19], [33]. This led to the hypothesis that other mechanical properties may be heightened within the gel once proteins were added. In addition,

another question was asked: Could a double network be forming within these gels? If a network was being formed, this would be considered remarkable, as the proteins are in such low concentration and molar fraction when compared to the PDMAAm network. Indeed, classical double network theory would suggest that concentrations of about 200-fold would be necessary for such formation. However, the results of the mechanical tests show that this is not the case.

4.4.3 Cohesive and Adhesive Strength

Two tests were run to determine the adhesive properties of the SGP-DMAAm gels. A lap shear test was used to measure the cohesive forces, while a pull-off test was used to measure adhesive forces. Both forces are important aspects of the total adhesive performance of the material.

Adhesive forces are derived from the bonds between the adhesive and the substrate, while cohesive forces are derived from the bonds that occur between the material and itself [38].

Certain types of mechanical tests used to measure the adhesive properties of materials are more favorable for measuring only one of these forces over the other. For example, the lap shear test is known for being dominated by the cohesive forces [39], [40], while a pull-off test is dominated by the adhesive forces [39]. To this end, both tests were employed to get a better understanding of both forces present within the gels.

Analyzing the results of the lap shear tests as shown in Figure 4.5, no composition was found to be significantly different from the others. The large variations in the 40 mg DMAAm/mL, 0.5 mg SGP/mL and the 40 mg DMAAm/mL, 0.8 mg SGP/mL compositions are also worth noting, but outlier testing indicated that none of the collected results were significant outliers. It should also be noted that the results of this test show that these materials have low cohesive forces in comparison to some bioadhesive materials developed recently. While these materials show

strengths in the hundreds of Pascals, materials developed for bioadhesive applications have been shown to have cohesive strengths in the kPa and even MPa range [41]–[43].

The results of this test would suggest no significant changes to the cohesive forces in the materials once loaded with SGP's. This would make sense considering the results of the rheometry and hysteresis tests, which indicated that no SGP network was being formed. If an SGP network was being formed, it would be expected that the cohesive forces increase, as there is another network forming crosslinking bonds within the gel. This increase in crosslinking bonds are important for providing the rigid structure necessary for high cohesive strength [38], [44].

The results of the pull-off test, as shown in Figure 4.6, show a pattern that was opposite of that hypothesized. It was expected that by increasing the concentration of proteins, the adhesion would increase, as there would be more adhesive proteins within the system. For both the 50 and 60 mg/mL DMAAm batches, incorporating the slug glue proteins into the gels had no significant effect on the adhesive strength. For the 40 mg/mL DMAAm batches, it was found that high SGP concentration decreased the adhesive strength. It is also interesting to note that the 40 mg/mL DMAAm, 0.0 and 0.5 mg/mL SGP samples had higher adhesive strengths than the other samples. A possible explanation for this could be due to the relationship between flowability and cohesion, which is necessary for adhesive polymers [1], [45], [46]. It is possible that this concentration is the best ratio between these two contradictory variables, leading to a higher adhesive strength for the pull-off test.

The hypothesized reason as to why adhesion occurs within the raw slug glue is that the asmp-15 proteins have an open adhesion site upon the surface of their structure, most likely mediated by a calcium ion [21]. If there is no sign of increased adhesion with increased SGP concentration, one

possibility for such a result would be that the adhesive site is no longer open or functioning, which would be caused by the protein denaturing during synthesis. It is also a possibility that the proteins go through a conformational change when placed in the gel, and this conformation change makes it so that the binding sites necessary for adhesion are not present at the surface of the material. Alternatively, this could also be due to the same reason as the results seen in the hysteresis and lap shear tests; the concentration of the proteins is too small for there to be any direct effect on the mechanical properties. Currently, there is more evidence to suggest that the latter is the likely case considering the results of the other mechanical tests. However, future work with more concentrated samples could be used to determine whether denaturing is occurring or not.

4.5 Conclusions

A synthetic DMAAm polymer was loaded with SGP's and multiple types of metal ions for the purposes of determining if this material setup could be used to elucidate how protein and metal-ion interactions affect the mechanical properties of a defensive slug glue. Through a series of mechanical tests, it was found that there was no discernable difference between the controls and protein-loaded samples. This is believed to be due to the low concentration of proteins, which is not conducive to the formation of a protein network.

To create a functional protein network within the current system, SGP solutions will need to be made with protein concentrations of approximately 200 mg/mL, about 200 times more concentrated than the average concentration used during this study. This limitation is compounded by two problems with the current setup. First, when collecting samples from slugs, the protein extraction process limits the SGP solution to concentrations that range from 0.6 mg/mL to 1.5 mg/mL. Concentrating these solutions to the desired level would require large

collections of raw glue, which can be difficult to obtain. Second, the SGP's are known to self-aggregate and separate out of solutions when the concentration gets too high (> 3 mg/mL).

In order for this setup to be a viable option, it may be necessary that more advances are done when it comes to creating methods to collect and solubilize these proteins. One option is to develop a bacterium that could synthesize the proteins of interest. This would allow not only high throughput and collection of the proteins but allow for more control over the specific concentrations of individual proteins. The large variations in the Results section may be a product of differences in individual protein concentrations between batches, so the use of bacteria could help minimize this. The solubilization problem is one that may have to be investigated and solved by a biochemist, who would have better knowledge on how to best tackle the issue.

The results of this project show what limitations currently exist for using this setup as a viable method to determine the effects on mechanical properties due to protein-ion interactions. Once these problems are solved, the current setup could be reviewed and investigated as a practical methodology.

4.6 Schemes, Figures, and Tables

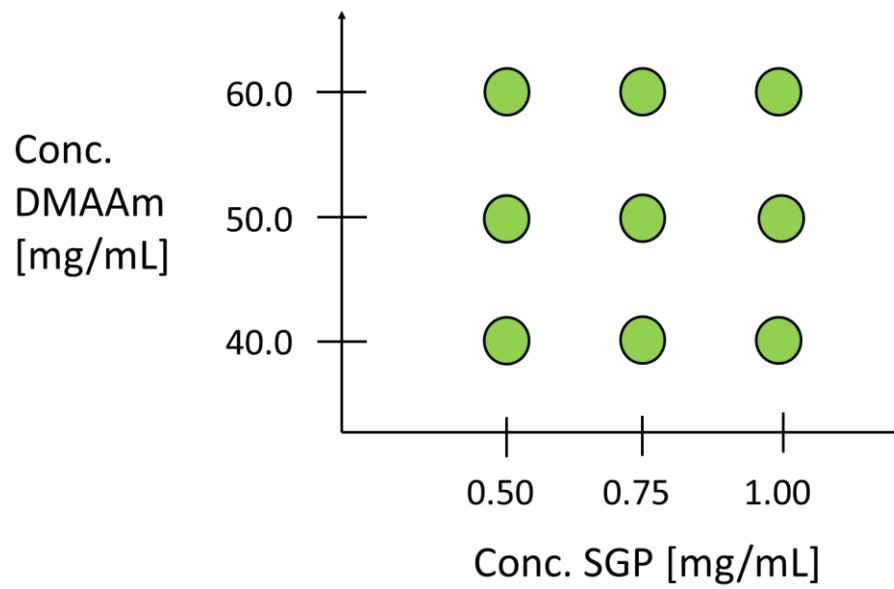


Figure 4.1 The design space used to investigate the effects of polymer and protein concentration on the adhesive and mechanical properties of the gels.

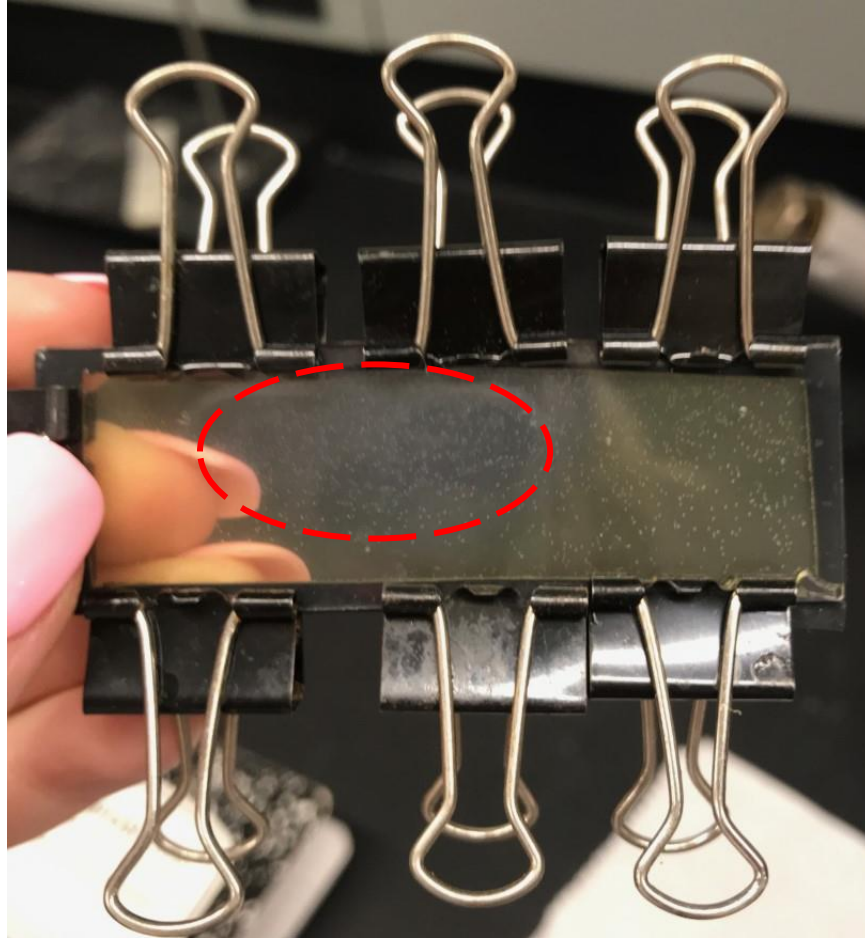


Figure 4.2 A slug glue protein, poly(dimethylacrylamide) gel that has been exposed to UV light from the OmniCure® S2000 Spot UV Cure System. For this particular light source, it was found that the beam was too focused, and would cause denaturing or damaging of the proteins in the area where the light directly shone unto the sample (red dashed circle). These samples were considered unusable.

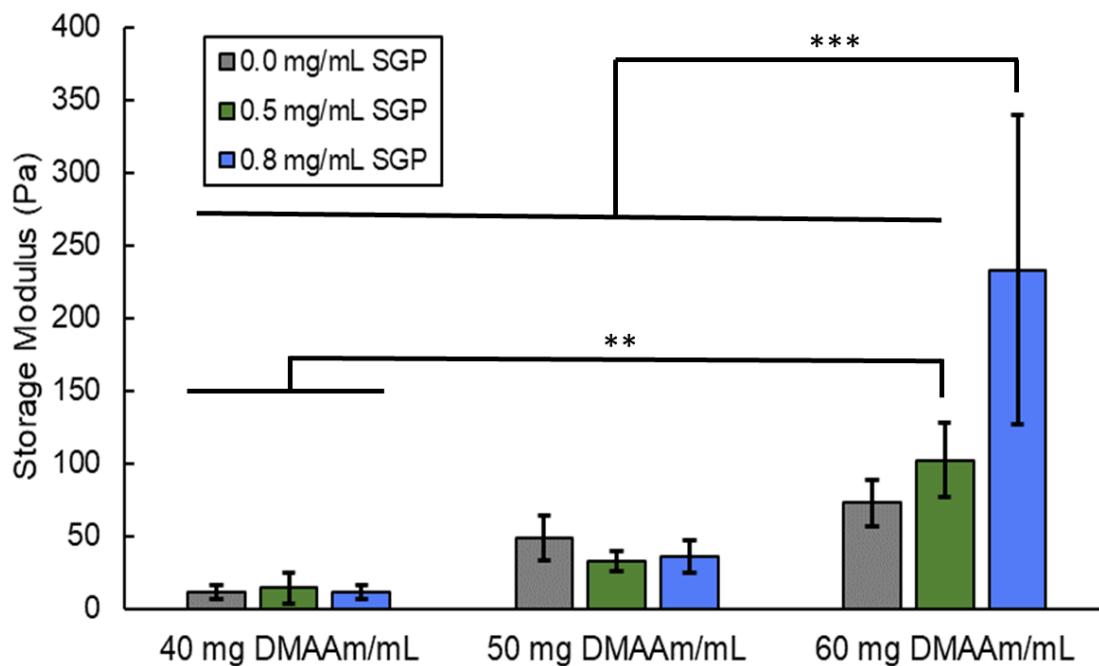


Figure 4.3 The results of the rheometry experiments with the SGP-DMAAm gels. The order of magnitude increase in storage modulus in the 60 mg DMAAm/mL, 0.8 mg SGP/mL sample was seen as a potential indication of a SGP network being formed. Error bars are standard deviation. ** - p-value < 0.01. *** - p-value < 0.001.

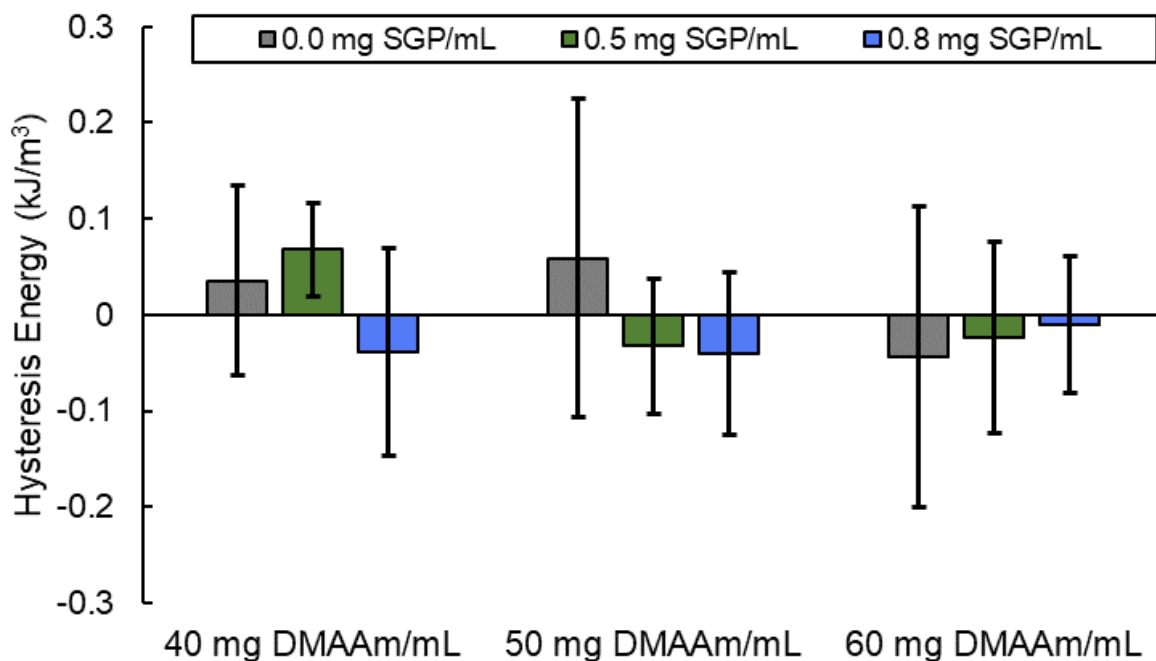


Figure 4.4 The hysteresis energy of the SGP-DMAAm gels. One point to note is that all error bars cross the 0-point. This indicates that there is little to no energy dissipation that occurs within the gels. If an SGP network was forming, it would be expected that the energy dissipation would increase with incorporation of SGP's into the gel.

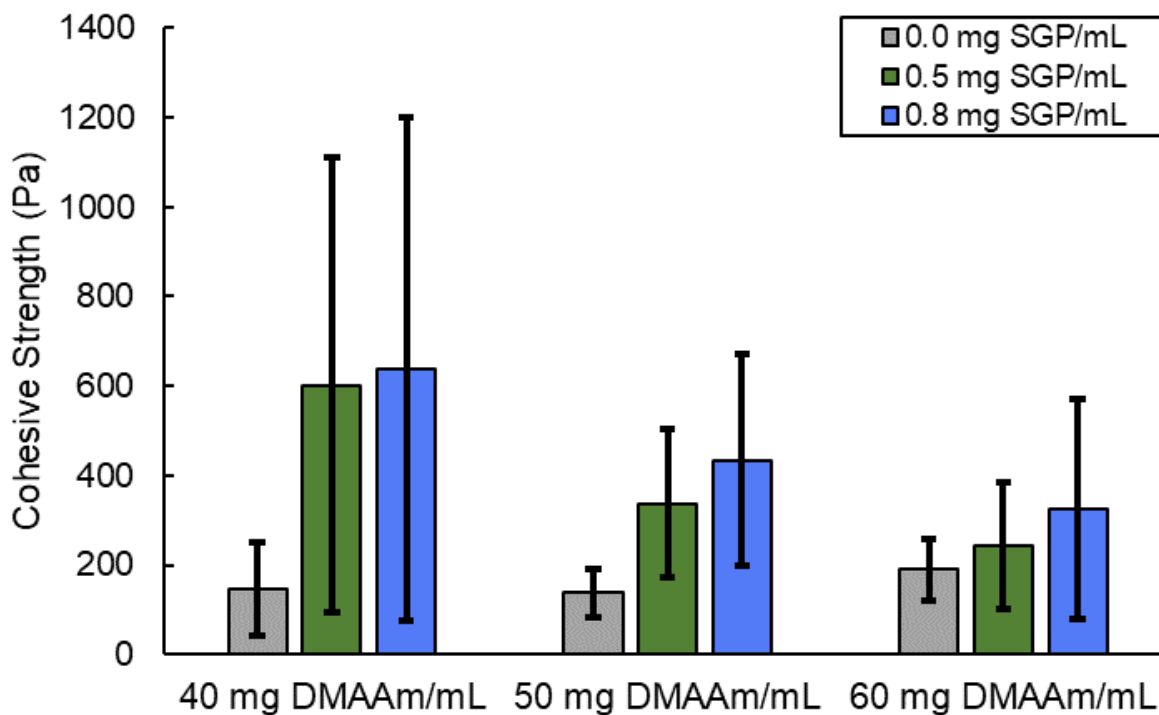


Figure 4.5 The cohesive strength of the SGP-DMAAm gels as observed from a lap shear test. No statistical difference could be inferred when comparing the compositions. This could be due to the high variations seen in the SGP-loaded 40 mg DMAAm/mL samples. It should be noted that outlier testing was conducted on all samples, and no outliers could be determined. This data also conforms with the results of the hysteresis testing, which indicated a lack of SGP network formation. An SGP network being formed within the gels would be seen as an increase in the cohesive strength.

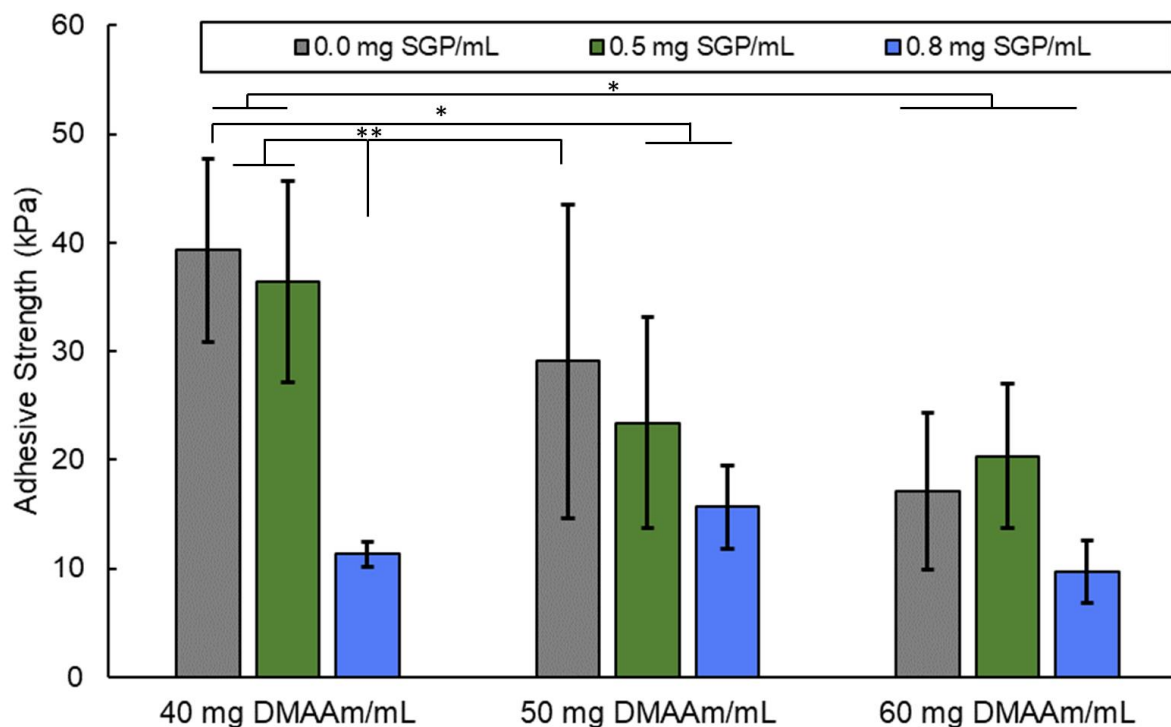


Figure 4.6 The adhesive strength of the SGP-DMAAm gels based on the results of a pull-off test. Interestingly, the 40 mg DMAAm/mL, 0.0 mg SGP/mL and 40 mg DMAAm/mL, 0.5 mg SGP/mL compositions had the highest adhesive energy. This is believed to be due to the high water content of these gels, and an increase in the surface tension that would result when a force is applied to the gel and then released. * - p-value < 0.05. ** - p-value < 0.01.

4.7 References

- [1] N. A. Peppas and J. J. Sahlin, "Hydrogels as mucoadhesive and bioadhesive materials: A review," *Biomaterials*, vol. 17, no. 16, pp. 1553–1561, 1996.
- [2] T. B. Reece, T. S. Maxey, and I. L. Kron, "A prospectus on tissue adhesives," *Am. J. Surg.*, vol. 182, no. 2 SUPPL. 1, pp. S40–S44, 2001.
- [3] C. W. Peak, J. J. Wilker, and G. Schmidt, "A review on tough and sticky hydrogels," *Colloid Polym. Sci.*, vol. 291, no. 9, pp. 2031–2047, 2013.
- [4] A. Abbott, "Bioadhesives: potential for exploitation," *Sci. Prog. Oxford*, vol. 74, no. 1, pp. 131–146, 1990.
- [5] H. J. Cha, D. S. Hwang, and S. Lim, "Development of bioadhesives from marine mussels," *Biotechnol. J.*, vol. 3, no. 5, pp. 631–638, 2008.
- [6] L. Li and H. Zeng, "Marine mussel adhesion and bio-inspired wet adhesives," *Biotribology*, vol. 5, pp. 44–51, 2016.
- [7] D. G. Barrett, G. G. Bushnell, and P. B. Messersmith, "Mechanically Robust, Negative-Swelling, Mussel-Inspired Tissue Adhesives," *Adv. Healthc. Mater.*, vol. 2, no. 5, pp. 745–755, 2013.
- [8] L. Han *et al.*, "Tough, self-healable and tissue-adhesive hydrogel with tunable multifunctionality," *NPG Asia Mater.*, vol. 9, no. 4, 2017.
- [9] C. Fan, J. Fu, W. Zhu, and D. A. Wang, "A mussel-inspired double-crosslinked tissue adhesive intended for internal medical use," *Acta Biomater.*, vol. 33, pp. 51–63, 2016.
- [10] M. Kamperman, E. Kroner, A. Del Campo, R. M. McMeeking, and E. Arzt, "Functional adhesive surfaces with 'Gecko' effect: The concept of contact splitting," *Adv. Eng. Mater.*, vol. 12, no. 5, pp. 335–348, 2010.
- [11] E. P. Chan, E. J. Smith, R. C. Hayward, and A. J. Crosby, "Surface wrinkles for smart adhesion," *Adv. Mater.*, vol. 20, no. 4, pp. 711–716, 2008.
- [12] N. Lang *et al.*, "A Blood-Resistant Surgical Glue for Minimally Invasive Repair of Vessels and Heart Defects," *Sci. Transl. Med.*, vol. 6, no. 218, 2015.
- [13] A. M. Smith, T. M. Robinson, M. D. Salt, K. S. Hamilton, B. E. Silvia, and R. Blasiak, "Robust cross-links in molluscan adhesive gels: Testing for contributions from hydrophobic and electrostatic interactions," *Comp. Biochem. Physiol. - B Biochem. Mol. Biol.*, vol. 152, no. 2, pp. 110–117, 2009.
- [14] A. M. Smith, "Multiple Metal-Based Cross-Links: Protein Oxidation and Metal Coordination in a Biological Glue," in *Biological and Biomimetic Adhesives: Challenges and Opportunities*, Cambridge: Royal Society of Chemistry, 2013, pp. 3–15.
- [15] J. P. Gong, "Why are double network hydrogels so tough?," *Soft Matter*, vol. 6, no. 12, pp. 2583–2590, 2010.
- [16] J. P. Gong, Y. Katsuyama, T. Kurokawa, and Y. Osada, "Double-Network Hydrogels with

- Extremely High Mechanical Strength,” *Adv. Mater.*, vol. 15, no. 14, pp. 1155–1158, 2003.
- [17] J.-Y. Sun *et al.*, “Highly stretchable and tough hydrogels,” *Nature*, vol. 489, no. 7414, pp. 133–136, 2012.
- [18] A. M. Smith and M. C. Morin, “Biochemical differences between trail mucus and adhesive mucus from marsh periwinkle snails,” *Biol. Bull.*, vol. 203, no. 3, pp. 338–346, 2002.
- [19] J. M. Pawlicki, L. B. Pease, C. M. Pierce, T. P. Startz, Y. Zhang, and A. M. Smith, “The effect of molluscan glue proteins on gel mechanics,” *J. Exp. Biol.*, vol. 207, no. 7, pp. 1127–1135, 2004.
- [20] M. Braun, M. Menges, F. Opoku, and A. M. Smith, “The relative contribution of calcium, zinc and oxidation-based cross-links to the stiffness of *Arion subfuscus* glue,” *J. Exp. Biol.*, vol. 216, no. 8, pp. 1475–1483, 2013.
- [21] A. M. Smith, C. Papaleo, C. W. Reid, and J. M. Bliss, “RNA-Seq reveals a central role for lectin, C1q and von Willebrand factor A domains in the defensive glue of a terrestrial slug,” *Biofouling*, vol. 33, no. 9, pp. 741–754, 2017.
- [22] U. R. S. Rutishauser and L. E. O. Sachs, “Cell-to-Cell Binding Induced by Different Lectins,” *J. Cell Biol.*, vol. 65, pp. 247–257, 1975.
- [23] M. Brudner *et al.*, “Lectin-Dependent Enhancement of Ebola Virus Infection via Soluble and Transmembrane C-type Lectin Receptors,” *PLoS One*, vol. 8, no. 4, 2013.
- [24] A. N. Zelensky and J. E. Gready, “The C-type lectin-like domain superfamily,” *FEBS J.*, vol. 272, no. 24, pp. 6179–6217, 2005.
- [25] A. Cambi and C. Figdor, “Necrosis : C-Type Lectins Sense Cell Death,” *Curr. Biol.*, vol. 19, no. 9, pp. R375–R378.
- [26] J. F. Sanchez *et al.*, “Biochemical and structural analysis of *Helix pomatia* agglutinin: A hexameric lectin with a novel fold,” *J. Biol. Chem.*, vol. 281, no. 29, pp. 20171–20180, 2006.
- [27] J. W. Han, K. S. Yoon, T. A. Klochkova, M. S. Hwang, and G. H. Kim, “Purification and characterization of a lectin, BPL-3, from the marine green alga *Bryopsis plumosa*,” *J. Appl. Phycol.*, vol. 23, no. 4, pp. 745–753, 2011.
- [28] S. Ressler, B. K. Vu, S. Vivona, D. C. Martinelli, T. C. Südhof, and A. T. Brunger, “Structures of C1q-like proteins reveal unique features among the C1q/TNF superfamily,” *Structure*, vol. 23, no. 4, pp. 688–699, 2015.
- [29] M. Paulsson and R. Wagener, “Matrilins,” in *Methods in Cell Biology*, vol. 143, L. Wilson and P. Tran, Eds. Cambridge: Elsevier, 2018, pp. 429–446.
- [30] C. A. Whittaker and R. O. Hynes, “Distribution and Evolution of von Willebrand / Integrin A Domains : Widely Dispersed Domains with Roles in Cell Adhesion and Elsewhere,” *Mol. Biol. Cell*, vol. 13, pp. 3369–3387, 2002.
- [31] T. M. Fung, C. Gallego Lazo, and A. M. Smith, “Elasticity and energy dissipation in the

- double network hydrogel adhesive of the slug *Arion subfuscus*,” *Philos. Trans. R. Soc. B Biol. Sci.*, vol. 374, no. 1784, 2019.
- [32] A. Bradshaw, M. Salt, A. Bell, M. Zeitler, N. Litra, and A. M. Smith, “Cross-linking by protein oxidation in the rapidly setting gel-based glues of slugs,” *J. Exp. Biol.*, vol. 214, no. Pt 10, pp. 1699–1706, 2011.
- [33] S. W. Werneke, C. Swann, L. A. Farquharson, K. S. Hamilton, and A. M. Smith, “The role of metals in molluscan adhesive gels,” *J. Exp. Biol.*, vol. 210, no. 12, pp. 2137–2145, 2007.
- [34] J. Li *et al.*, “Tough adhesives for diverse wet surfaces,” *Science (80-.)*, vol. 357, no. 6349, pp. 378–381, 2017.
- [35] ASTM International, “ASTM F2255-05(2015) Standard Test Method for Strength Properties of Tissue Adhesives in Lap-Shear by Tension Loading,” *Annu. B. ASTM Stand.*, vol. 05, no. Reapproved 2015, pp. 1–6, 2015.
- [36] J. M. Robertson, “Mechanically Active Electrospun Materials,” Syracuse University, 2015.
- [37] R. E. Webber, C. Creton, H. R. Brown, and J. P. Gong, “Large strain hysteresis and Mullins effect of tough double network hydrogels,” *Macromolecules*, vol. 40, pp. 2919–2927, 2007.
- [38] W. Zhu, Y. J. Chuah, and D. A. Wang, “Bioadhesives for internal medical applications: A review,” *Acta Biomater.*, vol. 74, pp. 1–16, 2018.
- [39] A. Della Bona and R. Van Noort, “Shear vs. Tensile Bond Strength of Resin Composite Bonded to Ceramic,” *J. Dent. Res.*, vol. 74, no. 9, pp. 1591–1596, 1995.
- [40] F. C. Campbell, “Adhesive Bonding and Integrally Cured Structure: A Way to Reduce Assembly Costs through Parts Integration,” in *Manufacturing Processes for Advanced Composites*, Amsterdam: Elsevier, 2004, pp. 241–301.
- [41] T. Wang, J. Nie, and D. Yang, “Dextran and gelatin based photocrosslinkable tissue adhesive,” *Carbohydr. Polym.*, vol. 90, no. 4, pp. 1428–1436, 2012.
- [42] S. Y. Yang *et al.*, “A Bio-Inspired Swellable Microneedle Adhesive for Mechanical Interlocking with Tissue,” *Nat. Commun.*, vol. 4, no. 1702, pp. 1–23, 2013.
- [43] Y. J. Lee *et al.*, “Enhanced biocompatibility and wound healing properties of biodegradable polymer-modified allyl 2-cyanoacrylate tissue adhesive,” *Mater. Sci. Eng. C*, vol. 51, pp. 43–50, 2015.
- [44] P. J. M. Bouten *et al.*, “The chemistry of tissue adhesive materials,” *Prog. Polym. Sci.*, vol. 39, no. 7, pp. 1375–1405, 2014.
- [45] G. Sudre, D. Hourdet, F. Cousin, C. Creton, and Y. Tran, “Structure of surfaces and interfaces of poly(N,N-dimethylacrylamide) hydrogels,” *Langmuir*, vol. 28, no. 33, pp. 12282–12287, 2012.
- [46] M. Shen, Y. Sun, J. Xu, X. Guo, and R. K. Prud’Homme, “Rheology and adhesion of

poly(acrylic acid)/Laponite nanocomposite hydrogels as biocompatible adhesives,”
Langmuir, vol. 30, no. 6, pp. 1636–1642, 2014.

Chapter 5 Summary

5.1 Conclusions

As shown in this thesis, the study of double network hydrogels can be taken into many different areas. In Chapter 2, a study was conducted into the underlying mechanics of double networks, to see how brittle network variables affect the mechanical properties of the gels. Chapter 3 highlights work performed to create a double network that could be synthesized using a novel photolithography setup, which allows us to make precise, complex 3D constructs. In Chapter 4, an attempt was made to create a synthetic-biological hybrid network for the purposes of investigating how proteins from a defensive slug secretion react when in the presence of different types of metal ions.

Chapter 2 used a methacrylated hyaluronic acid, poly(dimethylacrylamide) double network to determine how brittle network concentration and crosslinking can affect the mechanical properties of the double network gel. A central composite experimental design was used to systematically vary these two characteristics so that the interactions could also be quantified. It was found that the modulus and tearing energy of the double networks were affected by the interactions of the concentration and crosslinking ratio. From surface response plots, the elongation at break was found to have a local maxima at middling crosslinking ratios of 3:1. This means that materials can be designed where ductility is not forfeited for tougher or stronger gels. From model equations developed from results of the central composite design, the modulus, tearing energy, and maximum swelling equations were accurately predicted for gels of a tested composition.

Chapter 3 reported on efforts to make a double network gel that could be used in an additive printing photolithography machine. Results showed that double networks were formed using this

novel synthesis method. By altering the concentration of the brittle network, as well as the crosslinker and photoinitiator concentration of the second network, the mechanical properties of the system could be tuned. The same is true for the power setting of the laser as well as the fabrication speed of the setup. This tuning of material properties would be helpful for researchers who would need to make gels with specific material properties for tissue engineering or other biomedical applications.

Chapter 4 focused on the attempt to make poly(acrylamide) gels that were laden with proteins from a defensive slug glue. The goal of this work was to create a hybrid synthetic-biologic double network, and then use this network to investigate how metallic ions and protein concentrations would affect the mechanical properties of the gel. This would help to determine the role of the several types of proteins that exist within the slug glue and would hopefully lead to the design of novel biomaterials. Unfortunately, these gels did not show any signs of protein network formation. After review, several aspects of this project would need to be refined before this process is revisited. These are highlighted in the next subsection of this chapter.

5.2 Future Work

From the work completed in Chapter 2, the next steps would be to run similar types of central composite designs to further investigate the interplay between material variables and how they affect the overall gel mechanics. One experimental design that would be of particular interest would be to investigate the interactions between a brittle network variable and a ductile network variable. An example could be the crosslinking concentration of either, or the concentrations of either. For a particularly robust study, a complex experimental design could be implemented which would test for the importance and interactions of several variables at once. The drawback

to an experimental design such as that discussed above is the complexity of the design, which would require several compositions, and therefore be strenuous both on resources and time.

From the work completed in Chapter 3, alginate, poly(acrylamide) double networks were synthesized in a novel photolithography setup. It might be interesting to see if other materials could be made and how this change in materials could lead to gels with different mechanical properties. In addition, the self-healing properties of this material was not investigated. This could be an interesting property to examine and could lead to other applications that this material and synthesis process could be used for. To further expand on whether this material could be used in tissue engineering applications, tests should also be run to determine cytocompatibility. It would also be interesting to expand upon the complex 3D shapes made in this work, and perhaps try to make 3D structures that contain hollow channels that could be used for making bioreactors or complex tissue constructs.

From the work completed in Chapter 4, the limitations of the current setup were highlighted. Specifically, the concentration of proteins collected from raw glue samples was found to be too low to make viable samples. Advances in biochemistry, particularly the development of making bacterial strains that can produce the targeted proteins, would need to be completed. In addition, it may be necessary to determine how to keep the proteins from aggregating out of solutions when the concentrations get too high. Both problems would best be solved outside the area of expertise of the author, and so these issues might best be solved with collaborations with other researchers.

Appendices

Appendix A.1. All tensile, tearing, and swelling data collected for the CCD. Each value is the average \pm standard deviation.

Composition	Modulus (kPa)	Elongation at Break (%)	Max Stress (kPa)	Tearing Energy (J/m ²)	Q _{max} (g/g)
2 wt% 4:1	282.4 (\pm 92)	222.1 (\pm 94)	314.6 (\pm 59)	102.1 (\pm 41)	4.58 (\pm 1.6)
2 wt% 2:1	109.8 (\pm 50)	224.3 (\pm 53)	139.6 (\pm 60)	29.82 (\pm 2.7)	8.91 (\pm 0.72)
1 wt% 4:1	94.90 (\pm 52)	281.1 (\pm 30)	145.7 (\pm 68)	31.92 (\pm 20)	10.2 (\pm 1.7)
1 wt% 2:1	19.19 (\pm 2.9)	269.8 (\pm 64)	30.32 (\pm 7.6)	23.70 (\pm 11)	12.9 (\pm 1.1)
1.5 wt% 3:1	106.9 (\pm 37)	269.6 (\pm 39)	147.2 (\pm 53)	28.84 (\pm 4.8)	7.60 (\pm 0.90)
2.207 wt% 3:1	222.9 (\pm 29)	237.4 (\pm 30)	288.7 (\pm 39)	52.98 (\pm 9.2)	6.53 (\pm 0.55)
0.793 wt% 3:1	22.59 (\pm 6.9)	305.2 (\pm 31)	34.44 (\pm 11)	6.164 (\pm 2.4)	16.9 (\pm 1.6)
1.5 wt% 4.414:1	211.2 (\pm 30)	269.9 (\pm 60)	262.2 (\pm 14)	26.23 (\pm 11)	7.08 (\pm 0.27)
1.5 wt% 1.586:1	34.24 (\pm 21)	248.0 (\pm 56)	46.70 (\pm 25)	25.27 (\pm 9.0)	11.0 (\pm 0.43)

Appendix A.2. ANOVA Results. Tabular ANOVA data for each of the mechanical responses. Obtained from MINITAB software.

Modulus:

Source	DF	Adj SS	Adj MS	F-Value	P-Value
Model	5	365468	73094	40.70	0.000
Linear	2	352310	176155	98.08	0.000
MHA wt%	1	196971	196971	109.67	0.000
[PEGDA]/[MHA]	1	155339	155339	86.49	0.000
Square	2	1409	704	0.39	0.678
MHA wt%*MHA wt%	1	1152	1152	0.64	0.428
[PEGDA]/[MHA]*[PEGDA]/[MHA]	1	1153	1153	0.64	0.428
2-Way Interaction	1	11749	11749	6.54	0.015
MHA wt%*[PEGDA]/[MHA]	1	11749	11749	6.54	0.015
Error	39	70045	1796		
Lack-of-Fit	3	170	57	0.03	0.993
Pure Error	36	69876	1941		
Total	44	435513			

Elongation at Break:

Source	DF	Adj SS	Adj MS	F-Value	P-Value
Model	5	27764	5552.7	1.97	0.104
Linear	2	26084	13042.2	4.64	0.016
MHA wt%	1	25074	25074.5	8.92	0.005
[PEGDA]/[MHA]	1	1010	1009.9	0.36	0.552
Square	2	1450	725.2	0.26	0.774
MHA wt%*MHA wt%	1	139	138.8	0.05	0.825
[PEGDA]/[MHA]*[PEGDA]/[MHA]	1	1256	1255.7	0.45	0.508
2-Way Interaction	1	229	228.7	0.08	0.777
MHA wt%*[PEGDA]/[MHA]	1	229	228.7	0.08	0.777
Error	39	109659	2811.8		
Lack-of-Fit	3	2852	950.6	0.32	0.811
Pure Error	36	106807	2966.9		
Total	44	137423			

Max Stress:

Source	DF	Adj SS	Adj MS	F-Value	P-Value
Model	5	480909	96182	51.69	0.000
Linear	2	475708	237854	127.83	0.000
MHA wt%	1	254304	254304	136.67	0.000
[PEGDA]/[MHA]	1	221404	221404	118.99	0.000
Square	2	755	378	0.20	0.817
MHA wt%*MHA wt%	1	732	732	0.39	0.534
[PEGDA]/[MHA]*[PEGDA]/[MHA]	1	182	182	0.10	0.756
2-Way Interaction	1	4446	4446	2.39	0.130
MHA wt%*[PEGDA]/[MHA]	1	4446	4446	2.39	0.130
Error	39	72567	1861		
Lack-of-Fit	3	4266	1422	0.75	0.530
Pure Error	36	68302	1897		
Total	44	553476			

Tearing Energy:

Source	DF	Adj SS	Adj MS	F-Value	P-Value
Model	5	22592.0	4518.4	10.20	0.000
Linear	2	17061.6	8530.8	19.27	0.000
MHA wt%	1	12371.0	12371.0	27.94	0.000
[PEGDA] / [MHA]	1	4690.6	4690.6	10.59	0.002
Square	2	405.7	202.8	0.46	0.636
MHA wt%*MHA wt%	1	347.7	347.7	0.79	0.381
[PEGDA] / [MHA] * [PEGDA] / [MHA]	1	314.7	314.7	0.71	0.404
2-Way Interaction	1	5124.7	5124.7	11.57	0.002
MHA wt%*[PEGDA] / [MHA]	1	5124.7	5124.7	11.57	0.002
Error	39	17267.9	442.8		
Lack-of-Fit	3	7149.7	2383.2	8.48	0.000
Pure Error	36	10118.3	281.1		
Total	44	39859.9			

Maximum Swelling:

Source	DF	Adj SS	Adj MS	F-Value	P-Value
Model	5	300.194	60.039	26.75	0.000
Linear	2	263.556	131.778	58.72	0.000
MHA wt%	1	209.914	209.914	93.54	0.000
[PEGDA] / [MHA]	1	53.642	53.642	23.90	0.000
Square	2	33.090	16.545	7.37	0.004
MHA wt%*MHA wt%	1	25.508	25.508	11.37	0.003
[PEGDA] / [MHA] * [PEGDA] / [MHA]	1	1.188	1.188	0.53	0.475
2-Way Interaction	1	3.548	3.548	1.58	0.222
MHA wt%*[PEGDA] / [MHA]	1	3.548	3.548	1.58	0.222
Error	21	47.126	2.244		
Lack-of-Fit	3	23.010	7.670	5.72	0.006
Pure Error	18	24.116	1.340		
Total	26	347.320			

Appendix A.3. Explanation of the Tearing Energy Results.

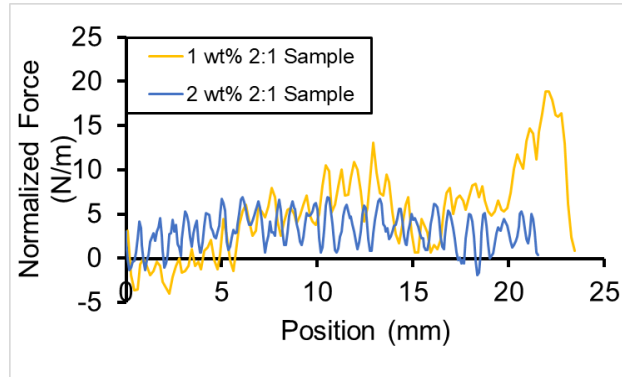


Figure A.1 Model behavior of low wt% and low crosslinking ratio gel (1 wt% 2:1) and a high wt% and low crosslinking gel (2 wt% 2:1). From the data, the low wt% low crosslinking network takes more energy to propagate the defect. An explanation for this is that the low wt% and low crosslinking ratio gel propagates the defect slower than the other due to a higher critical length before crack propagation can occur.

Appendix B.1. Quantification of volume increase during the immersion of DN gel structures in calcium solution.

The DN gel structure undergoes significant increase in volume after it is immersed to the calcium bath. To quantify the increase in the volume due to absorption of calcium solution, we fabricated DN gel rectangular slab by digital masked based optical lithography. The as-fabricated structure was immersed into the calcium solution and the dimension of the structure is recorded every 24 hrs. Series of photographs show the increase of the volume of the sample before immersing (0 hrs) and after immersing the structure to 24 hrs, 48 hrs and 72 hrs to the calcium bath (Figure B-1). Photographs show that the most of increment takes place within the 24 hrs of immersion. There is still increment of the volume after 24 hrs of immersion, however the increase in volume is significantly lower compared to that of first 24 hrs immersion. The volume change is quantified in bar diagram, which shows almost 100% increase in volume in 24 hrs. However, in the next 48 hrs, the volume of structure only increases by ~20%.

Appendix B.2. Study of the mechanical properties of fabricated DN gel structures with different fabrication speed and fixed laser power.

The tensile properties of the DN gel structures are studied by fabricating structures with varying scanning speed (also referred as fabrication speed) of 0.045 mm/s, 0.06 mm/s, 0.075 mm/s and 0.09 mm/s at constant laser intensity of 100 mW (laser intensity of 1.65 mW/cm²). A stress vs strain plot was recorded using a tensile tester and is depicted in Figure 6A. The tensile parameters (elastic modulus, strain, and maximum stress) are plotted as a function of fabrication speed (Figure B-2).

Appendix B.3. Schemes, Tables, and Figures for Appendix B.

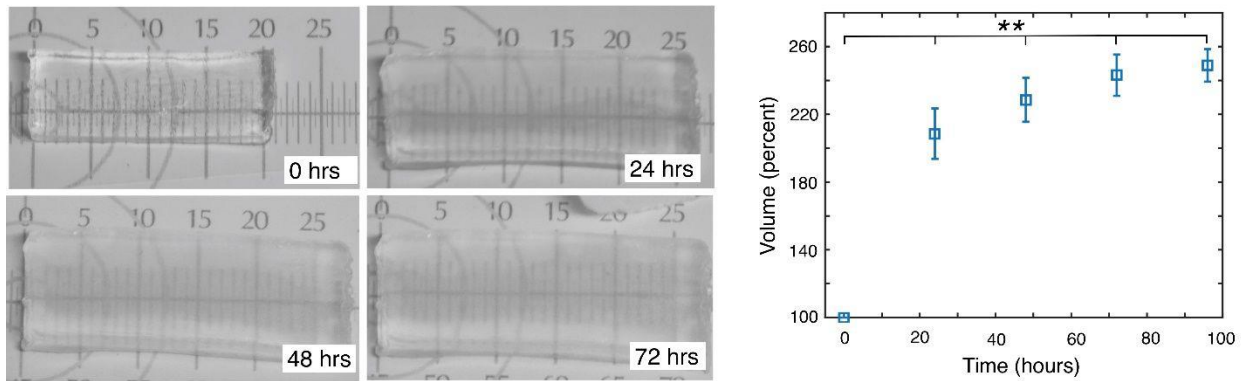


Figure B.1 Photographs of the rectangular slab fabricated of DN gel using a digital mask based optical projection lithography. The first photo was taken right after optical fabrication of the structure (0 hrs). The three other photos were recorded after the structure is immersed into the calcium chloride bath for 24 hrs, 48 hrs and 72 hrs respectively. Bar diagram shows quantification of volume increment before and after dipping the fabricated structure to the calcium bath for different periods of time. ** p value <0.001 (Error bars: Mean±SD)

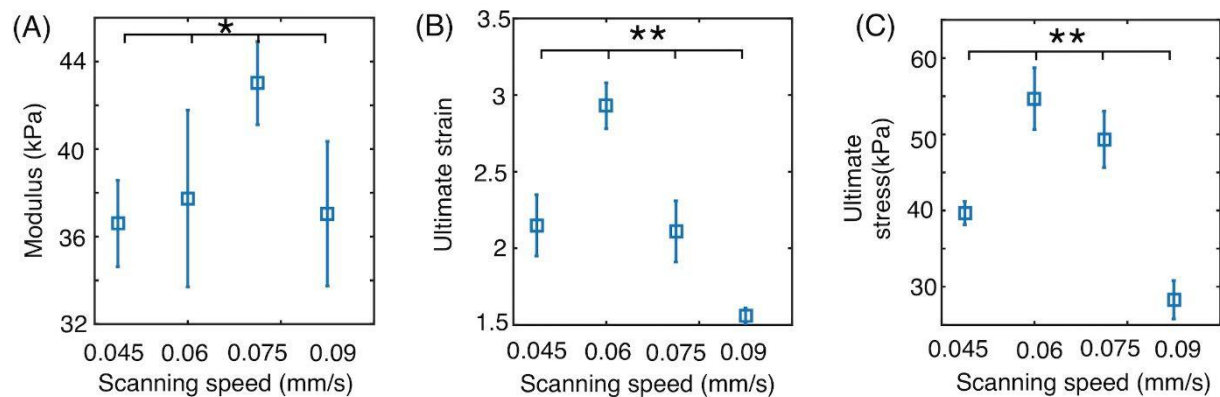


Figure B.2 Tensile parameters (A) elastic modulus, (B) strain, and (C) maximum stress are plotted for DN gel structure printed at varying scanning speed and fixed laser power. * p value < 0.05, ** p value < 0.001 (Error bars: Mean \pm SD)

Appendix C. The Strain and Frequency Sweeps of PDMAAm-SGP gels.

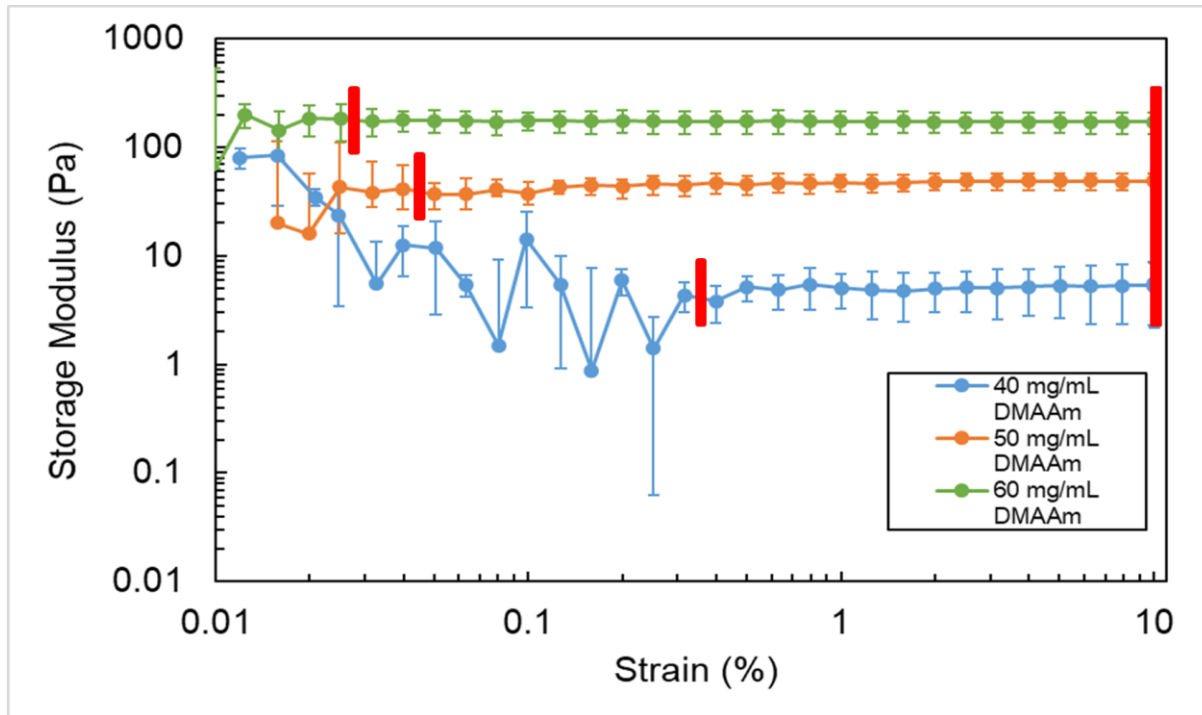


Figure C.1 Strain sweep data for DMAAm gels at a concentration of 40, 50, and 60 mg/mL. The linear viscoelastic region is highlighted as the region between the red bars. For all frequency sweeps, it was determined that a strain of 0.5 % would be used for all other studies, as it is a strain in which the LVE is evident for all concentrations.

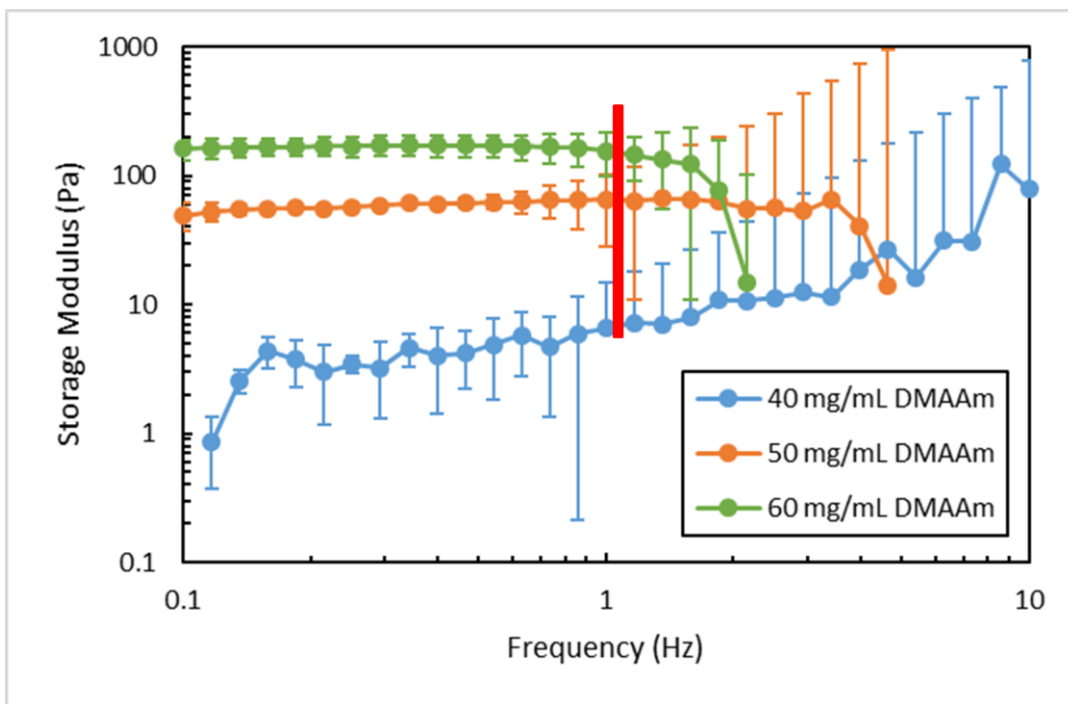


Figure C.2 Frequency sweep data for DMAAm gels at a concentration of 40, 50, and 60 mg/mL. The gels are not viable at frequencies above 1 Hz, as the gels appear to mechanically fail. It was determined that for rheometry data collection, a frequency value of 0.5 Hz would be used.

Vita

ALEXANDER VINCENT STRUCK JANNINI

Phone: (856) 469-1094
avstruck@syr.edu
avjannini@comcast.net

105 Remington Avenue Apt. 9
Syracuse, NY 13210
DOB: August 24, 1991

EDUCATION

- MS** Biomedical Engineering, Syracuse University Expected Date May 2020
Thesis: “Design of Adhesive, Tough, Self-Healing Double Network Hydrogels with Tunable Mechanics Using Slug Glue Proteins”
Advisors: Dr. J. M. Hasenwinkel and Dr. J. H. Henderson
- MS** Chemical Engineering, Rowan University August 2014
Thesis: “Development of Experiments Involving Pharmaceutical Manufacturing Principles”
Advisor: Dr. C. S. Slater
- BS** Chemical Engineering, Rowan University May 2013
Graduated Cum Laude
Concentrations: Materials and Biological Engineering

HONORS AND AWARDS

- Teaching Assistantship** 2019
Acted as a teaching assistant for the Engineering Computation Tools course. Awarded by the Biomedical and Chemical Engineering Department at Syracuse University.
- Teaching Assistantship** 2017-2018
Acted as a teaching assistant for the Mass and Energy Balance course of Fall 2017 and the Biomedical Controls course of Spring 2018. Awarded by the Biomedical and Chemical Engineering Department at Syracuse University.
- Integrative Graduate Education and Research Traineeship Fellowship** 2015-2017
Awarded an interdisciplinary fellowship which focused on biomaterials and soft interfaces. Awarded by the Syracuse Biomaterials Institute at Syracuse University in August 2015.
- Outstanding Teaching Fellow Award** 2014
Recognition for outstanding service during teaching fellowship. Awarded by the Rowan University chemical engineering faculty in May 2014.
- Teaching Fellowship** 2013-2014

Awarded one of the first teaching fellowship positions at Rowan University. Responsible for a clinic team in pharmaceutical engineering research. Supervised and managed undergraduates in a unit operations course. Completed this while completing master's degree requirements.

New Jersey Space Grant Consortium Fellow

2012-2013

Received one year stipend for junior year research. Participated in poster presentation for all Space Grant Fellows.

TEACHING EXPERIENCE

Syracuse University, Syracuse NY

Jan 2019 to May 2019

Teaching Assistant, Biomedical and Chemical Engineering Department

- Introduced students to several different computer programs such as MATLAB, Excel, and Autodesk Inventor
- Helped guide students through exercise problems given during laboratory sessions
- Graded homework assignments, quizzes, and exams

Syracuse University, Syracuse NY

Sep 2017 to May 2018

Teaching Assistant, Biomedical and Chemical Engineering Department

- Responsible for leading class discussions on mass and energy balance topics
- Guided students through problems involving mass balances, separation heuristics, and vapor-liquid equilibrium
- Graded homework assignments, quizzes, and exams

Rowan University, Glassboro NJ

Sep 2014 to May 2015

Adjunct Professor, Chemical Engineering Department

- Taught Freshman Engineering Clinic, a project-based introduction to engineering course
- Developed and supervised semester-long projects for the course on sustainability, chocolate manufacturing, and thin film manufacturing
- Developed exams, homework, surveys, lectures, and laboratory write-ups

Rowan University, Glassboro NJ

May 2013 to Aug 2014

Teaching Assistant, Chemical Engineering Department

- Supervised approximately 36 undergraduates during unit operation experimentation
- Equipment included packed columns, V-mixers, reverse osmosis system, heat exchangers, gas permeation membrane, and baffled mixer
- Responsible for grading student presentations
- Gave lectures on design of experiments and advanced statistical methods

RESEARCH EXPERIENCE

Master's Thesis: Understanding Double Network Theory and Applying it to Synthesis and Biological Applications, Syracuse University, Syracuse NY

May 2020

Advisor: Dr.'s J.M. Hasenwinkel and J.H. Henderson

- Investigated how brittle network variables affect the mechanical properties of the double network to expand knowledge of double network behavior

- Collaborated with another lab to develop a double network hydrogel that could be synthesized using a novel photolithography setup for making complex 3D microstructures
- Developed a slug glue protein laden hydrogel to investigate the effects of glue protein and metal ion interactions

Rowan University, Glassboro NJ

September 2014 – May 2015

Adjunct Professor

- Creating a semester-long project for undergraduates focusing on thin films
- Researching the effectiveness of experiments involving sustainability and chocolate manufacturing
- Researching educational concepts dealing with continuous pharmaceutical manufacturing processes

Master's Thesis: Development of Experiments Involving Pharmaceutical Manufacturing Principles, Rowan University, Glassboro NJ 2014

Advisor: Dr. C.S. Slater

- Incorporated pharmaceutical engineering principles into laboratory experiments
- Areas Researched: Thin films, drug delivery, statistical analysis, fluidization, reverse engineering
- Skills Obtained: Creation of polymers, using laboratory equipment, good manufacturing practices, design of experiments

Rowan University, Glassboro NJ

2012-2013

Senior Clinic Researcher, Advisor: Dr. C.S. Slater

- Devised methods of incorporating pharmaceutical engineering principles into the undergraduate curriculum
- Developed labs for undergraduate students
- Skills Obtained: Team management, design of experiments, using laboratory equipment

Rowan University, Glassboro NJ

2012-2013

Student Researcher, Advisor: Dr. C.S. Slater

- Began basic design of laboratory experiments involving reverse engineering asthma inhalers
- Compiled data on the current state of pharmaceutical engineering education in academia
- Tested solubility and swelling characteristics of hydrogels

Rowan University, Glassboro NJ

2011-2012

Junior Clinic Researcher, Advisor: Dr. A.J. Vernengo

- Researched use of polymeric microspheres as drug carriers
- Targeted site was spinal cord injuries
- Skills Obtained: creation of polymers, drug delivery applications, biomedical applications

PUBLICATIONS

- *Journal Publications*

Kunwar, P., **Jannini, A.**, Xiong, Z., Ransbottom, M., Perkins, J., Henderson, J., Hasenwinkel, J., and Soman, P. “Quick and high-resolution 3D printing of stretchable hydrogel structures using optical projection lithography,” *ACS Applied Materials & Interfaces*, vol. 12, no. 1, 2020.

Fillioe, S., Bishop, K., **Jannini, A.**, Kim, J., McDonough, R., Ortiz, S., Goodisman, J., Hasenwinkel, J., Peterson, C., and Chaiken, J. “In vivo, noncontact, real-time, PV[O]H imaging of the immediate local physiological response to spinal cord injury in a rat model,” *Journal of Biomedical Optics*, vol. 25, no. 3, 2019.

Struck Jannini, A., Slater, C.S., and Savelski, M.J., “Development of Experiments in Strip Film Drug Delivery and Manufacture,” *Global Journal of Engineering Education*, vol. 17, no. 1, 2015.

Struck Jannini, A.V., Slater, C.S., and Savelski, M.J., “Experiments in Pharmaceutical Engineering for Introductory Courses,” *Chemical Engineering Education*, vol. 48, no. 4, 2014, pp. 239-249.

- *Book Chapter*

Struck Jannini, A.V., Wisniewski, C.M., Staehle, M.M., Stanzone III, J.F., and Savelski, M.J., “An Edible Education in Sustainable Development: Investigating Chocolate Manufacturing in a Laboratory-Based Undergraduate Engineering Course,” in: Leal Filho W., Nesbit S. (eds) *New Developments in Engineering Education for Sustainable Development*. World Sustainability Series. Springer.

PRESENTATIONS

Jannini, A., Henderson, J.H., Smith, A., and Hasenwinkel, J.M. “Incorporation of Slug-Glue Proteins to Increase the Stiffness of Double Networks.” *Biomedical Engineering Society*, Oct. 16-19, 2019.

Fillioe, S., Bishop, K.K., **Struck Jannini, A.V.**, Kim, J., McDonough, R., Ortiz, S., Goodisman, J., Hasenwinkel, J., and Chaiken, J. “Use of the PV[O]H algorithm as a noninvasive imaging modality for spinal cord injury *in vivo* in a rat model,” *Novel Techniques in Microscopy*, Apr. 14-17, 2019.

Struck Jannini, A.V., Sheplock, J., Henderson, J.H., and Hasenwinkel, J.M. “A Factorial Analysis to Determine the Effects of Brittle Network Variables on Double Network Properties,” *Biomedical Engineering Society*, Oct. 18-20, 2018.

Perkins, J. **Jannini, A.**, Sheplock, J., Henderson, J.H., and Hasenwinkel, J.M. “Investigating Rigid Network Variables Effects on Double Network Gels Mechanical Properties Using Design of Experiments.” *LSAMP @ SU Undergraduate Poster Session*. Aug. 2018.

Buffington, S.L., Falkenstein-Smith, R.L., Johnson, A., Pieri, K., and **Jannini, A.V.** “Soft Skills Boot Camp: Designing a Three-day Student-run Seminar and Workshop Series for Graduate Students,” American Society for Engineering Education, Jun. 24-27, 2018.

Jannini, A.V., Buffington, S.L., Henderson, J.H., and Mitchell, S.B. “Polymers in the Classroom: Developing a Summer Workshop for High School Science Teachers,” American Society for Engineering Education, Jun. 24-27, 2018.

Jannini, A., Sheplock, J., Henderson, J.H. and Hasenwinkel, J.M. “Development of a Double Network Hydrogel and the Effects of Network Variables on Mechanical Performance.” Stevenson Lecture Day Poster Session. Apr. 23, 2018.

Fillioe, S., Bishop, K.K., **Struck Jannini, A.V.**, Kim, J., McDonough, R., Ortiz, S., Goodisman, J., Hasenwinkel, J.M., and Chaiken, J. “In vivo, noncontact, real-time, optical and spectroscopic assessment of the immediate local physiological response to spinal cord injury in a rat model,” SPIE, Jan. 27-Feb.1, 2018.

Struck Jannini, A.V., Wisniewski, C.M., Staehle, M.M., Stanzione III, J.F., and Savelski, M.J., “Chocolate in the Shark Tank – Investigating the Sustainable Development of Chocolate Manufacturing in a Laboratory-Based Undergraduate Engineering Course,” American Society for Engineering Education, Jun. 14-17, 2015.

Struck Jannini, A.V., Wisniewski, C.M., Staehle, M.M., Stanzione III, J.F., and Savelski, M.J., “An Edible Education in Sustainable Development: Investigating Chocolate Manufacturing in a Laboratory-Based Undergraduate Engineering Course,” Engineering Education in Sustainable Development, Jun. 3-12, 2015, PAPERID-38.

Slater, C.S., Savelski, M.J., and **Struck Jannini, A.V.**, “Exposing Chemical Engineering Students to Pharmaceutical Concepts through Introductory-Level Experiments and Illustrative Exercises,” American Institute for Chemical Engineers, Nov. 16-21, 2014, PAPERID-686h.

Slater, C.S., Savelski, M.J., **Struck Jannini, A.V.**, and Krause, D., “Simple Introductory Experiments Involving Pharmaceutical Engineering Concepts,” American Institute for Chemical Engineers, Nov. 3-8, 2013, PAPERID-510e.

LEADERSHIP EXPERIENCES

Graduate Assistant to the Dean’s Diversity Council July 2018 to November 2018

- Responsible for notetaking and meeting minute writeups for the Council
- Conducted research on the design and infrastructure needed to create an Office of Inclusive Excellence

President – American Society of Engineering Education at Syracuse University (ASEE@SU) May 2017 to Present

- Developed the annual plan and budget for the organization
- Defended a request for funding for the organization
- Responsible for distribution of responsibilities among other board members of ASEE@SU

Workshop Facilitator July 2017 and July 2018

- Developed a two-day workshop for high school teachers highlighting how to incorporate polymer science into high school science classes
- Lead experiments for the workshop participants that allowed them to try the labs that could be incorporated into their curriculum

Secretary – American Society of Engineering Education at Syracuse University (ASEE@SU)

May 2016 to May 2017

- Responsible for creating and distributing promotional flyers for ASEE events
- Led workshops and seminars highlighting resources available on campus and increasing soft skills mastery
- Helped develop a three-day, soft skills retreat for graduate students in the College of Engineering

PROFESSIONAL AFFILIATIONS

American Institute of Chemical Engineers, 2009-2013

American Society of Engineering Education, 2015-Present

Biomedical Engineering Society, 2018-Present

OTHER

U.S. Citizen

Martial artist: Rank of 1st-dan in Taekwondo and Hapkido

Musician: Saxophone, clarinet, percussion, and voice